Searches for Lepton Flavor Violation

An Experimental Review

David Hitlin
Caltech
SLAC Lunchtime Seminar
January 12, 2018

Plus ça change, plus c'est la même chose

- The first Lunchtime Seminar I gave at SLAC was in February, 1969, as part of my interview for a postdoc position
- The topic was the measurement of the sizes and shapes of nuclei with a permanent quadrupole deformation, using detailed analysis of the hyperfine structure in muonic X-ray spectra. This involved stopping low momentum negative muons (~10^3/s) produced in the decay of pions at the 385 MeV Columbia synchrocyclotron in a variety of targets, from ^{152}Sm to ^{238}U

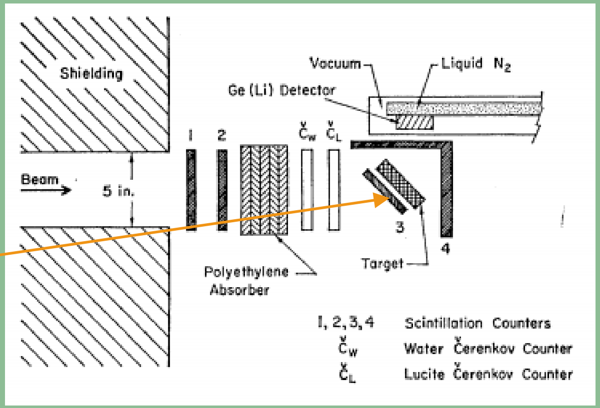

- My seminar today also involves, in part, stopping large numbers (10^{10}/s) of low momentum negative muons produced in the decay of pions produced at the 8 GeV Fermilab booster, stopped in an ^{27}Al target, a search for charged lepton flavor violation, henceforth CLFV

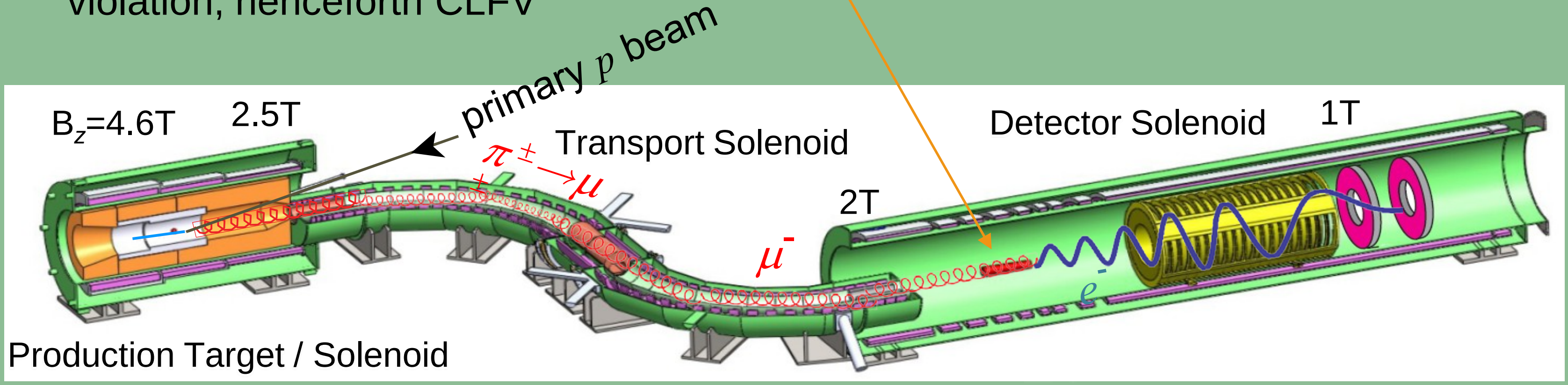

Charged lepton flavor violation (CLFV)

- CLFV denotes a transition among μ, e and τ lepton states that doesn't conserve lepton family number, *i.e.*, there are no neutrinos involved
  - A CLF conserving transition: $\mu^- \rightarrow e^- \nu_e \overline{\nu}_\mu$
  - A CLFV transition: $\mu \rightarrow e\gamma$, $\mu \rightarrow 3e$, $\mu N \rightarrow e N$ ($\mu \rightarrow e$ conversion)
- Family number is not a symmetry of the Standard Model Lagrangian
  - Quark family number is violated in weak decays (*c.f.* the CKM matrix)
  - Neutrino oscillations are proof of the violation of neutral lepton flavor conservation as well as evidence for BSM physics (*e.g.,* see-saw)
- A natural question: "Is there also observable charged lepton flavor violation?"
  - In the Standard Model (+ heavy neutrinos), CLFV is very small:

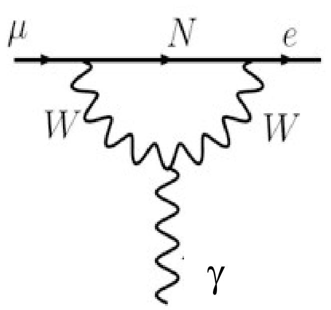

$$\mathcal{B}(\mu \rightarrow e\gamma) = \frac{3\alpha}{32\pi} \left| \sum_{i=2,3} U^*_{\mu i} U_{ei} \frac{\Delta m^2_{1i}}{M^2_W} \right|^2 < 10^{-54}$$

  - Thus CLFV searches are a clean probe of new physics

Searching for CLFV

- Many NP models predict CLFV processes to occur in an observable regime
- The sensitivity to CLFV in loop processes can exceed that in direct production
  - There are many distinct experimental probes and a rich phenomenology, leading to a robust experimental scene
    - $\mu \rightarrow e\gamma$: most powerful limits: MEG at PSI. Upgrade underway
    - $\mu N \rightarrow e N$ muon to electron conversion: three experiments upcoming: one at FNAL and two at JPARC
    - $\mu \rightarrow 3e$: unique effort at PSI
    - $\mu^- N \rightarrow e^+ N(Z\text{-}2)$ (Mu2e–II?)
    - $\mu^+ e^- \rightarrow \mu^- e^+$
    - $\tau \rightarrow \mu\gamma$ and many other τ decays (Belle II)
    - $K_L \rightarrow \mu e$, $B \rightarrow \mu e$, $K \rightarrow \mu e$, … (LHC*b*, expts at J-PARC, CERN)
    - $H^0 \rightarrow \mu, e, \tau + X$

$$R_{\mu e} = \frac{\Gamma(\mu^- + N(A,Z) \rightarrow e^- + N(A,Z))}{\Gamma(\mu^- + N(A,Z) \rightarrow \text{all muon captures})}$$

  - The form of the CLFV Yukawa coupling matrix is model-dependent, *e.g.*, it could be PMNS-like or CKM-like
  - Different theories predict distinct correlations between CLFV processes

CLFV Processes

- Low energy probes: rare μ, τ and h decays, $\mu \rightarrow e$ conversion, CLFV in meson decay

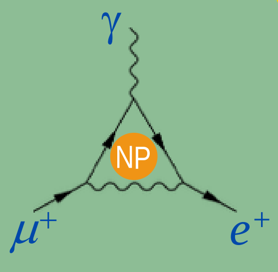

$\mu^+ \rightarrow e^+\gamma$

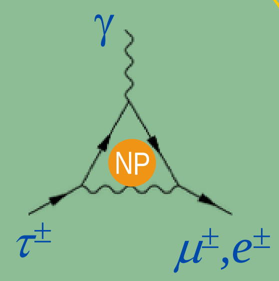

$\tau \rightarrow \mu\gamma$, e$\gamma$

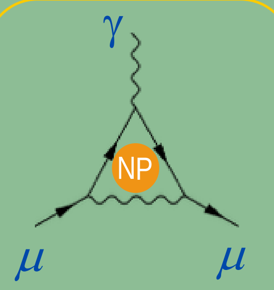

$(g\text{-}2)_\mu$

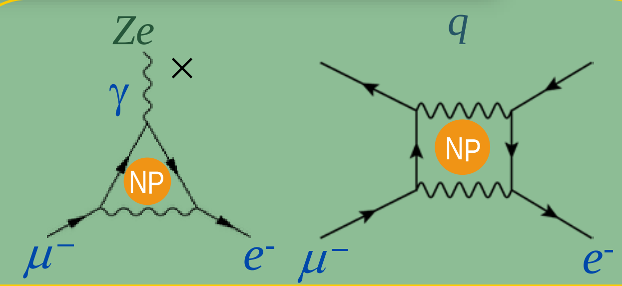

$\mu^- N \rightarrow e^- N$

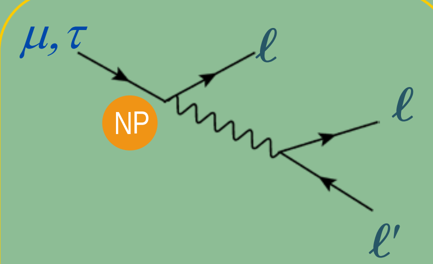

$\mu, \tau \rightarrow 3\ell$

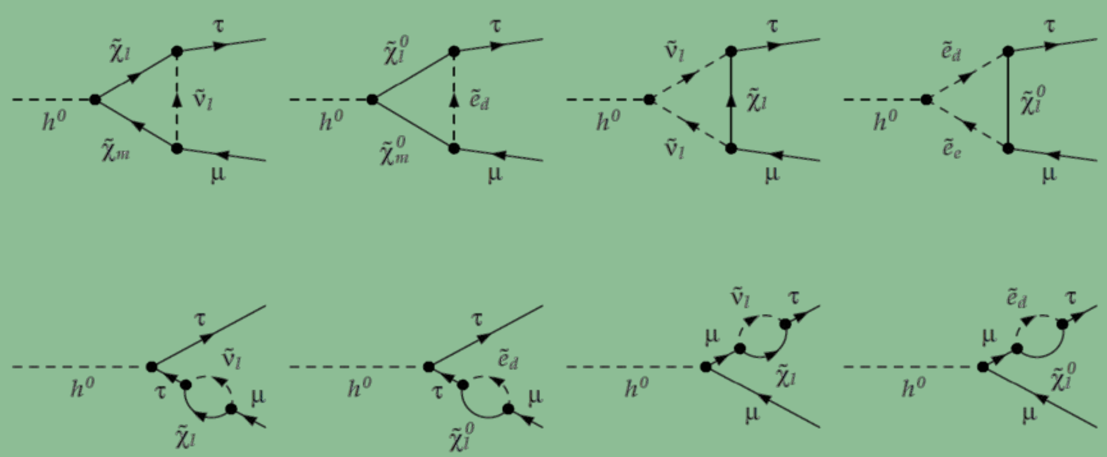

Higgs decay: $h^0 \rightarrow \tau\,\mu$ (also $\tau\, e$, $\mu\, e$)

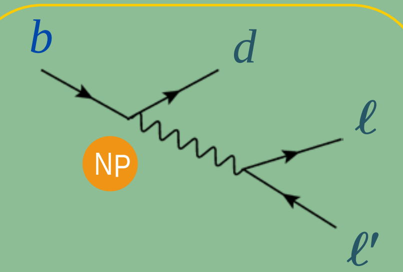

$B \rightarrow \ell\ell'$

$B \rightarrow X_s\ell\ell'$

The new CLFV physics NP

$$\mu^+ \to e^+\gamma \qquad \mu^- \mathrm{N} \to e^- \mathrm{N} \qquad \mu^+ \to e^+e^+e^-$$

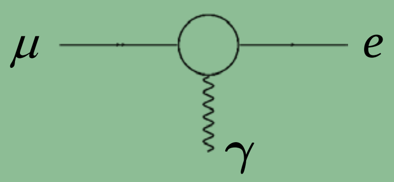

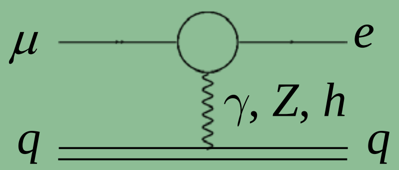

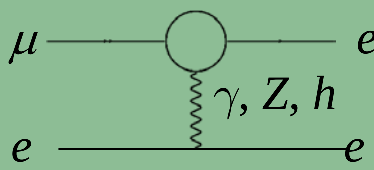

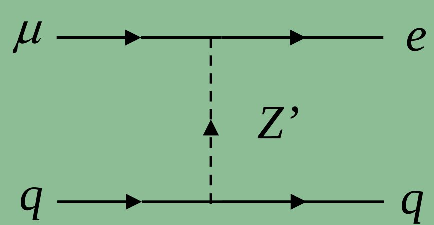

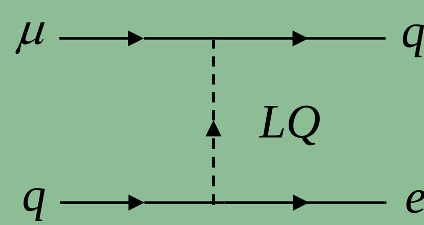

\+ analogous decay processes

CLFV process rates and ratios are thus sensitive probes of the underlying models

New Physics contributions to $\mu \to e$ conversion

$\mu N \to eN$ is sensitive to a wide variety of New Physics models, *e.g.*,

SUSY, 2HDM, Extra Dimensions, Leptoquarks, GUTs, LHT,…

Supersymmetry

rate ~ 10^{-15}

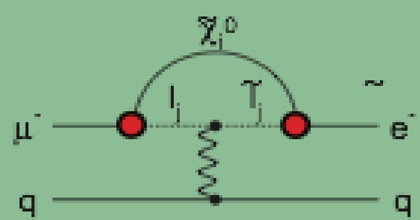

Compositeness

Λ_c ~ 3000 TeV

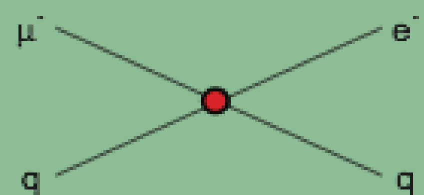

Leptoquark

$M_{LQ} = 3000\,(\lambda_{\mu d}\lambda_{ed})^{1/2}$ TeV/c^2

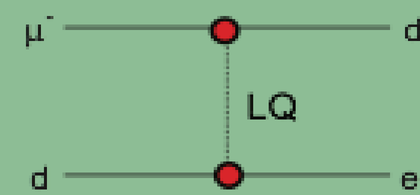

Heavy Neutrinos

$|U_{\mu N}U_{eN}|^2 \sim 8\times10^{-13}$

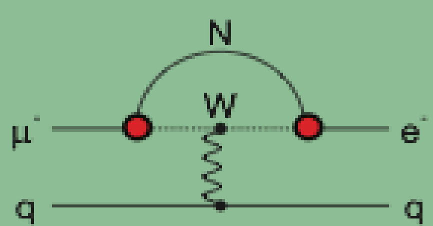

Second Higgs Doublet

$g(H_{\mu e}) \sim 10^{-4} g(H_{\mu\mu})$

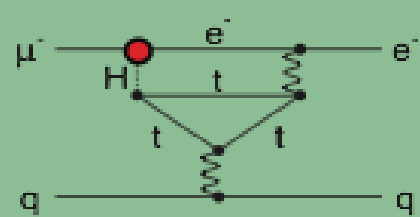

Heavy *Z′*
Anomalous *Z* Coupling

$M_{Z'}$ = 3000 TeV/c^2

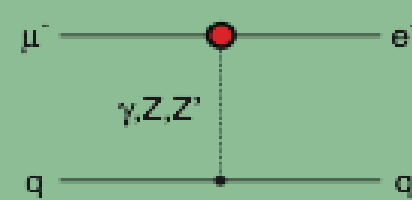

Model-independent effective Lagrangian

$$\mathcal{L}_{\rm CLFV} = \frac{m_\mu}{(1+\kappa)\Lambda^2}\bar{\mu}_R \sigma_{\mu\nu} e_L F^{\mu\nu} + \frac{\kappa}{(1+\kappa)\Lambda^2}\bar{\mu}_L \gamma_\mu e_L (\bar{u}_L \gamma_\mu u_L + \bar{d}_L \gamma_\mu d_L) + h.c.$$

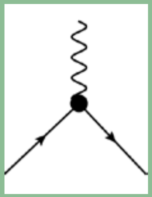

Dipole interaction
(SUSY, ……)

$\mu \to e\gamma$

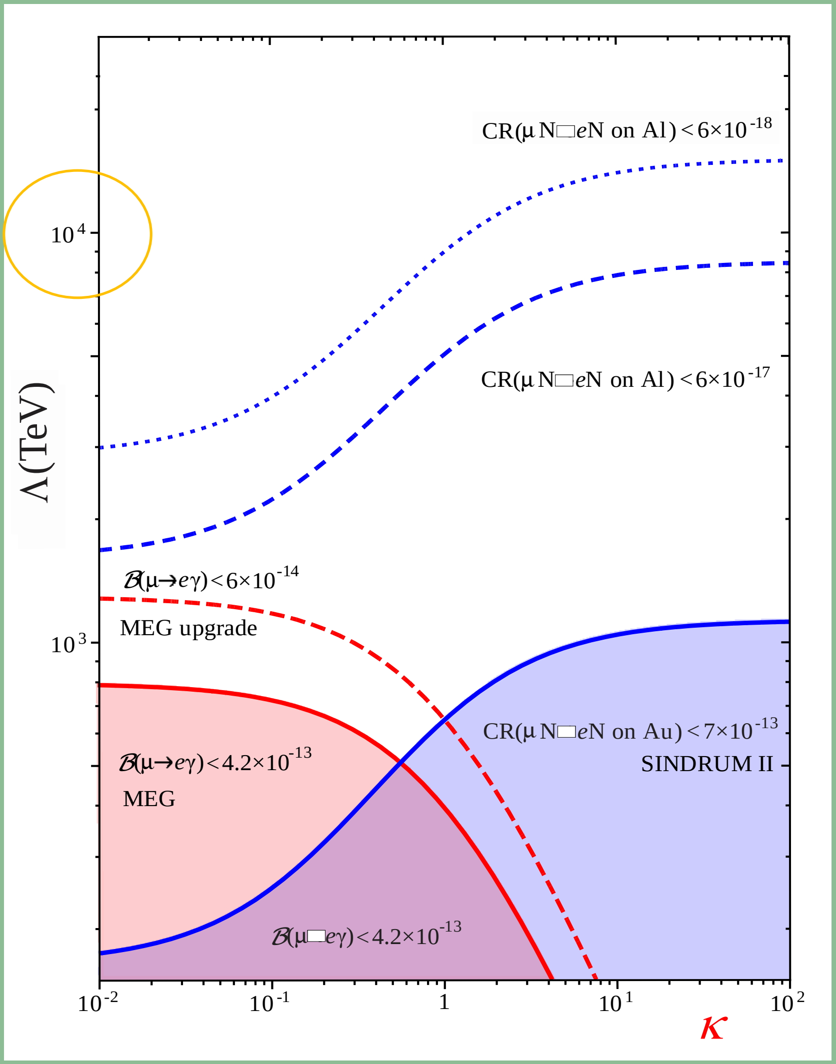

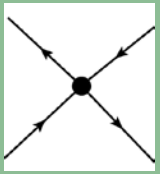

Contact interaction
(Z', leptoquarks, …

$\mu \to e$ conversion

CLFV processes have unique sensitivity to New Physics at high mass scales

Also [$\mu \to eee$]

Derived from A. de Gouvêa & P. Vogel, Prog.Part.Nucl. Phys 71, 75 (2013)

Purely leptonic case: $\mu \to e\gamma$, $\mu \to 3e$ ($\tau \to$)

$$\mathcal{L}_{\mathrm{CLFV}} = \frac{m_\mu}{(1+\kappa)\Lambda^2}\bar{\mu}_R \sigma_{\mu\nu} e_L F^{\mu\nu} + \frac{\kappa}{(1+\kappa)\Lambda^2}\bar{\mu}_L \gamma_\mu e_L (\bar{e}_L \gamma_\mu e_L) + h.c.$$

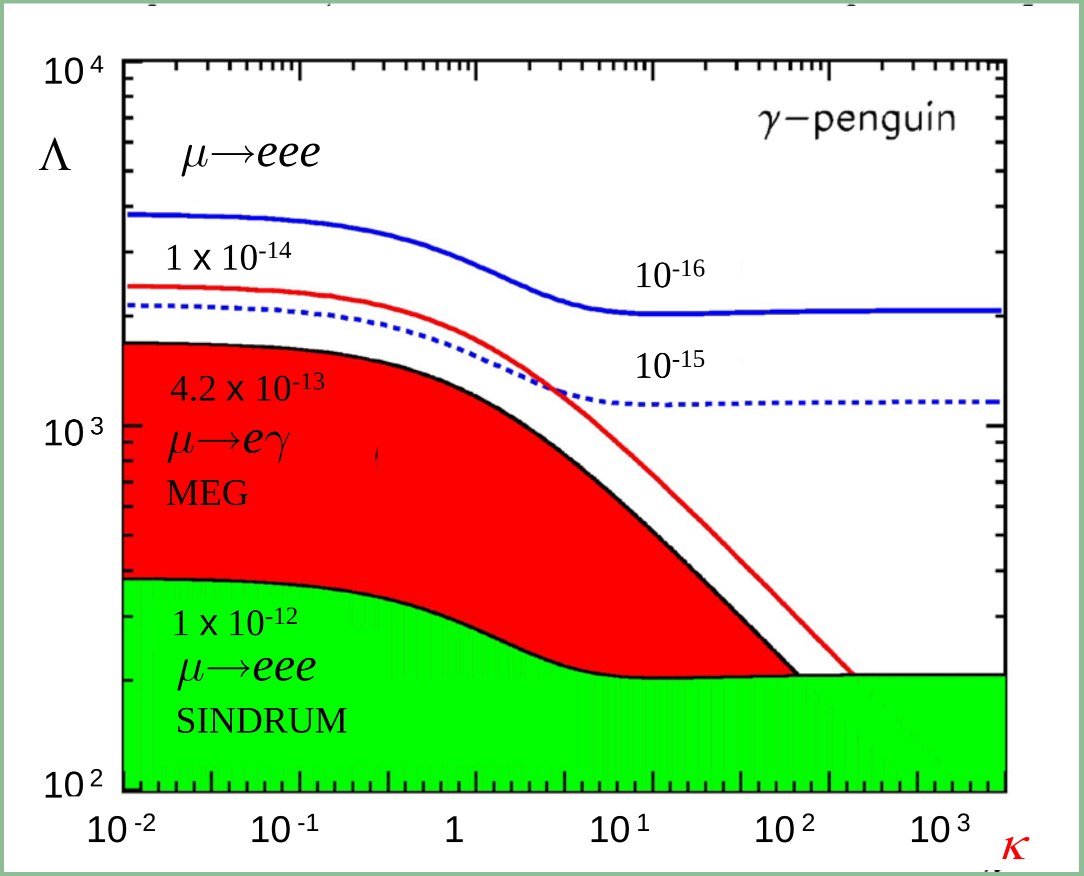

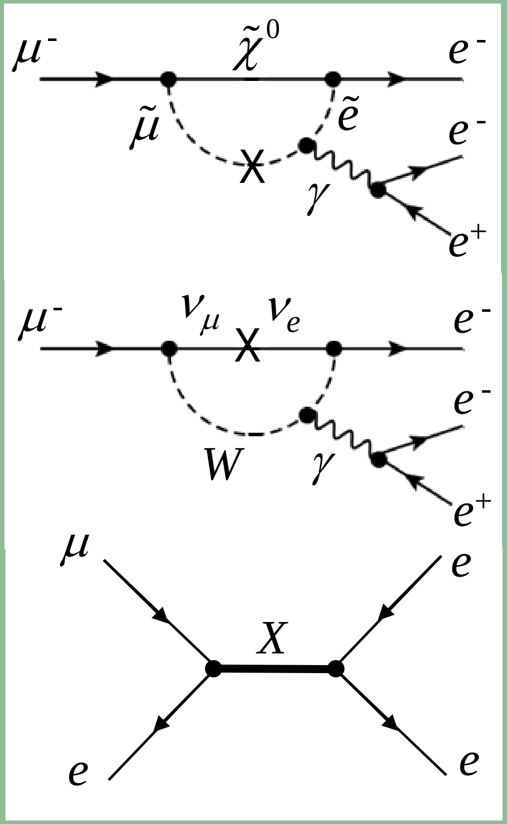

Hisano

Current and future CLFV limits (90%CL)

Process	Current Limit	Next Generation exp
$\tau \rightarrow \mu\eta$	BR < 6.5 x 10^{-8}	
$\tau \rightarrow \mu\gamma$	BR < 6.8 x 10^{-8}	10^{-9} - 10^{-10} (Belle II)
$\tau \rightarrow \mu\mu\mu$	BR < 3.2 x 10^{-8}	
$\tau \rightarrow eee$	BR < 3.6 x 10^{-8}	
$K_L \rightarrow e\mu$	BR < 4.7 x 10^{-12}	
$K^+ \rightarrow \pi^+ e^- \mu^+$	BR < 1.3 x 10^{-11}	
$B^0 \rightarrow e\mu$	BR < 7.8 x 10^{-8}	
$B^+ \rightarrow K^+ e\mu$	BR < 9.1 x 10^{-8}	
$\mu^+ \rightarrow e^+\gamma$	BR < 4.2 x x 10^{-13}	10^{-14} (MEG Upgrade)
$\mu^+ \rightarrow e^+e^+e^-$	BR < 1.0 x 10^{-12}	10^{-16} (Mu3e)
$\mu N \rightarrow eN$	$R_{\mu e}$ < 7.0 x 10^{-13}	10^{-17} (Mu2e, COMET)

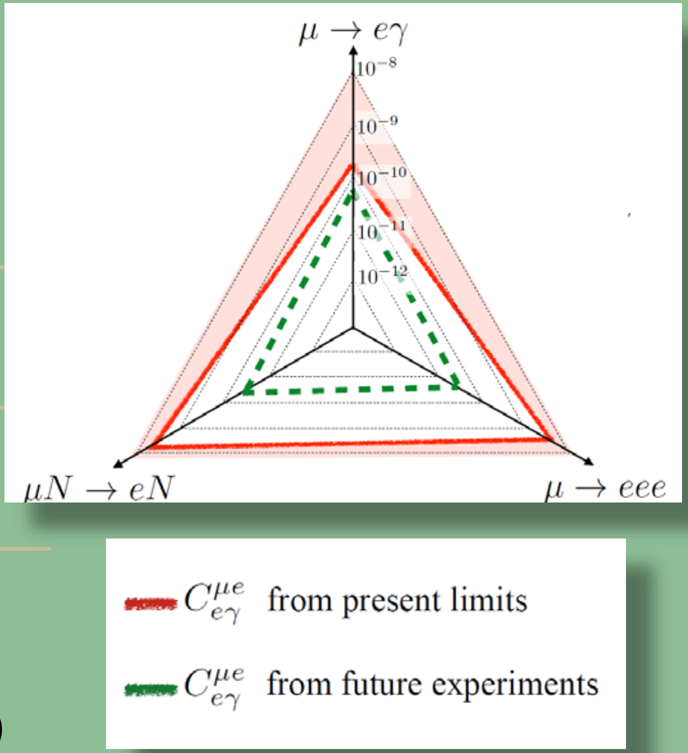

Calibbi and Signorelli
arXiv: 1709.00294 [hep-ph]

Bounds on Higgs exchange models

$$\begin{pmatrix} Y_{ee} & Y_{e\mu} & Y_{e\tau} \\ Y_{\mu e} & Y_{\mu\mu} & Y_{\mu\tau} \\ Y_{\tau e} & Y_{e\mu} & Y_{\tau\tau} \end{pmatrix}$$

- Bounds on CLFV couplings to the Higgs can be derived from LHC limits as well as conventional leptonic processes

$$\mathcal{L}_Y \supset -Y_{e\mu}\bar{e}_L\mu_R h - Y_{\mu e}\bar{\mu}_L e_R h - Y_{e\tau}\bar{e}_L\tau_R h - Y_{\tau e}\bar{\tau}_L e_R h - Y_{\mu\tau}\bar{\mu}_L\tau_R h - Y_{\tau\mu}\bar{\tau}_L\mu_R h + h.c..$$

CLFV Higgs decay $\quad \Gamma(h \to \ell^\alpha \ell^\beta) = \frac{m_h}{8\pi}\left(|Y_{\ell^\beta\ell^\alpha}|^2 + |Y_{\ell^\alpha\ell^\beta}|^2\right)$

$\mu \to e\gamma \;\; (\tau \to \mu\gamma)$

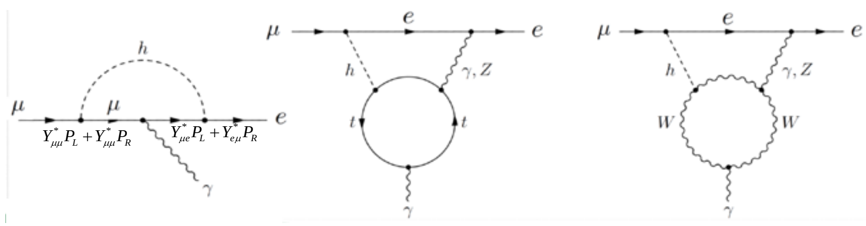

$\mu \to 3e \;\; (\tau \to \ell'\ell\ell)$

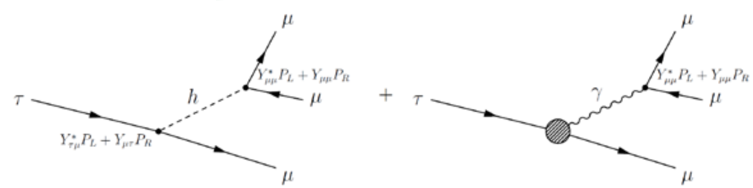

$\mu N \to eN$

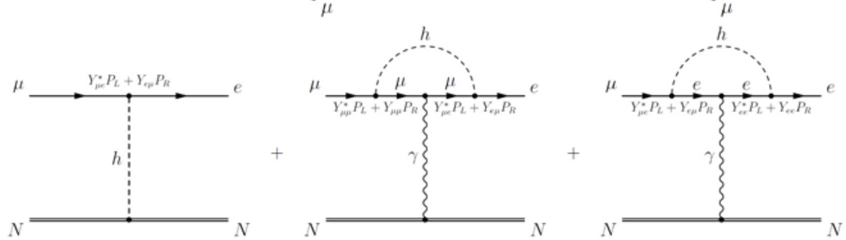

g-2

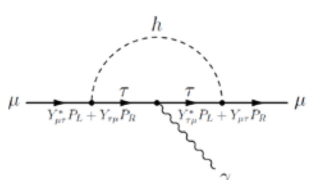

Higgs Yukawa coupling limits

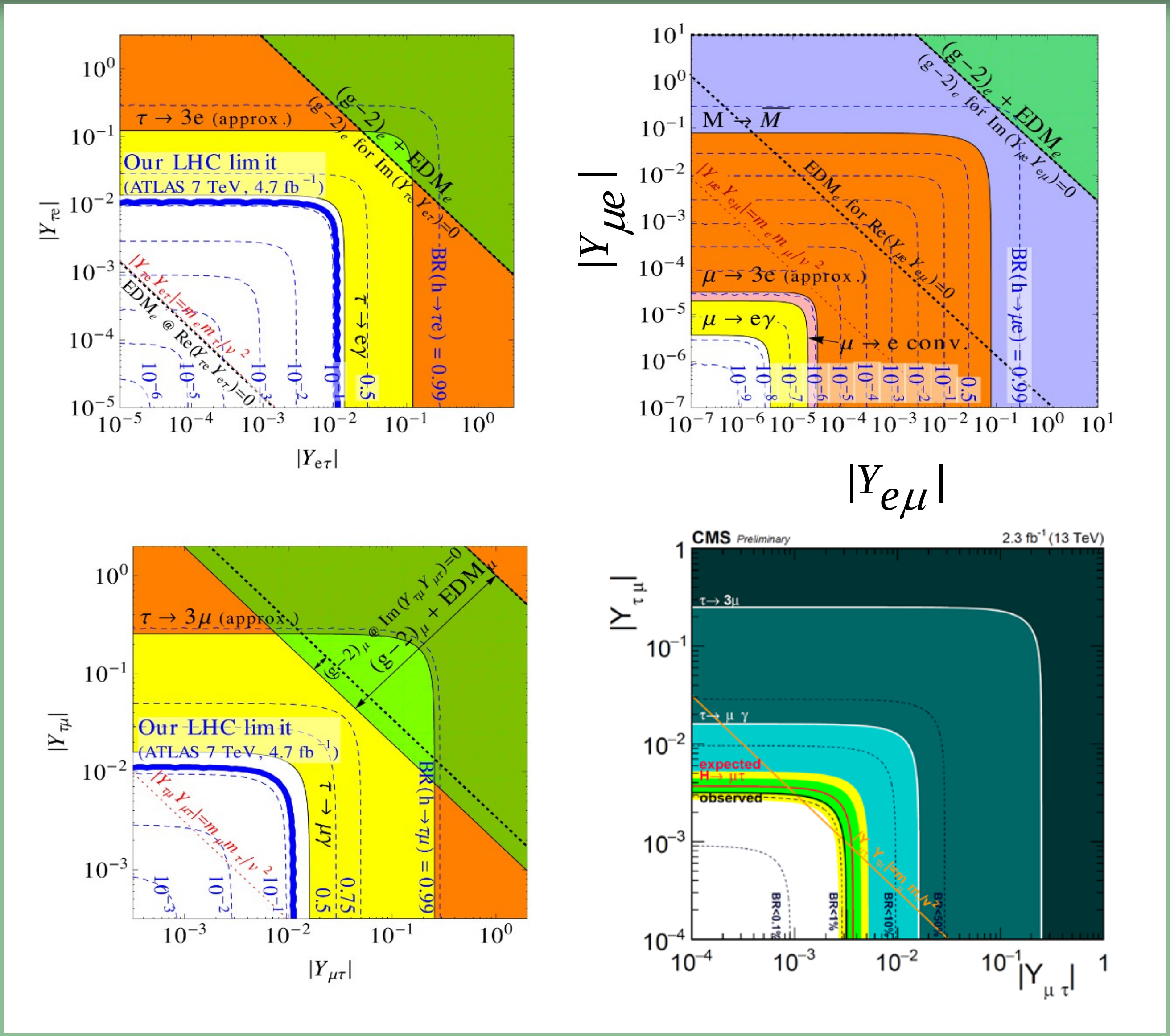

R. Harnik, J. Kopp, and J. Zupan, J. High Energ. Phys. (2013) 2013: 26

Limits on Higgs CLFV couplings

Channel	Coupling	Bound
$\mu \to e\gamma$	$\sqrt{\lvert Y_{\mu e}\rvert^2 + \lvert Y_{e\mu}\rvert^2}$	$< 3.6 \times 10^{-6}$
$\mu \to 3e$	$\sqrt{\lvert Y_{\mu e}\rvert^2 + \lvert Y_{e\mu}\rvert^2}$	< 0.31
electron $g-2$	$\mathrm{Re}(Y_{e\mu}Y_{\mu e})$	$-0.019\ldots0.026$
electron EDM	$\lvert\mathrm{Im}(Y_{e\mu}Y_{\mu e})\rvert$	$< 9.8 \times 10^{-8}$
$\mu \to e$ conversion	$\sqrt{\lvert Y_{\mu e}\rvert^2 + \lvert Y_{e\mu}\rvert^2}$	$< 4.6 \times 10^{-5}$
M-$\bar{M}$ oscillations	$\lvert Y_{\mu e} + Y^*_{e\mu}\rvert$	< 0.079
$\tau \to e\gamma$	$\sqrt{\lvert Y_{\tau e}\rvert^2 + \lvert Y_{e\tau}\rvert^2}$	< 0.014
$\tau \to e\mu\mu$	$\sqrt{\lvert Y_{\tau e}\rvert^2 + \lvert Y_{e\tau}\rvert^2}$	< 0.66
electron $g-2$	$\mathrm{Re}(Y_{e\tau}Y_{\tau e})$	$[-2.1\ldots2.9] \times 10^{-3}$
electron EDM	$\lvert\mathrm{Im}(Y_{e\tau}Y_{\tau e})\rvert$	$< 1.1 \times 10^{-8}$
$\tau \to \mu\gamma$	$\sqrt{\lvert Y_{\tau\mu}\rvert^2 + \lvert Y_{\mu\tau}\rvert^2}$	$< 3.16 \times 10^{-3}$
$\tau \to 3\mu$	$\sqrt{\lvert Y^2_{\tau\mu} + \lvert Y_{\mu\tau}\rvert^2}$	< 0.52
muon $g-2$	$\mathrm{Re}(Y_{\mu\tau}Y_{\tau\mu})$	$(2.7 \pm 0.75) \times 10^{-3}$
muon EDM	$\mathrm{Im}(Y_{\mu\tau}Y_{\tau\mu})$	$-0.8\ldots1.0$
$\mu \to e\gamma$	$(\lvert Y_{\tau\mu}Y_{\tau e}\rvert^2 + \lvert Y_{\mu\tau}Y_{e\tau}\rvert^2)^{1/4}$	$< 3.4 \times 10^{-4}$

Model discrimination through correlations

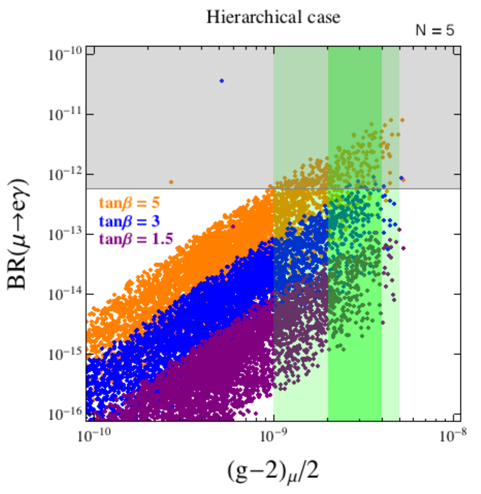

Calibbi *et al*. arXiv:1408.0754 [hep-ph]

arXiv:0702136v3 [hep-ph]

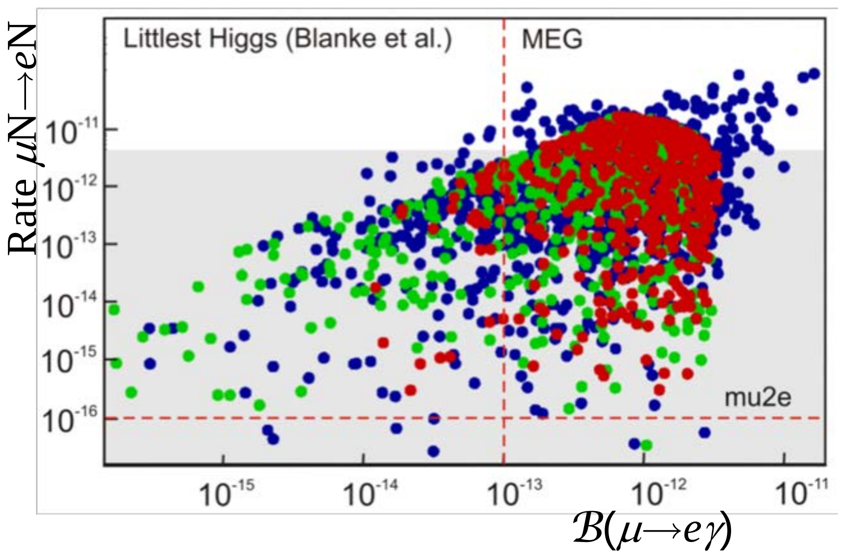

A. Vicente & C.E. Yaguna – Scotogenic model, N_1-N_1 annihilation region

arXiv: 1412.2545 [hep-ph]

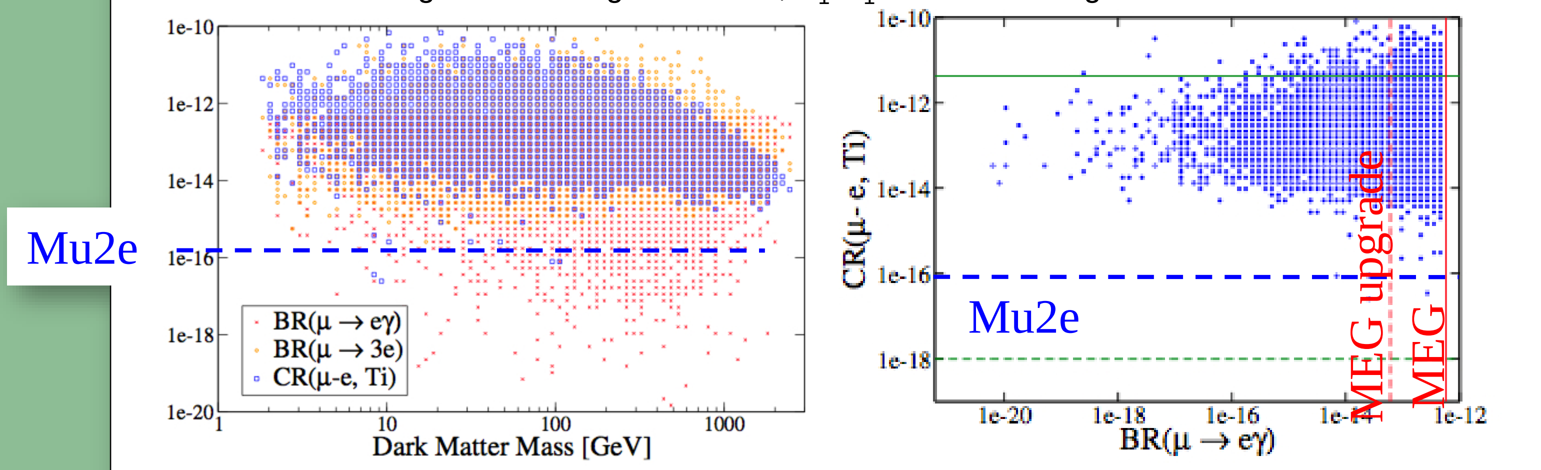

Model discrimination through correlations

ratio	LHT	MSSM (dipole)	MSSM (Higgs)
$\frac{Br(\mu^-\to e^-e^+e^-)}{Br(\mu\to e\gamma)}$	$0.02\ldots1$	$\sim 6\cdot10^{-3}$	$\sim 6\cdot10^{-3}$
$\frac{Br(\tau^-\to e^-e^+e^-)}{Br(\tau\to e\gamma)}$	$0.04\ldots0.4$	$\sim 1\cdot10^{-2}$	$\sim 1\cdot10^{-2}$
$\frac{Br(\tau^-\to \mu^-\mu^+\mu^-)}{Br(\tau\to \mu\gamma)}$	$0.04\ldots0.4$	$\sim 2\cdot10^{-3}$	$0.06\ldots0.1$
$\frac{Br(\tau^-\to e^-\mu^+\mu^-)}{Br(\tau\to e\gamma)}$	$0.04\ldots0.3$	$\sim 2\cdot10^{-3}$	$0.02\ldots0.04$
$\frac{Br(\tau^-\to \mu^-e^+e^-)}{Br(\tau\to \mu\gamma)}$	$0.04\ldots0.3$	$\sim 1\cdot10^{-2}$	$\sim 1\cdot10^{-2}$
$\frac{Br(\tau^-\to e^-e^+e^-)}{Br(\tau^-\to e^-\mu^+\mu^-)}$	$0.8\ldots2.0$	~ 5	$0.3\ldots0.5$
$\frac{Br(\tau^-\to \mu^-\mu^+\mu^-)}{Br(\tau^-\to \mu^-e^+e^-)}$	$0.7\ldots1.6$	~ 0.2	$5\ldots10$
$\frac{R(\mu\mathrm{Ti}\to e\mathrm{Ti})}{Br(\mu\to e\gamma)}$	$10^{-3}\ldots10^{2}$	$\sim 5\cdot10^{-3}$	$0.08\ldots0.15$

Correlations in the $\tau\to\mu\gamma$ and $\ell\ell\ell$ branching fractions

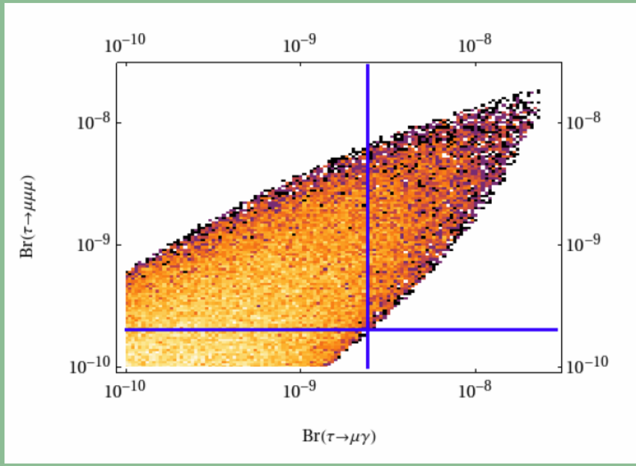

Blanke, Buras, Duling, Recksiegel & Tarantino, Acta Phys. Polon. B41, 657 (2010)

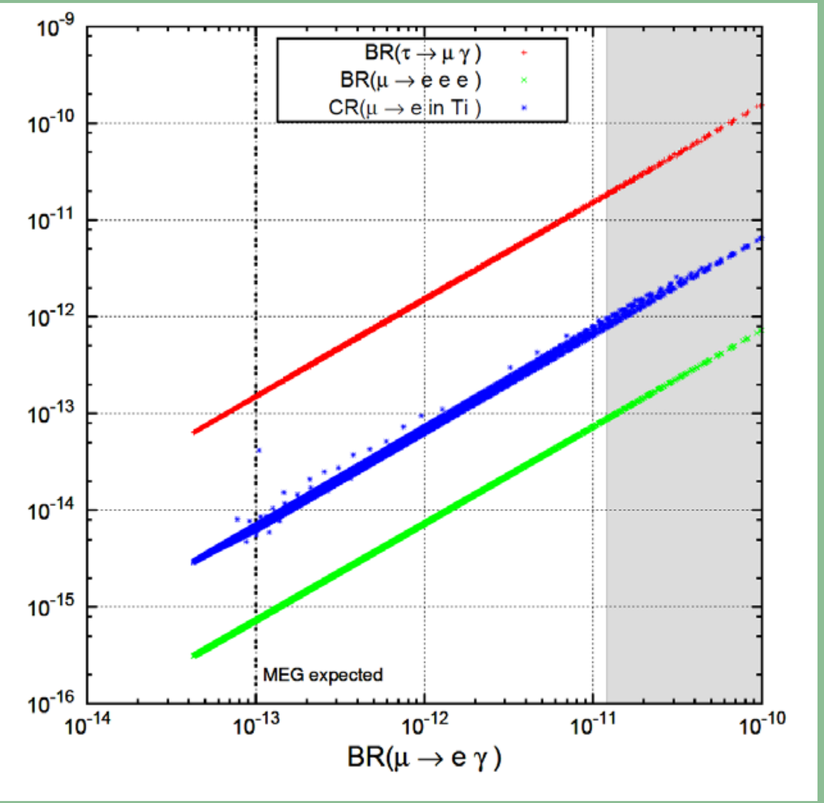

$\mathcal{B}(\tau\to\mu\gamma)$ *vs.* $\mathcal{B}(\mu\to eee)$ and CR($\mu\to$ e on Ti)
in an SO(10) Type II SUSY model
Calibbi, et al., JHEP 0912 057 (2009)

Chronology of μ and τ CLFV searches

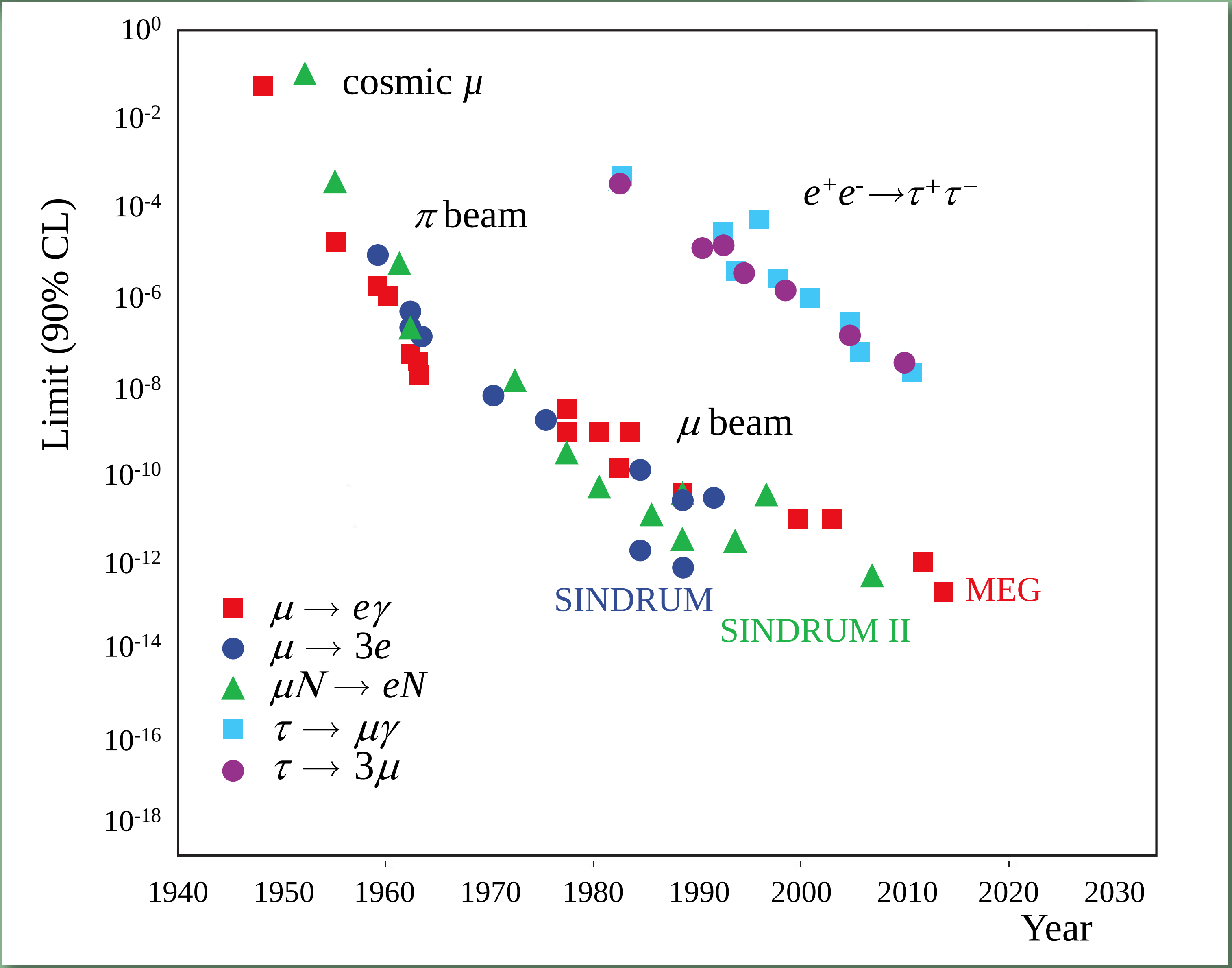

Chronology of μ and τ CLFV searches

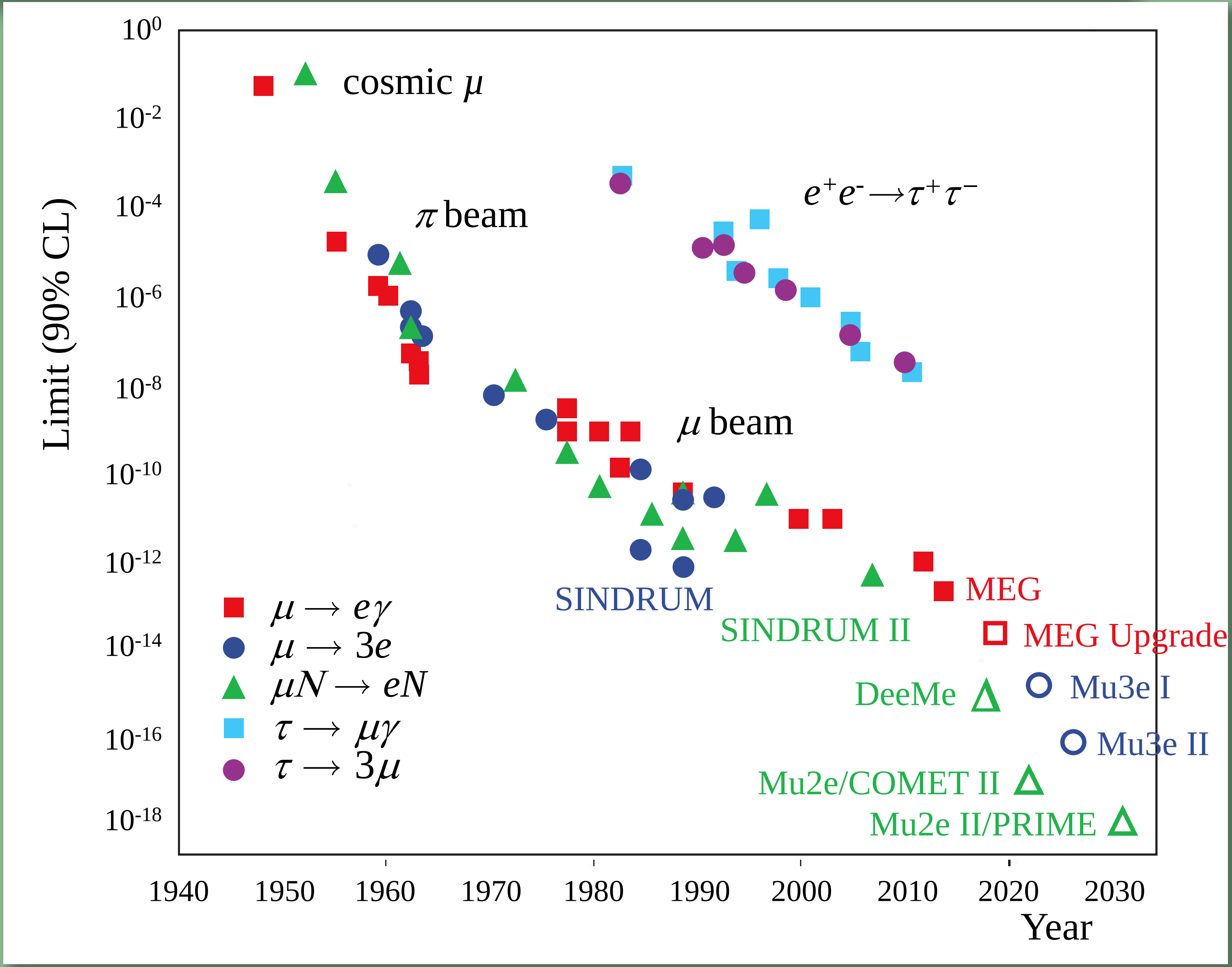

Limits on CLFV τ decays

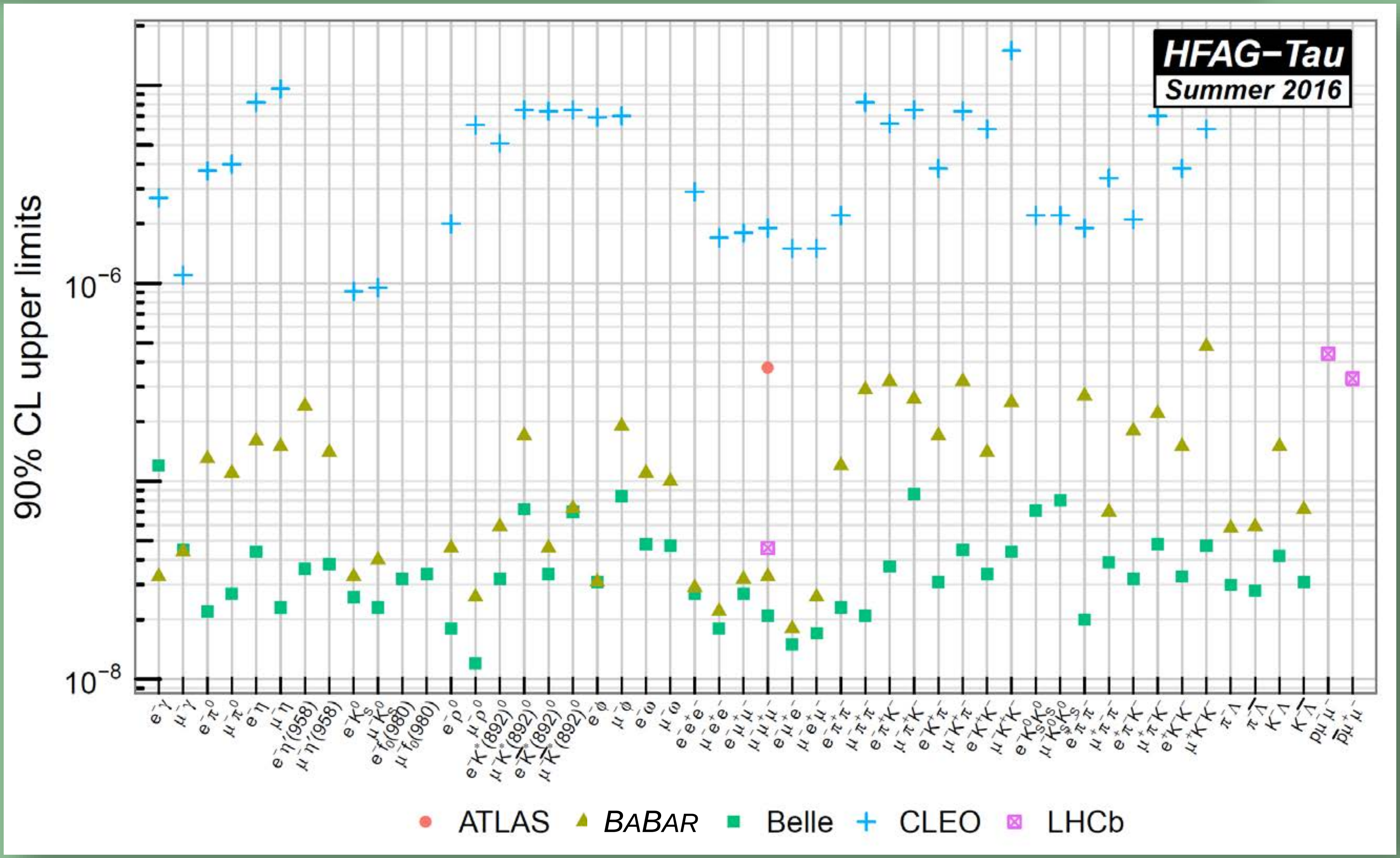

Friends in high places

- Sid Drell's involvement with the CIA/Air Force CORONA program of satellite reconnaissance proved to be crucial to the timely completion of *BABAR*
- The detector solenoid was built by Ansaldo in Genoa. It was originally planned to transport the coil to SLAC by ship, but when the completion fell behind schedule, we were able to make up time by shipping the coil using an Air Force C130
- At that time (1997) there was US involvement in the Balkan war, so that many planes were transporting matériel to The NATO base in Genoa and returning empty
- Sid was able to secure permission from one of his Air Force general friends to ship the *BABAR* solenoid to Moffett Field using a returning C130, thereby preserving the schedule

Backgrounds: the name of the game

- At the sensitivities required to advance the state of the art in both τ decays and muon experiments, the primary issue is control of backgrounds in a high rate environment
  - Irreducible backgrounds
  - Accidental backgrounds
- Problematic backgrounds are specific to the type of experiment
- Handles on background control are
  - Charged particle energy resolution
  - Neutral energy resolution
  - Time resolution
  - Particle identification
  - Prompt beam particle rejection
  - Cosmic ray rejection
- New muon experiments
  - MEG upgrade
  - Mu3e
  - DeeMe, Mu2e, COMET
- New τ decay experiments

  Belle II

  LHC*b*

Belle II τ CLFV limits

- The target integrated luminosity of 50 ab^{-1} (~$5x10^{10}$ $\tau\bar{\tau}$) will be reached in ~2025
- The improvement in sensitivity to CLFV τ decays depends on whether or not a particular mode has backgrounds
  - *e.g.*, limits on $\mathcal{B}(\tau\rightarrow\ell\ell\ell)$ improve as $1/\int\mathcal{L}dt$ if there is no background, but more slowly, as ~ $(1/\int\mathcal{L}dt)^{1/2}$, if there is background

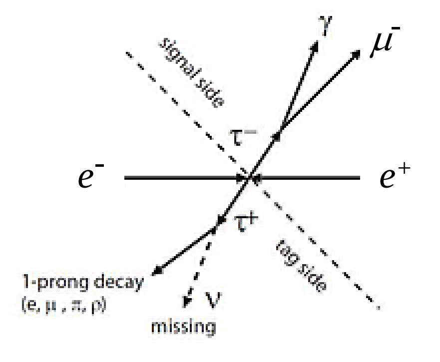

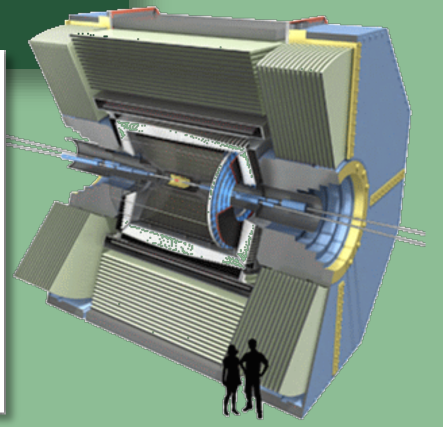

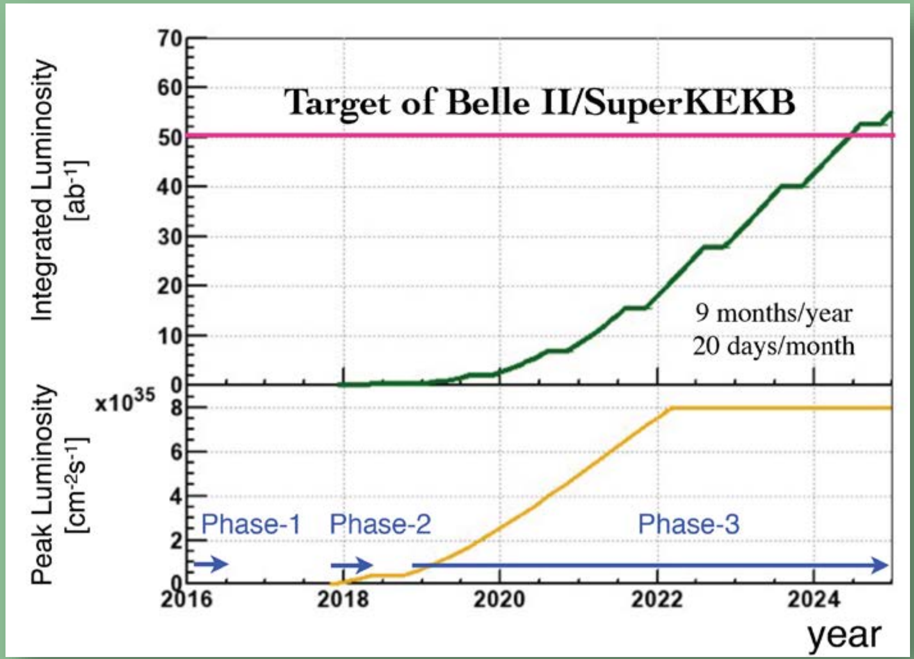

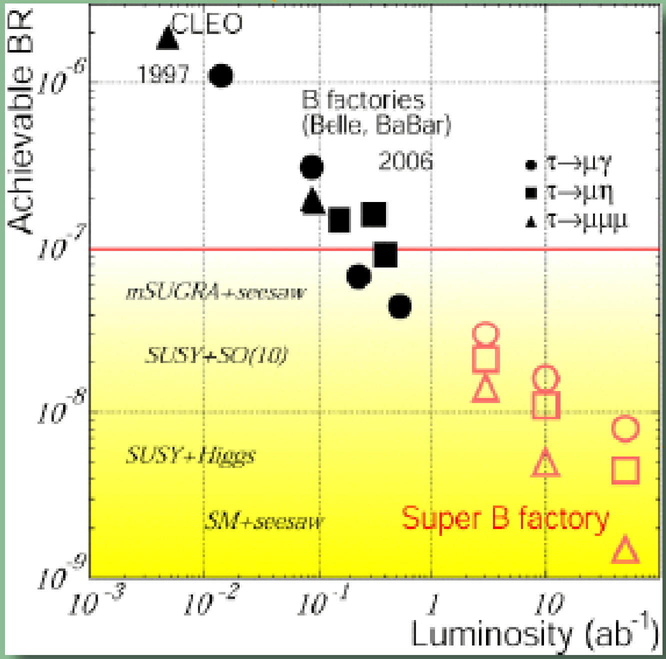

Muon experiments: CW *vs* pulsed beams

- Muon decay experiments $\mu\to e\gamma$, $\mu\to eee$ need a continuous μ^+ beam, such as the PSI synchrocyclotron surface muon beam
- The dominant backgrounds come from accidental coincidences of two decays
  - background $\propto$ (rate)^2
  - signal $\propto$ rate

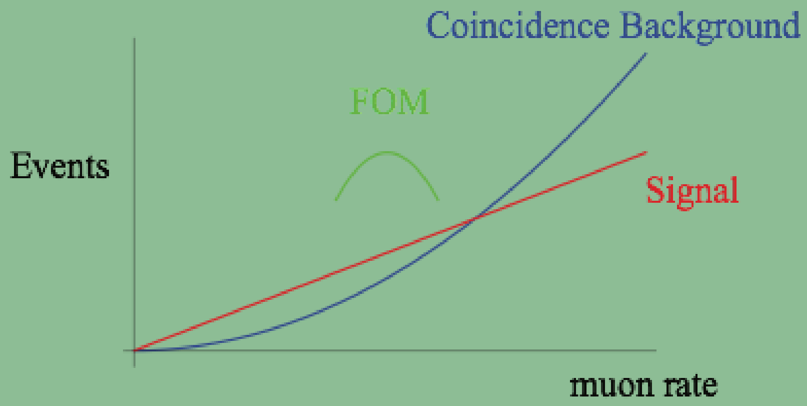

CW operation optimizes the S/N

- $\mu\to e$ conversion experiments need a pulsed μ^- beam, such as FNAL or J-PARC
  - many (prompt) pion-induced backgrounds immediately after the proton pulse
  - Use the muon/pion lifetime difference to reduce background

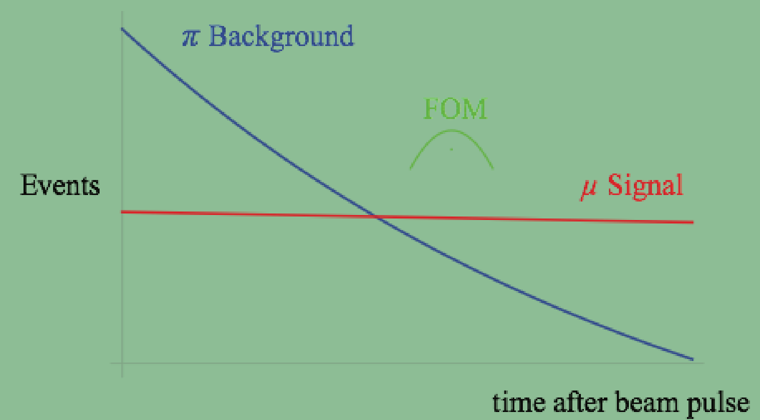

Pulsed operation optimizes the S/N

Muon experiments: CW *vs* pulsed beams

- Muon decay experiments $\mu \rightarrow e\gamma$, $\mu \rightarrow eee$ need a continuous μ^+ beam, such as the PSI synchrocyclotron surface muon beam
- The dominant backgrounds

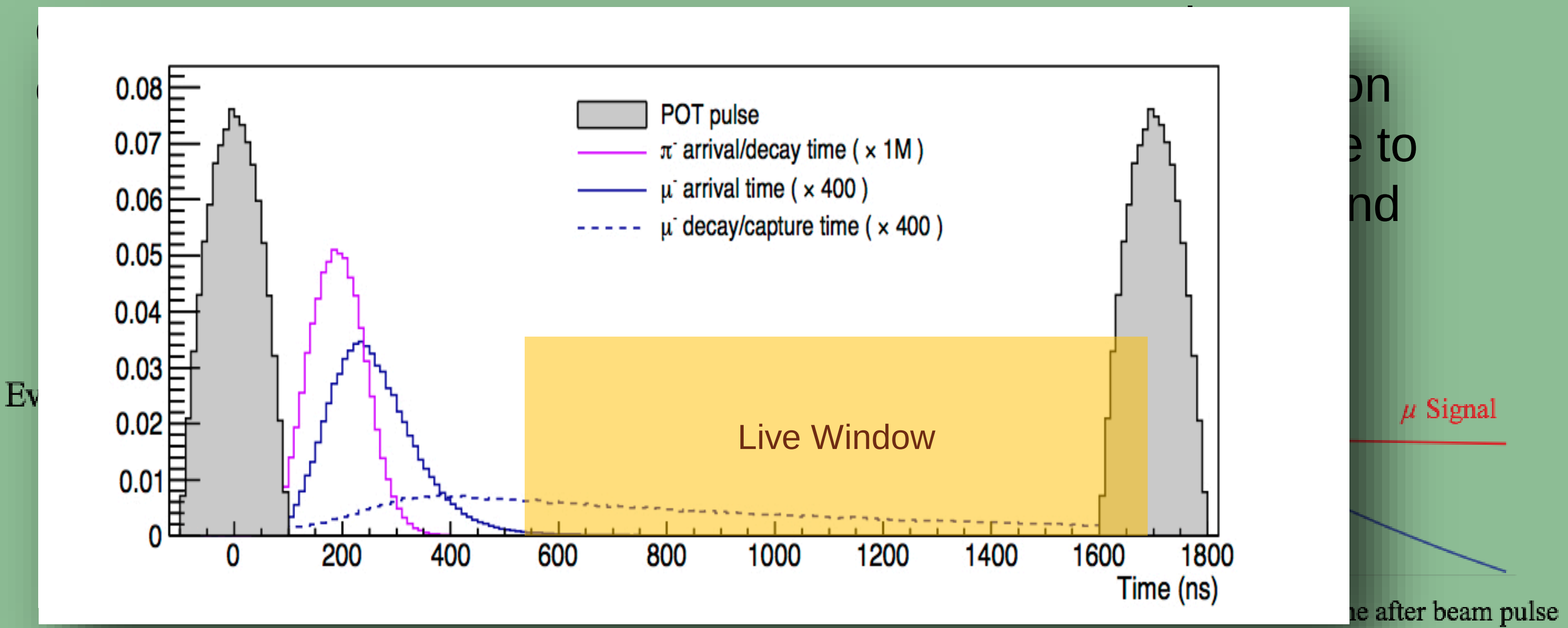

- $\mu \rightarrow e$ conversion experiments need a pulsed μ^- beam, such as FNAL or J-PARC
  - many (prompt) pion-induced backgrounds immediately after the

CW operation optimizes the S/N

Pulsed operation optimizes the S/N

MEG upgrade signal and backgrounds

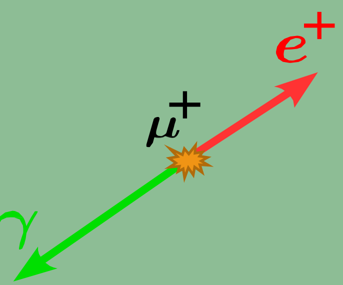

$\mu^+ \to e^+\gamma$

CLFV signal

$\propto R_\mu$

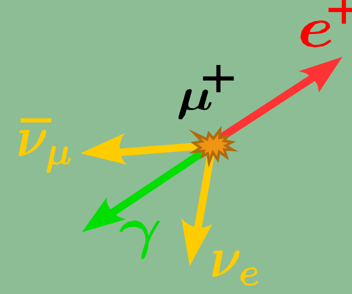

$\mu^+ \to e^+\bar{\nu}_\mu\nu_e\gamma$

Radiative muon decay

correlated $\propto R_\mu$

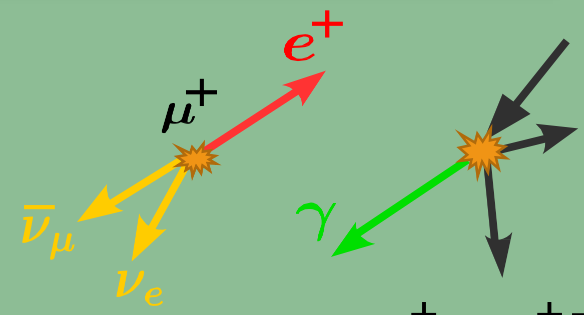

$\mu^+ \to e^+\bar{\nu}_\mu\nu_e$

$\mu^+ \to e^+\bar{\nu}_\mu\nu_e\gamma$
$e^+e^- \to \gamma\gamma$
$e^+N \to e^+N\gamma$

Accidental background

uncorrelated $\propto R_\mu^2$

Events are described by five variables: $E_\gamma, E_e, t_{e\gamma}, \theta_{e\gamma}, \phi_{e\gamma}$

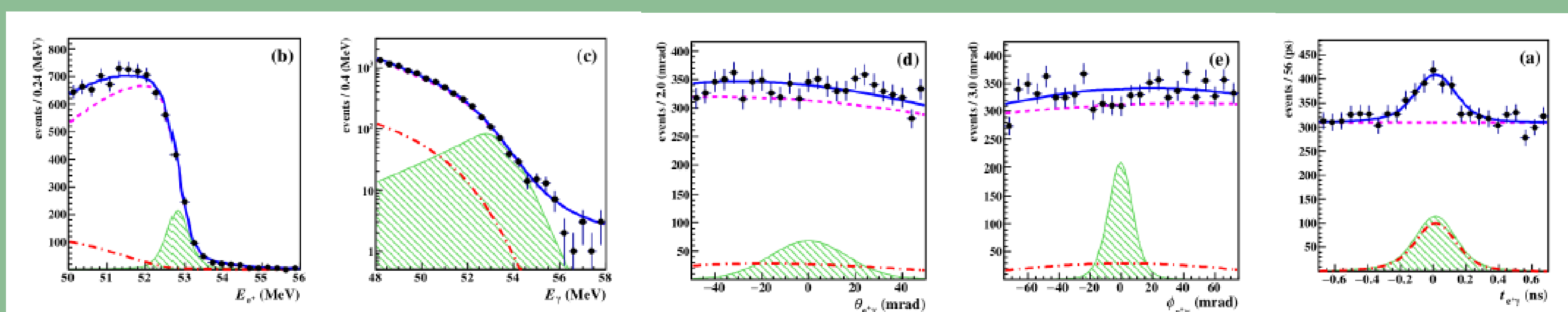

MEG backgrounds

- Backgrounds are proportional to: $\left(\frac{R_\mu}{D}\right)\left(\Delta t_{e\gamma}\right)\left(\frac{\Delta E_e}{m_\mu/2}\right)\left(\frac{\Delta E_\gamma}{15m_\mu/2}\right)^2\left(\frac{\Delta\theta_{e\gamma}}{2}\right)^2$
  - uncorrelated backgrounds $\propto$ instantaneous rate
  - electron-photon time resolution
  - electron momentum resolution
  - square of photon energy resolution, since background due to the integral of the photon spectrum of $\mu \to e\nu\nu\gamma \sim (1-2E_\gamma/m_\mu)$
  - Square of electron-photon angular resolution
- These considerations dictated the original MEG design and the improvements incorporated in the upgrade

Stop 10^7 muons/sec in 150μ kapton target

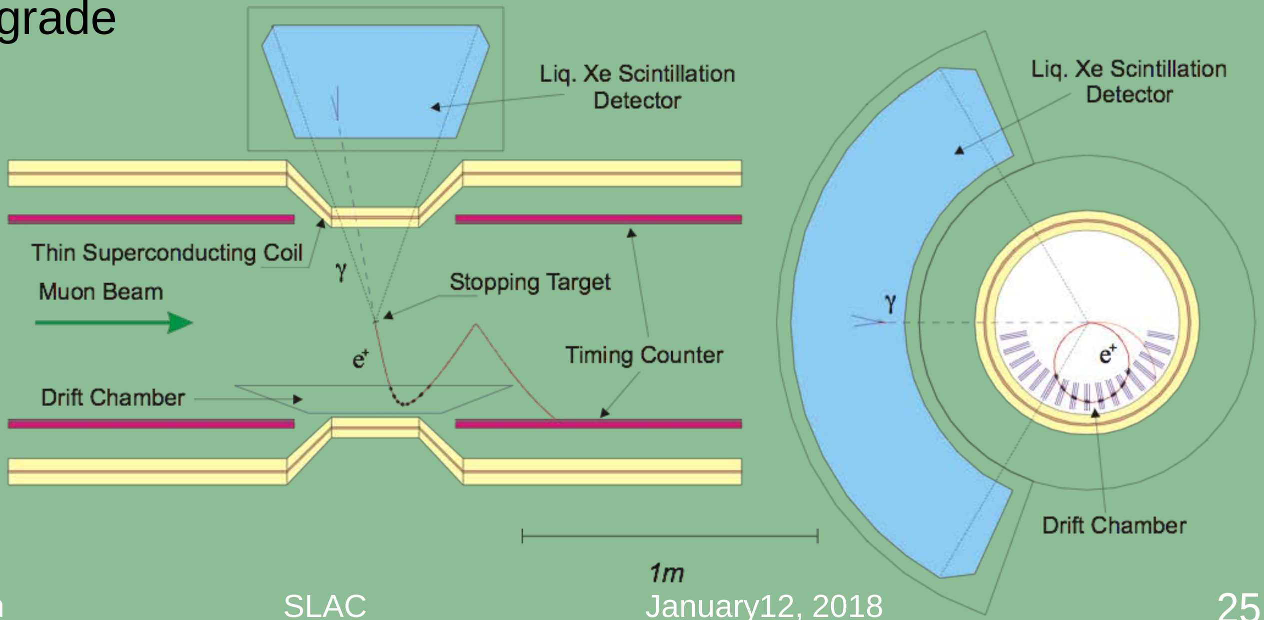

MEG upgrade

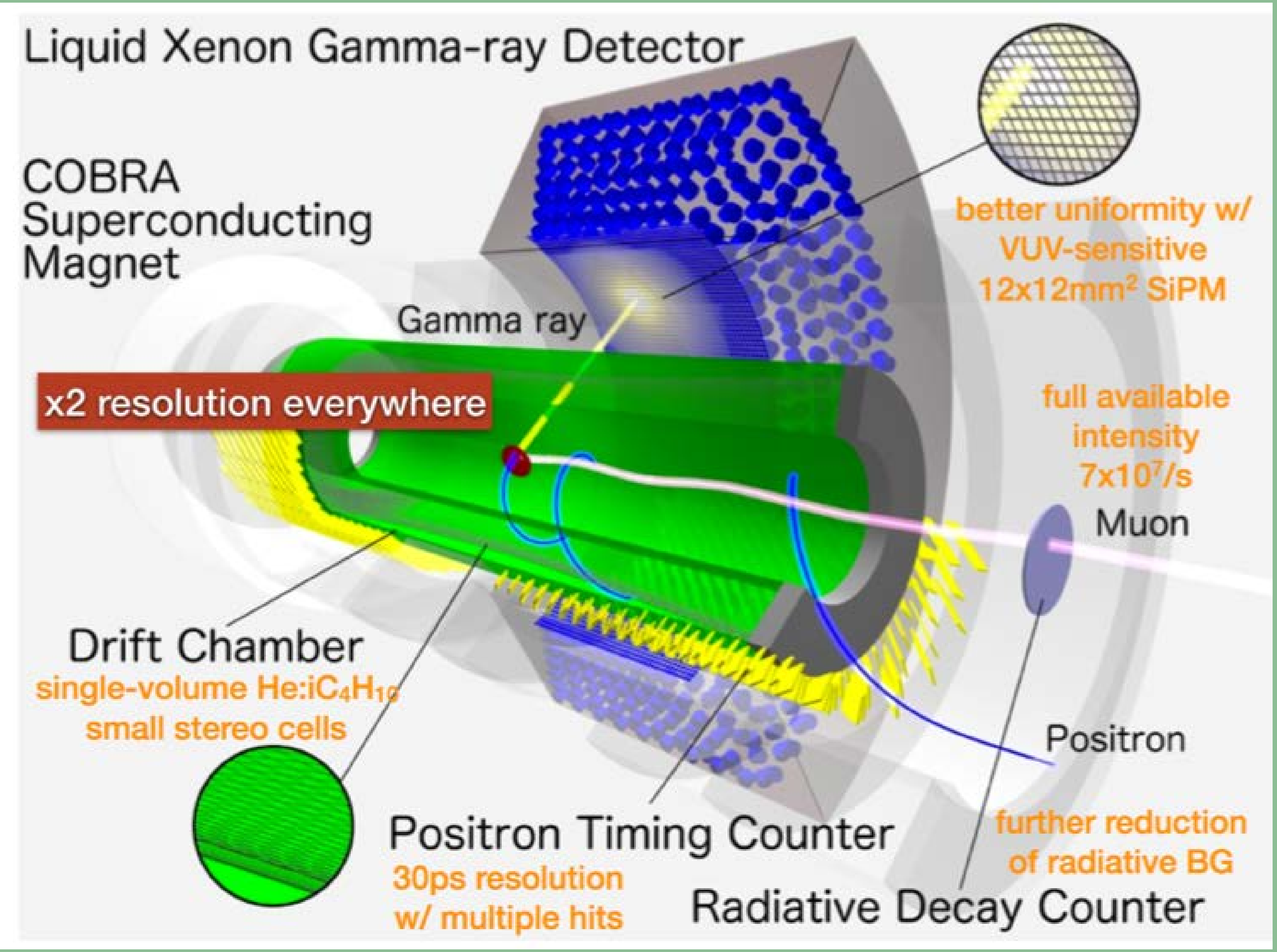
Liquid Xenon Gamma-ray Detector
COBRA Superconducting Magnet
Gamma ray
x2 resolution everywhere
better uniformity w/ VUV-sensitive 12x12mm² SiPM
full available intensity 7x10⁷/s
Muon
Drift Chamber
single-volume He:iC4H10 small stereo cells
Positron
Positron Timing Counter
30ps resolution w/ multiple hits
further reduction of radiative BG
Radiative Decay Counter

MEG upgrade

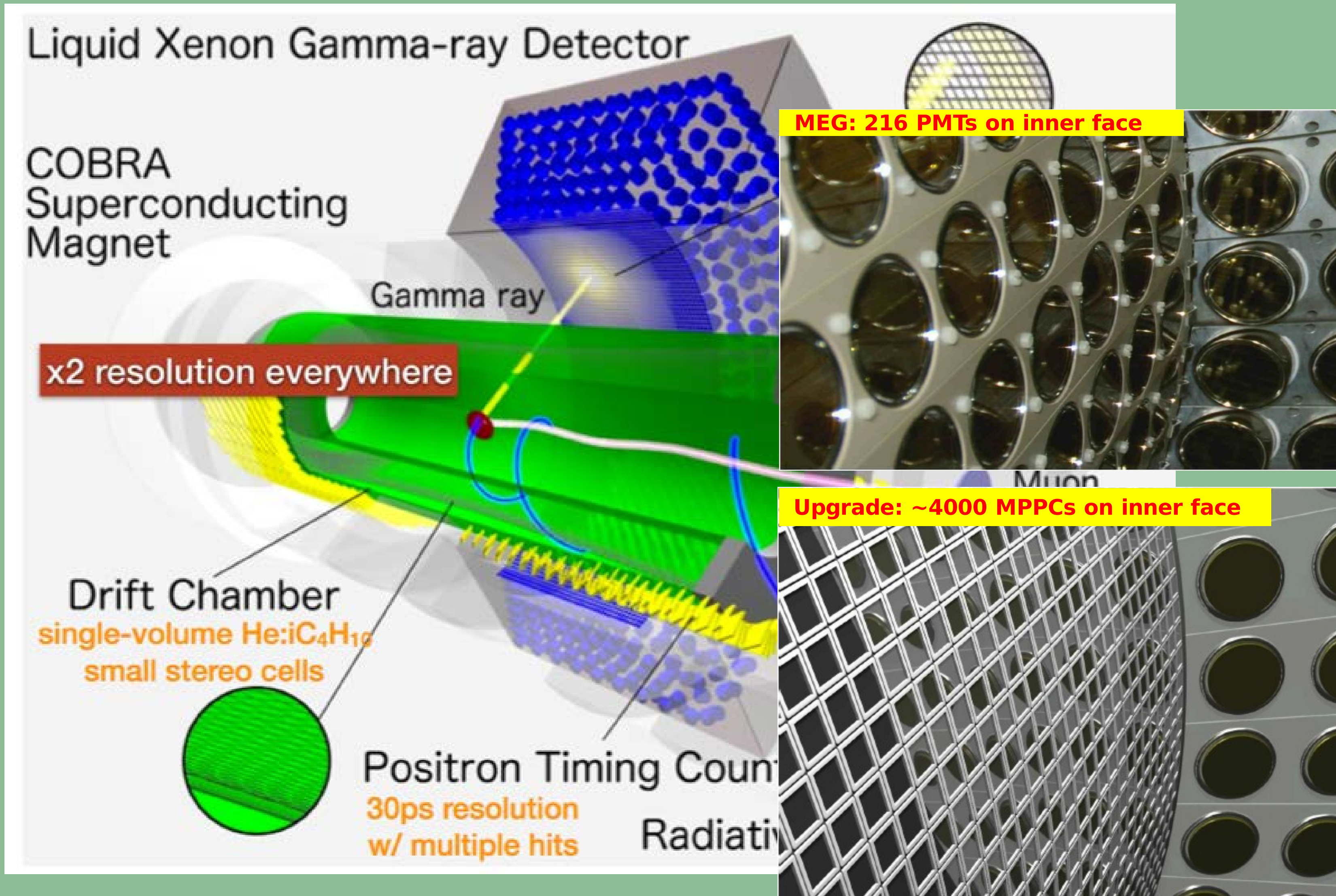
Liquid Xenon Gamma-ray Detector
COBRA Superconducting Magnet
Gamma ray
x2 resolution everywhere
Drift Chamber
single-volume He:iC4H10
small stereo cells
Positron Timing Coun
30ps resolution
w/ multiple hits
Radiati
Muon
MEG: 216 PMTs on inner face
Upgrade: ~4000 MPPCs on inner face

MEG result and upgrade goal

- MEG has the best current limit on $\mathcal{B}(\mu^+ \rightarrow e^+ \gamma)$
- Uses a surface muon beam: DC, $|p_\mu|$ 28 MeV/c, 10^8 μ/s
- With a total of $7.5\text{x}10^{14}$ stopped muons, gathered in runs from 2009 through 2013, they set a 90% CL limit of $< 4.2 \times 10^{-13}$ (Baldini *et al*., Eur.Phys.J. C76434, 2016)
- The MEG Upgrade will improve the detector to achieve a 90% CL limit of $< 5 \times 10^{-14}$ in a three year run

- Upgrade schedule
  - Engineering Run 2017 to test LXe modifications and timing
  - Full Engineering Run July 2018
  - Data Fall 2018
  - Upgrades to PSI to modify the surface beam target station

Mu3e

Signal

$E = m_\mu$
$\Sigma p_i = 0$
Vertex

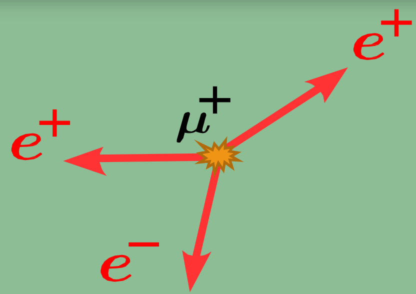

Background

Accidentals

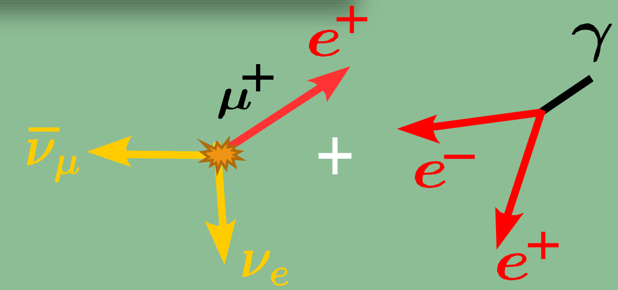

Radiative decay
w internal conversion

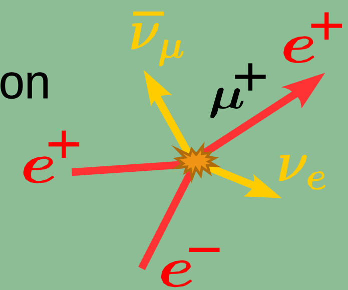

- **Current limit:** 1.0×10^{-12} (SINDRUM at PSI, 1988)
- Mu3e at PSI will provide substantial improvement
  - Uses a surface muon beam - πE5 beamline
  - Phase I
    - 2018 - 10^8 μ^+/s
    - Sensitivity 10^{-15}
  - Phase II HIMB 10^9 μ^+/s
    - Sensitivity 10^{-16}

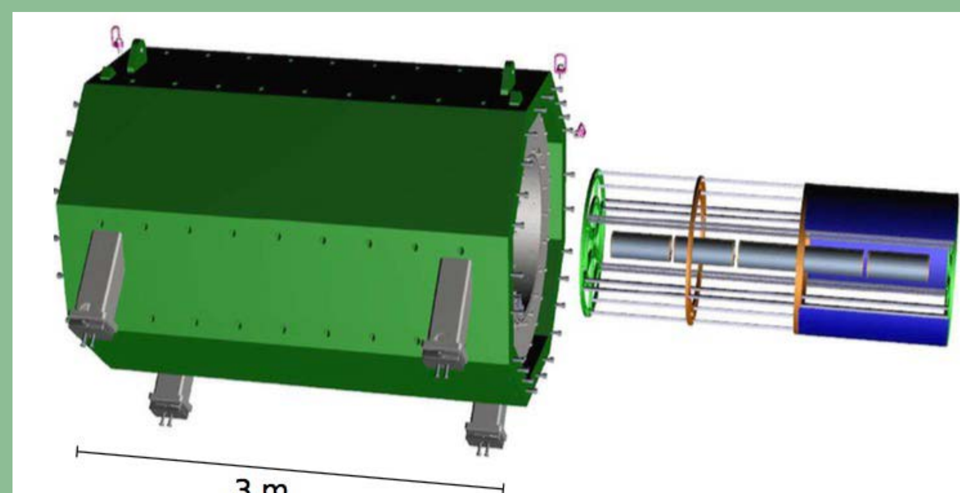

Mu3e detail

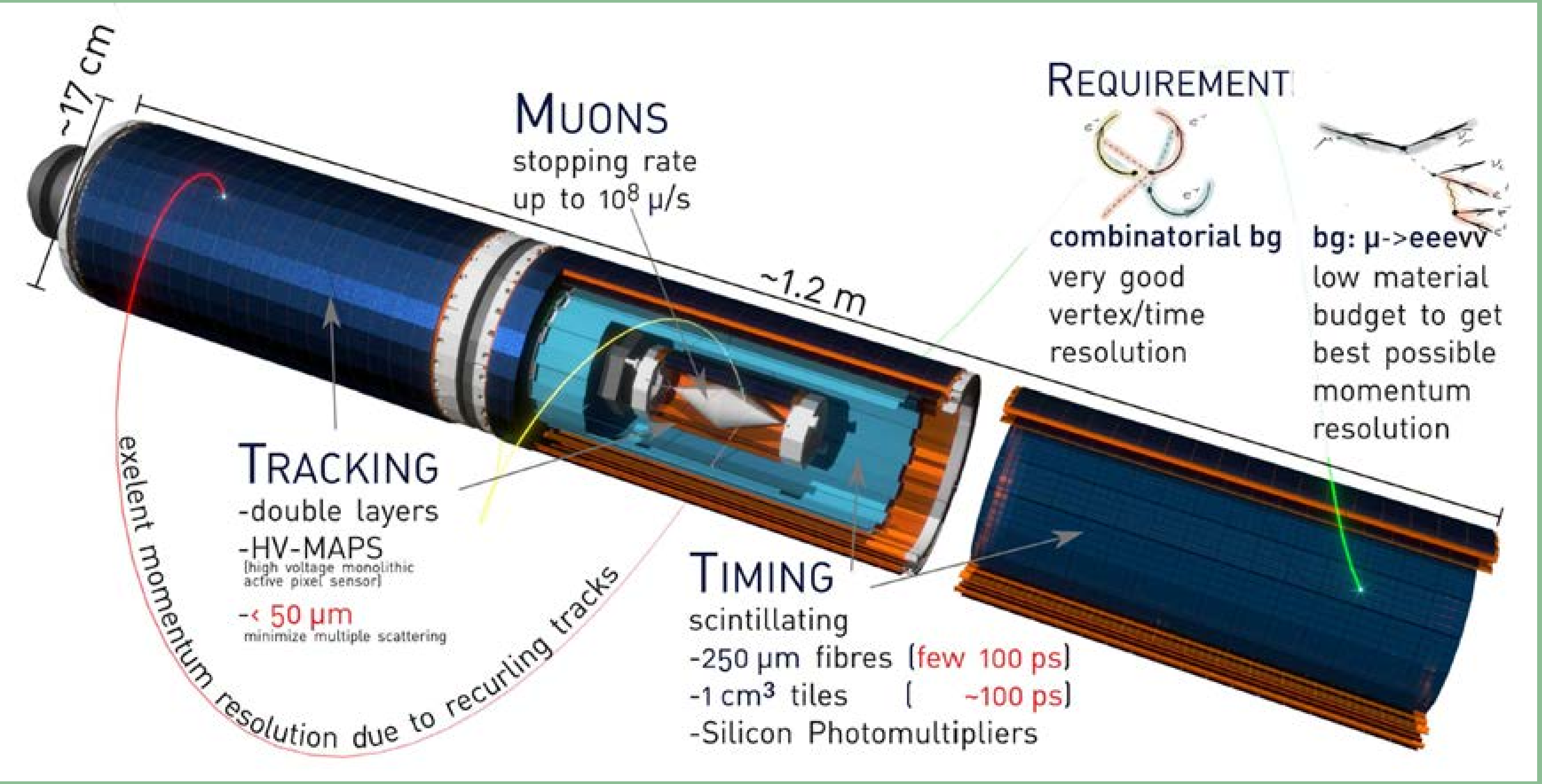

~17 cm
MUONS
stopping rate
up to 10^8 μ/s
~1.2 m
REQUIREMENT
combinatorial bg
very good
vertex/time
resolution
bg: μ->eeeνν
low material
budget to get
best possible
momentum
resolution
TRACKING
-double layers
-HV-MAPS
(high voltage monolithic active pixel sensor)
-< 50 μm
minimize multiple scattering
TIMING
scintillating
-250 μm fibres (few 100 ps)
-1 cm³ tiles (~100 ps)
-Silicon Photomultipliers
exelent momentum resolution due to recurling tracks

Mu3e sensitivity

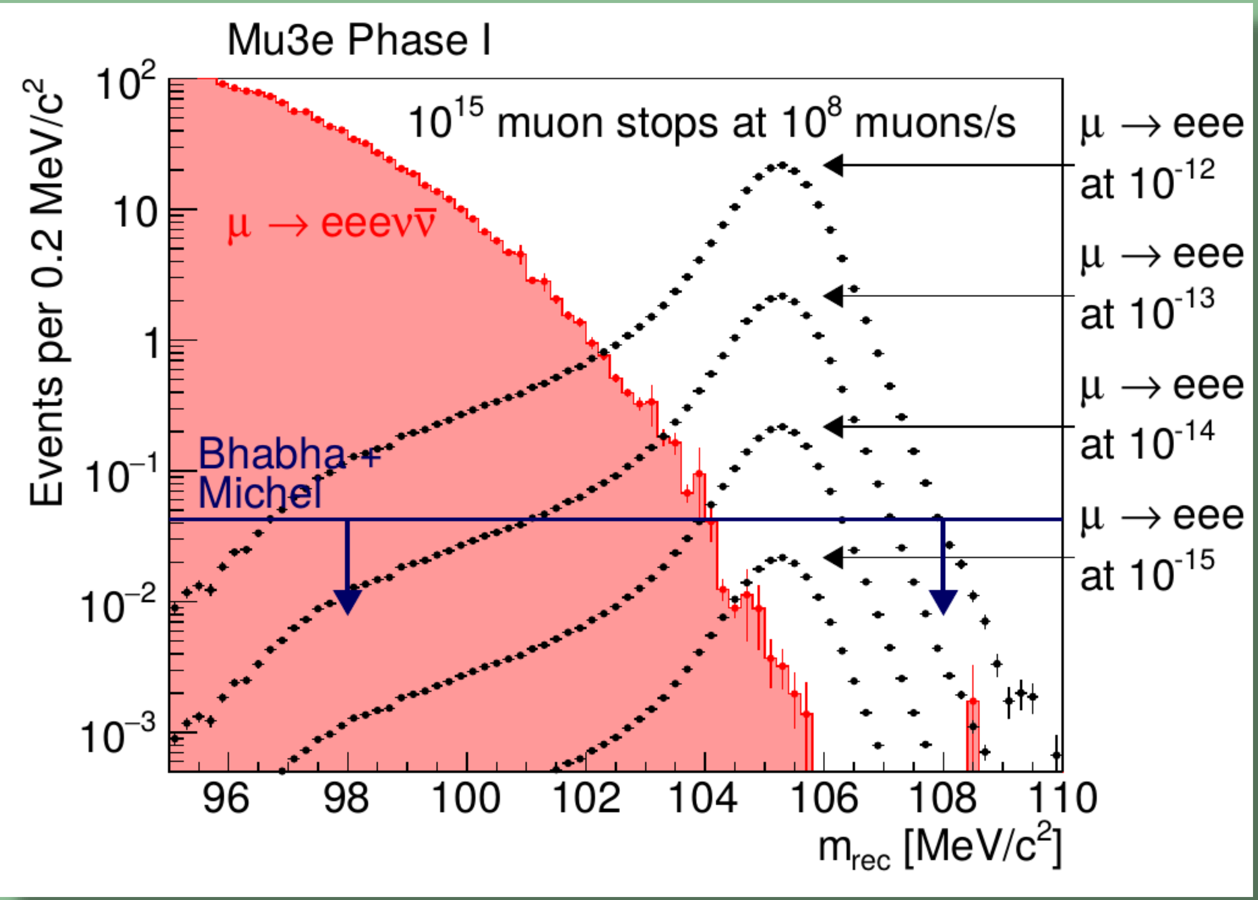

Mu3e sensitivity

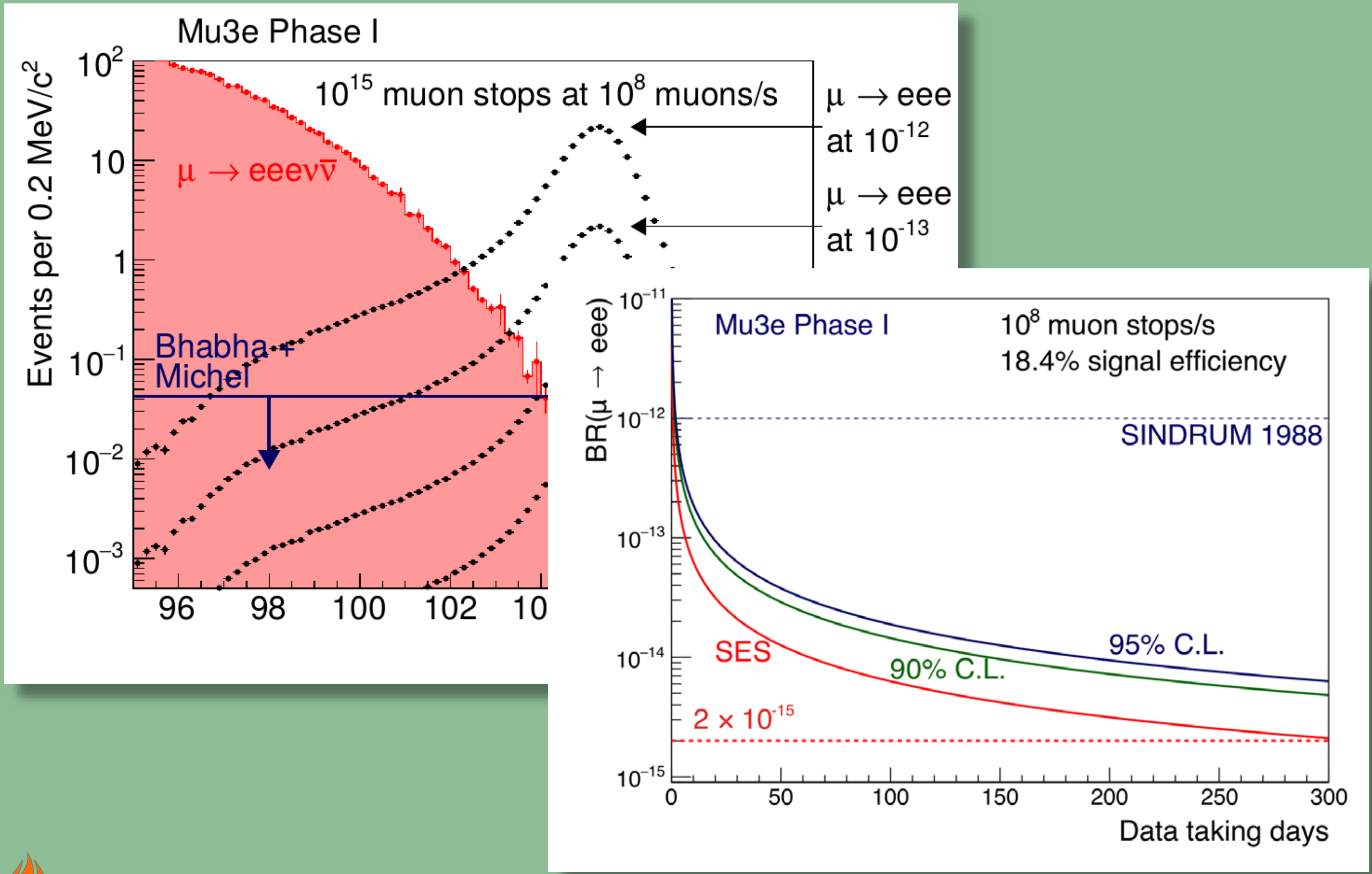

μ to e conversion experiments

- The signal is a single mono-energetic electron
- If N = Al, E_e ~105 MeV
  - electron energy depends on Z, due to atomic binding energy
- Coherent nuclear recoil

$$R_{\mu e} = \frac{\Gamma(\mu^- + N(A,Z) \to e^- + N(A,Z))}{\Gamma(\mu^- + N(A,Z) \to \text{all muon captures})}$$

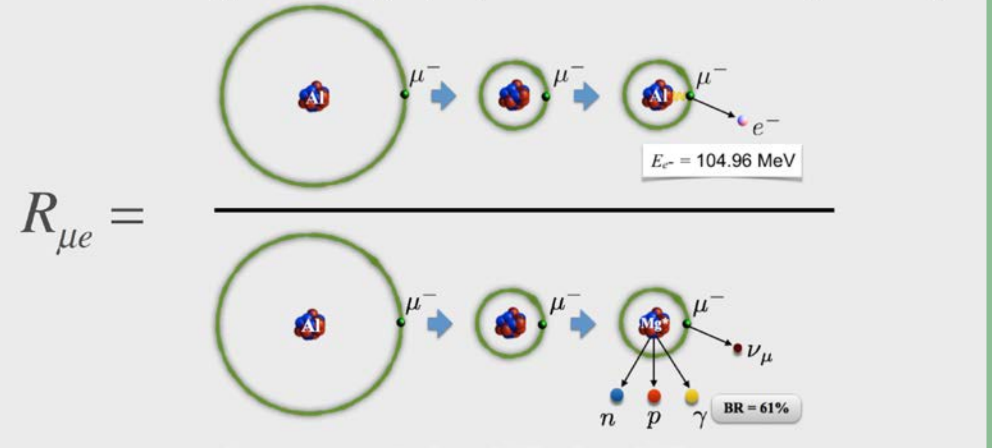

- There are four experiments in various stages of preparation
  - DeeMe
  - COMET Phase I and Phase II
  - Mu2e
  - PRISM/Prime

  } Origins trace to MELC and MECO proposals

      - All face similar challenges, addressed in specific ways
        - High rates to achieve required sensitivity
        - Prompt and delayed beam-related backgrounds
        - Cosmic ray backgrounds

$\mu \rightarrow e$ experiment schematic

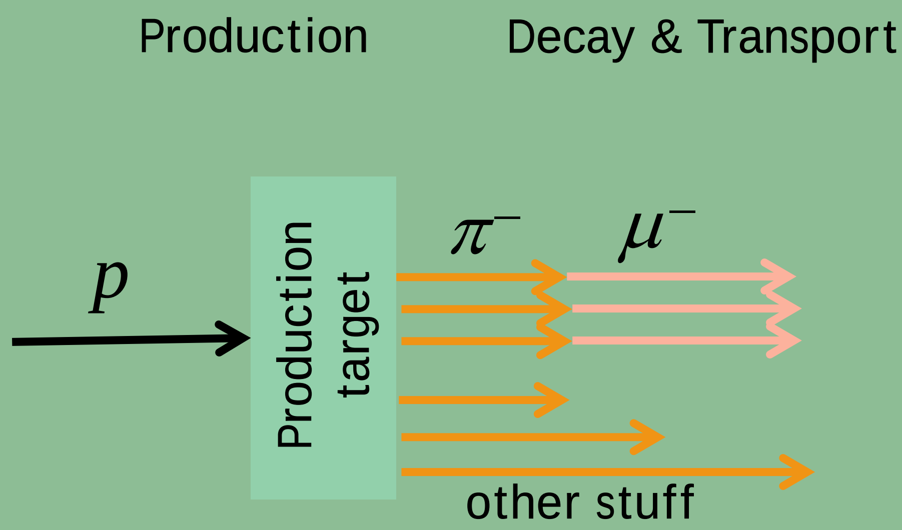

1) Generate a beam of low momentum negative muons

$\mu \rightarrow e$ experiment schematic

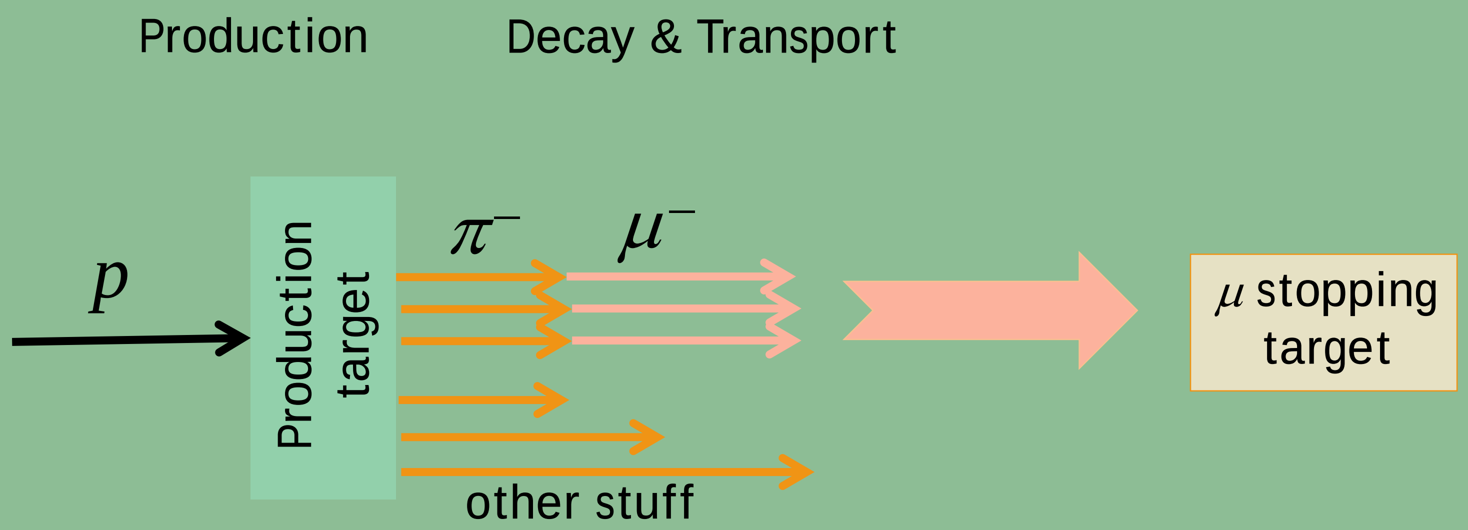

1) Generate a beam of low momentum negative muons
2) Stop the muons in a target (C, SiC, Al, Ti, …..)

$\mu \to e$ experiment schematic

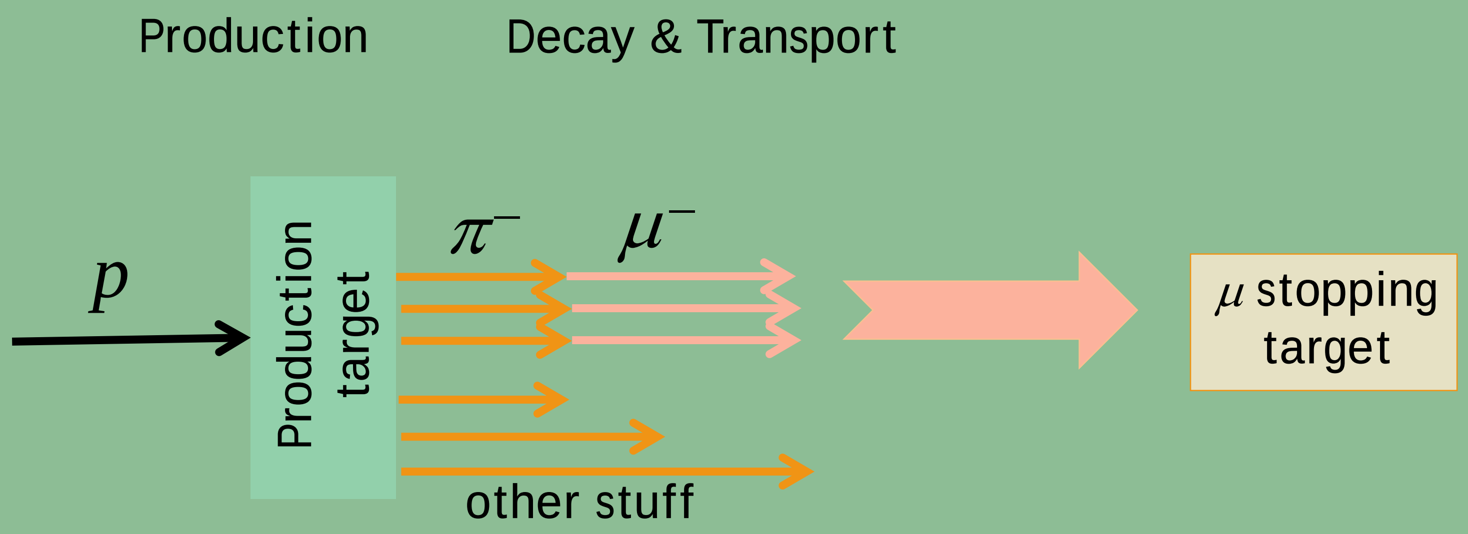

1) Generate a beam of low momentum negative muons
2) Stop the muons in a target (C, SiC, Al, Ti, …..)
   - In orbit around nucleus: τ_{μ}^{Al} = 864 ns
   - Large τ_{μ}^{N} is important for discriminating background

$\mu \rightarrow e$ experiment schematic

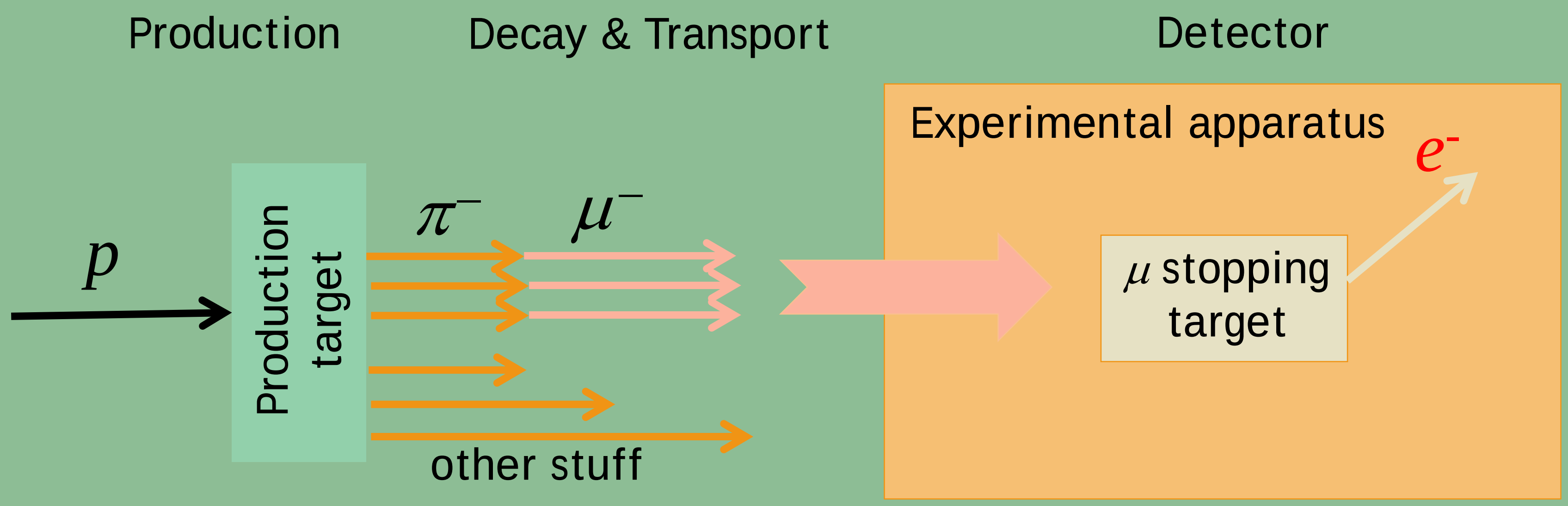

1) Generate a beam of low momentum negative muons
2) Stop the muons in a target (C, SiC, Al, Ti, …..)
3) Search for events consistent with $\mu N \rightarrow eN$
4) Discriminate against backgrounds from pion decays and interactions, muon decays in orbit (DIOs), radiative decays and cosmic rays

Decay-in-Orbit Shape

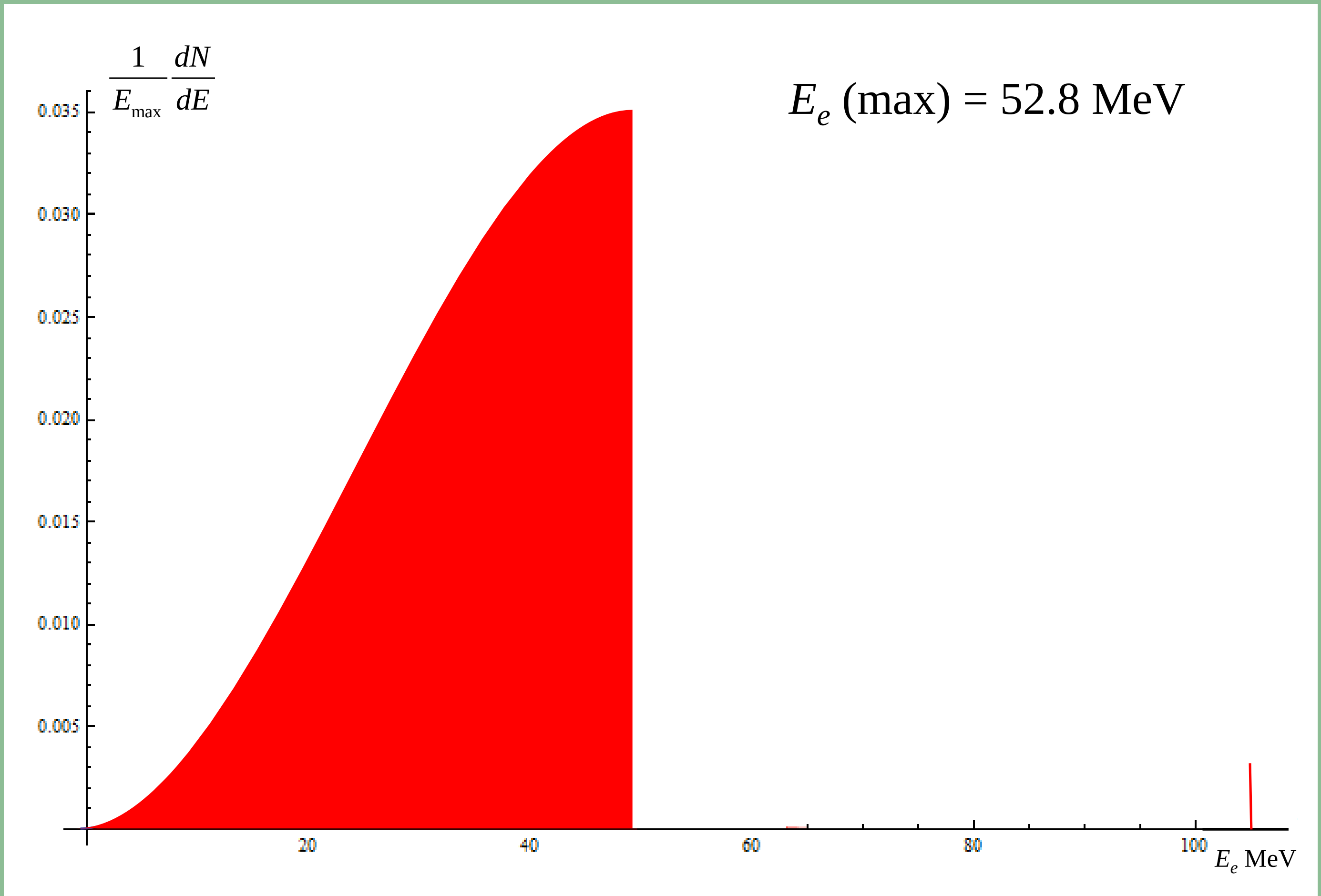

Decay-in-Orbit Shape

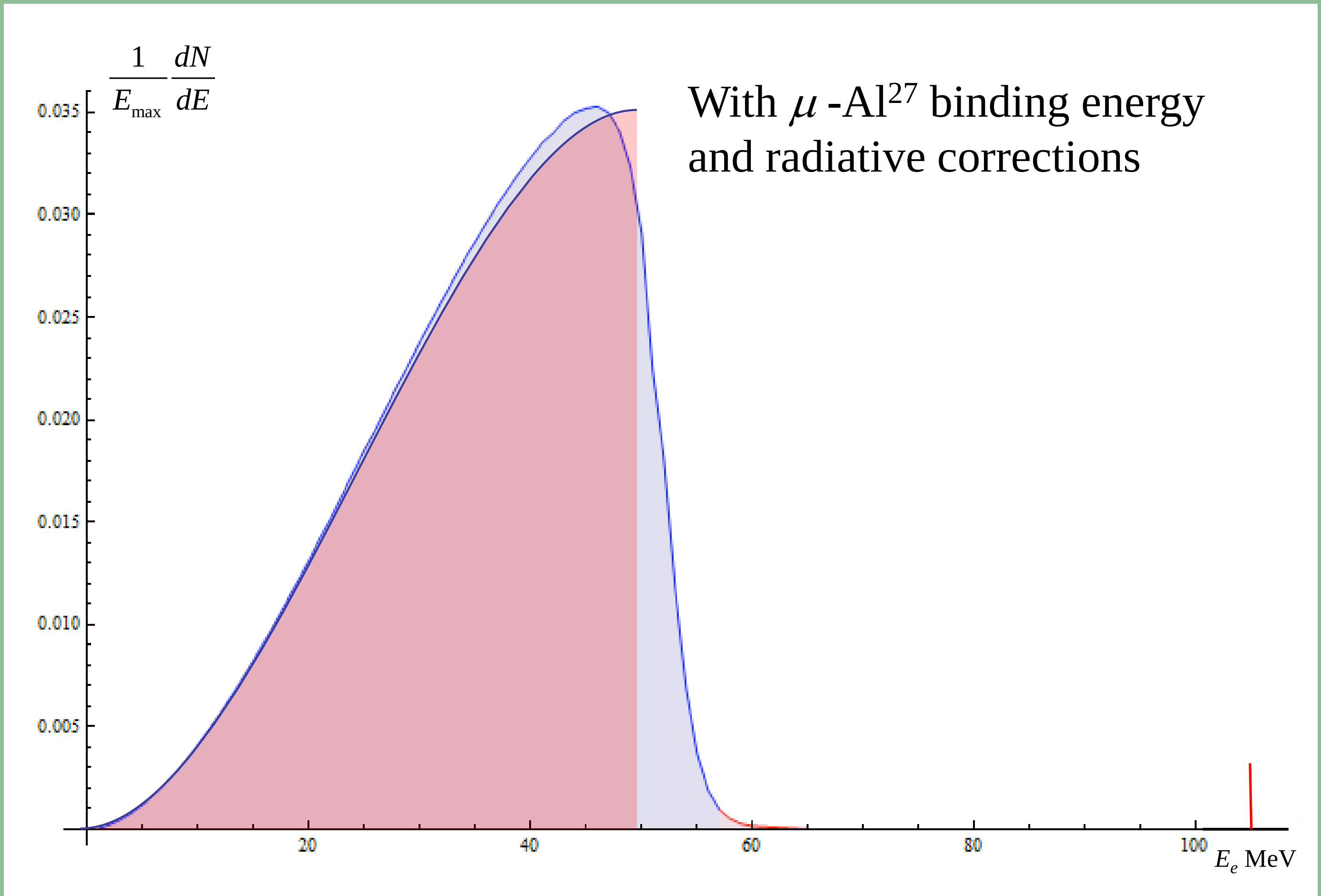

Czarnecki
Szafron

Decay-in-Orbit Shape

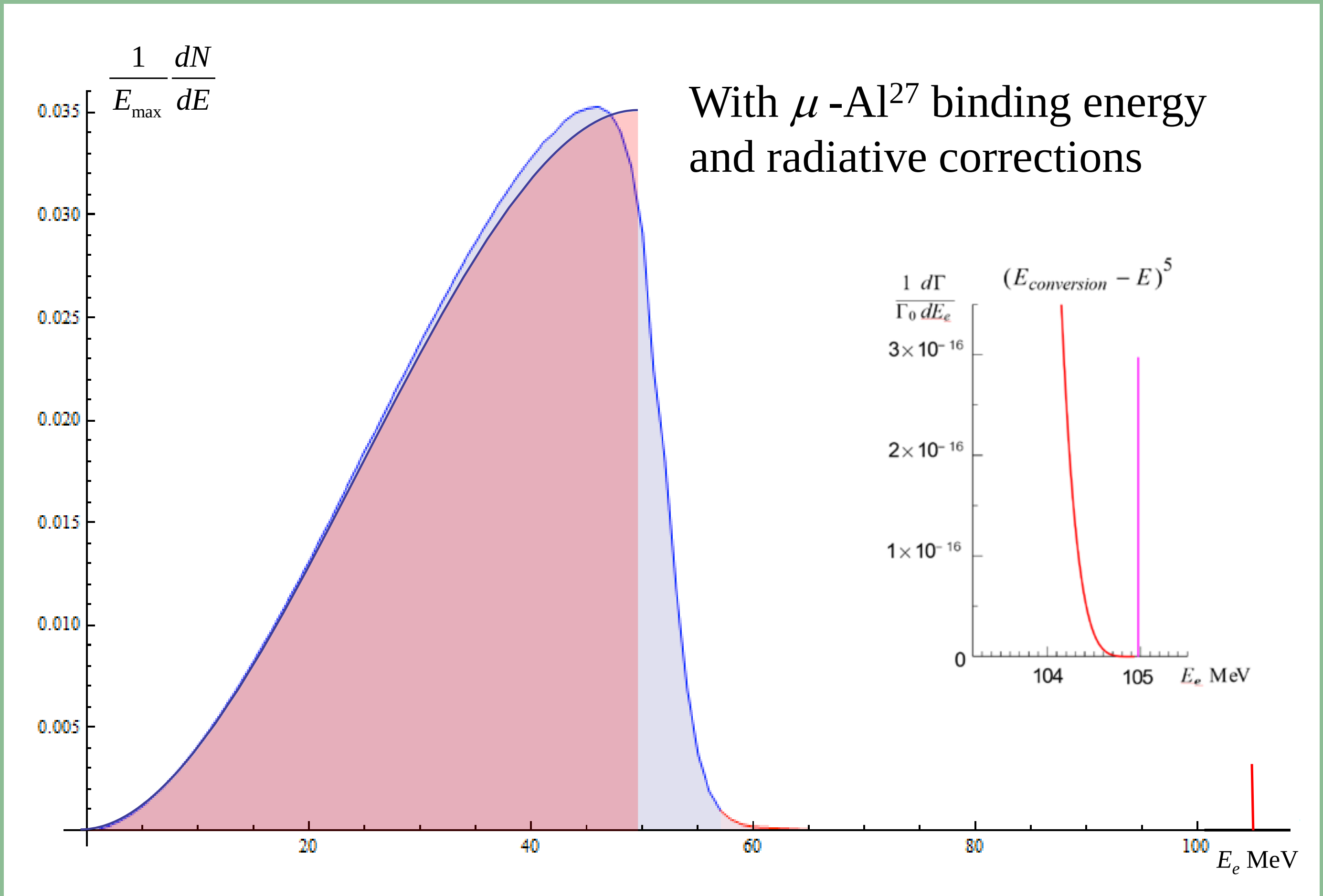

Czarnecki
Szafron

DeeMe

- Directly search for $\mu \rightarrow e$ conversion in a high power target
  - High power, high purity proton beam from MLF at J-PARC
  - initially a graphite target, then a rotating SiC target
  - production and conversion target are the same

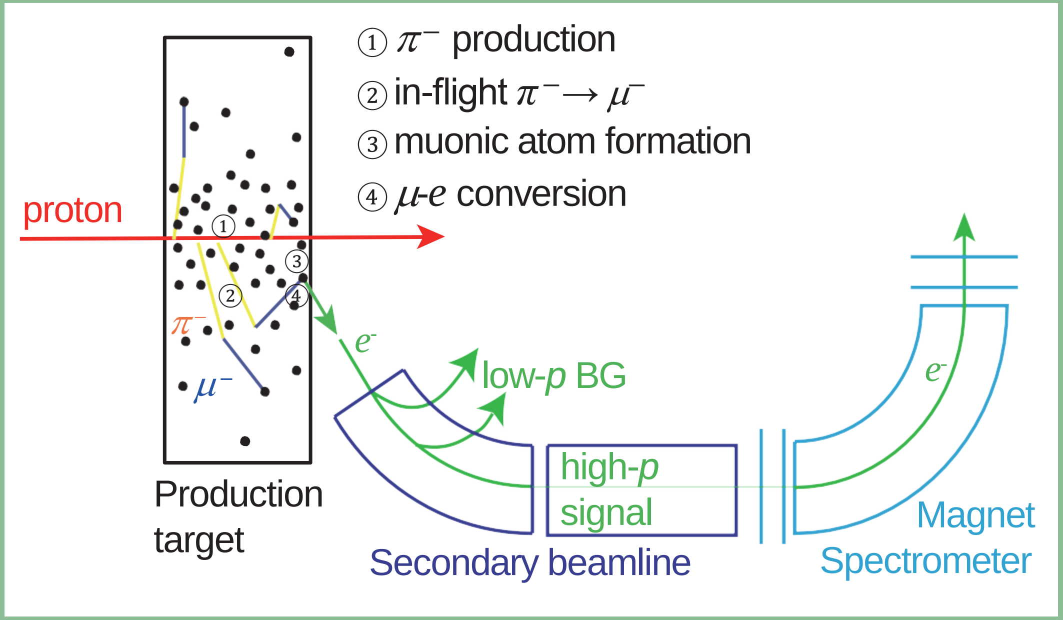

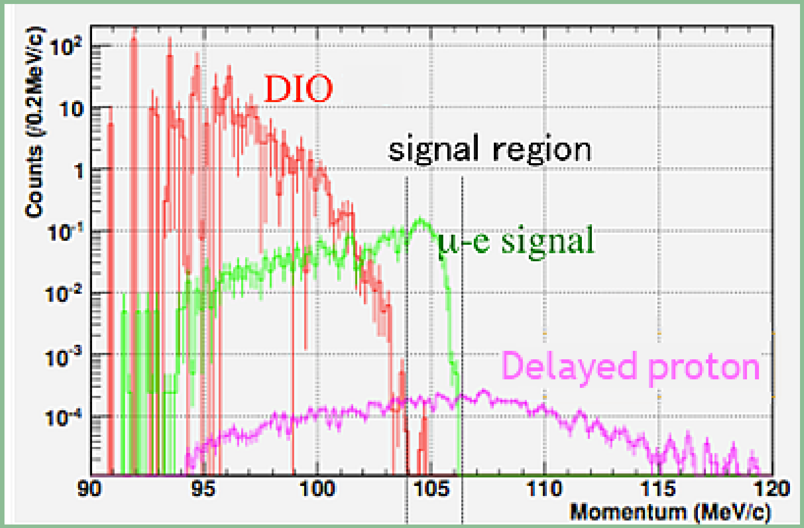

- Single event sensitivity (1 year = 2×10^{7} sec) with 1MW beam
  - 1.2×10^{-13}
  - 2.5×10^{-14} (4 years)

Upgrade to SiC

- 2.1×10^{-14}
- 5×10^{-15} (4 years)

DeeMe status

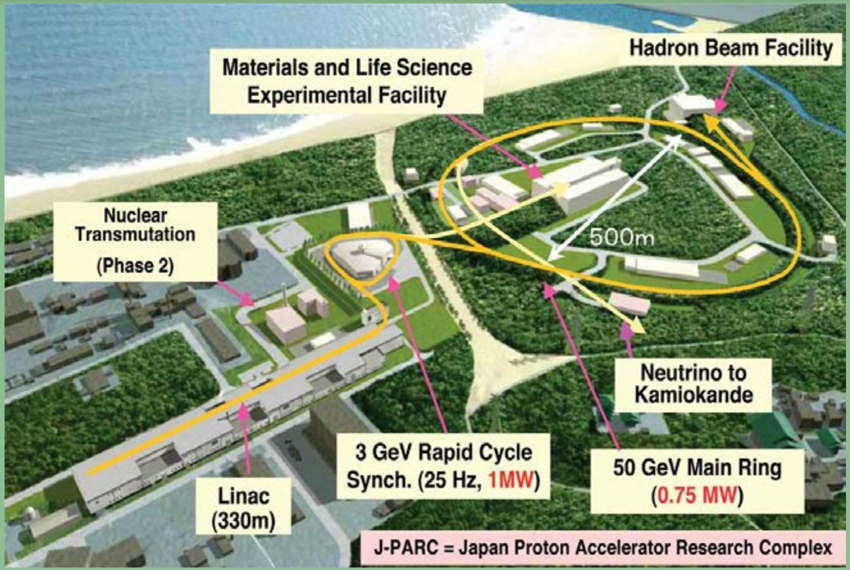

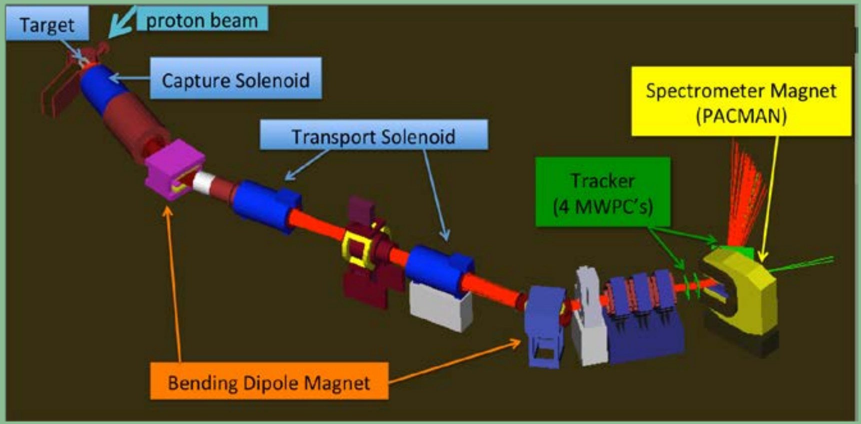

- Will start with graphite target
- Detector components built
- Beamline (to be shared with other experiments such as *g*-2 scheduled for 2018
- PACMAN spectrometer magnet moved from TRIUMF

Mu2e

- The Mu2e sensitivity goal 2.6 x 10^{-17} demands a total of ~ 6x10^{17} stopped muons in a 3 year run of ~ 6x10^{7} second total
- This requires a muon stopping rate of 10^{10}/sec

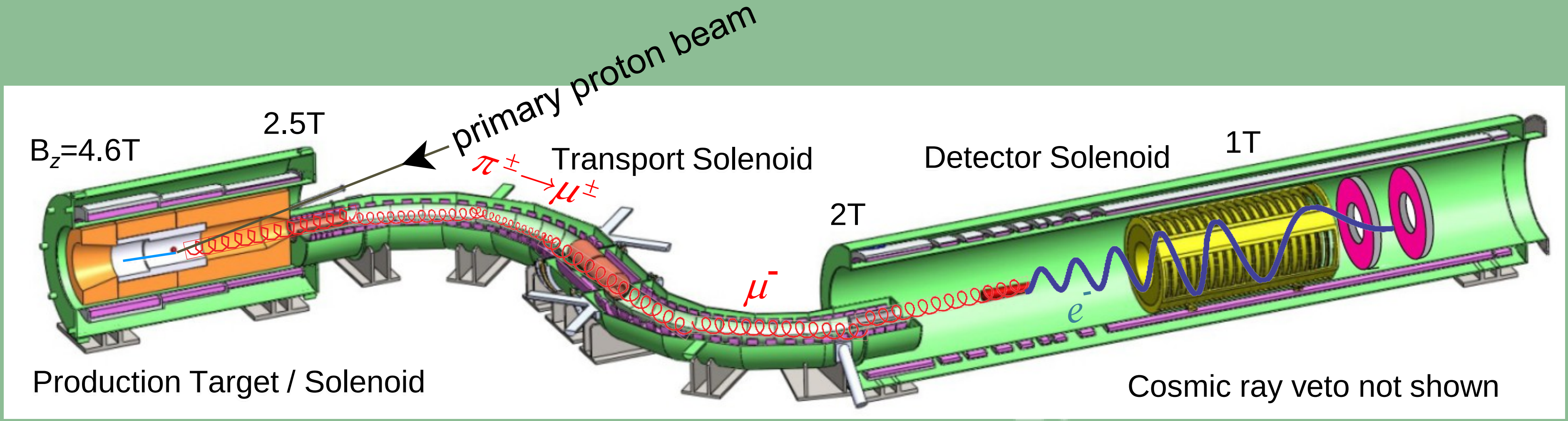

- Experimental design
  - Pulsed proton beam produce pions, which are captured in the backward direction
  - Transport muons from pion decay, with momentum and sign selection
  - Since electron backgrounds are at lower momentum than the sought conversion electrons, confine lower momentum particles to smaller helical radii in a solenoid and a provide hole in tracker and calorimeter for them to pass through
  - Reject cosmic ray events

The Muon Campus at Fermilab

The Muon Campus at Fermilab

The Collaboration in the Mu2e hall

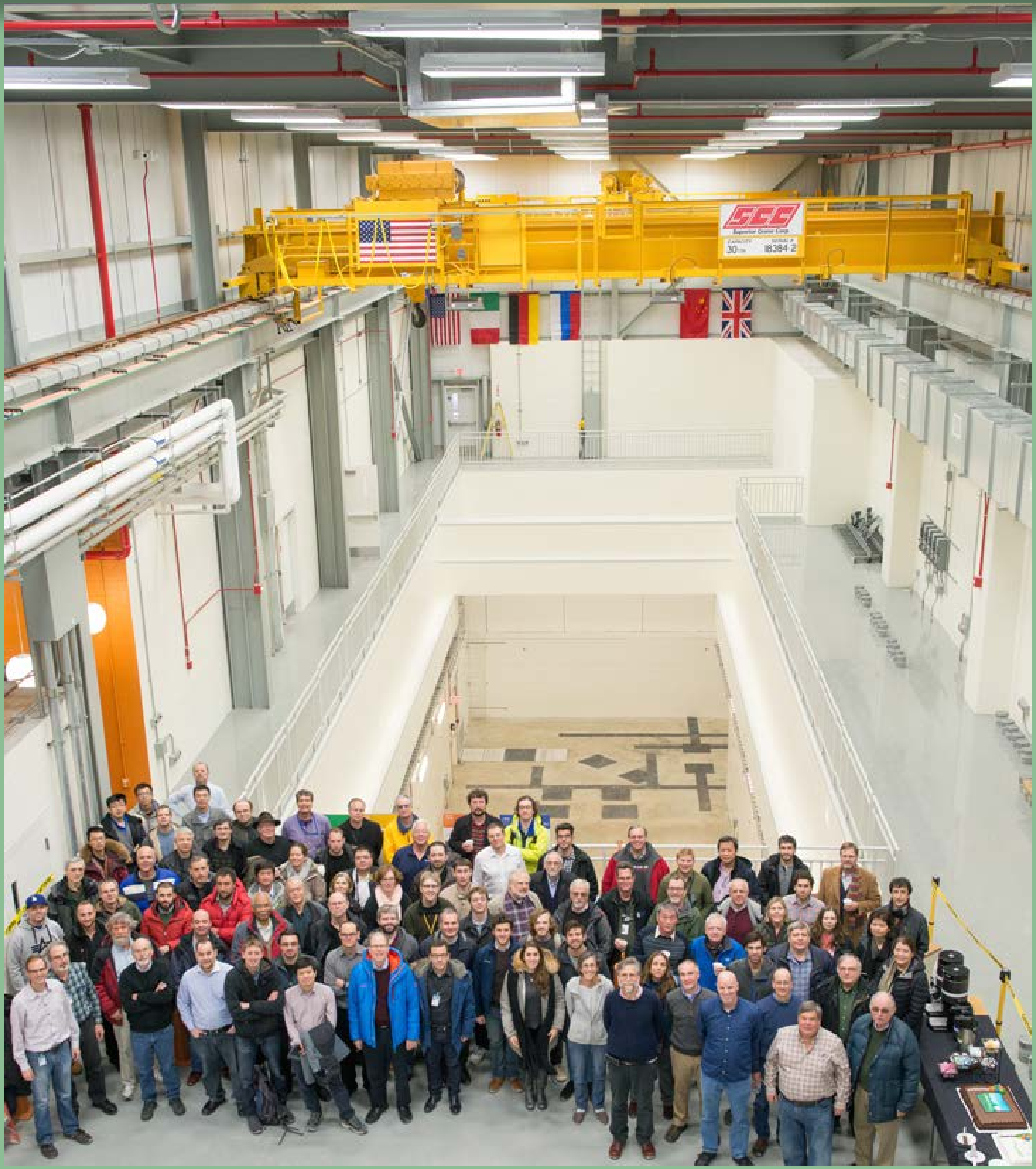

Beamline + detector layout

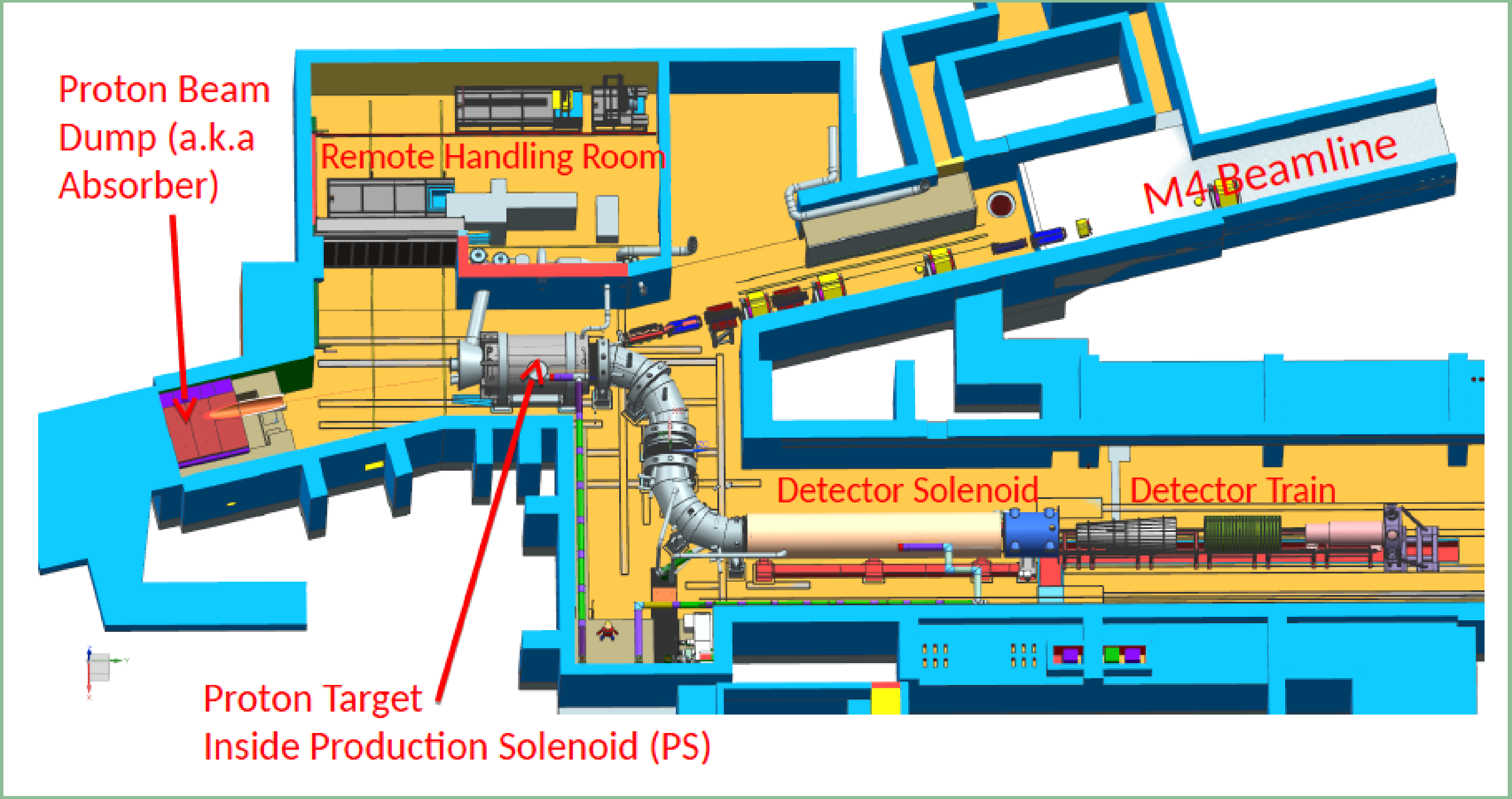

The Mu2e experiment

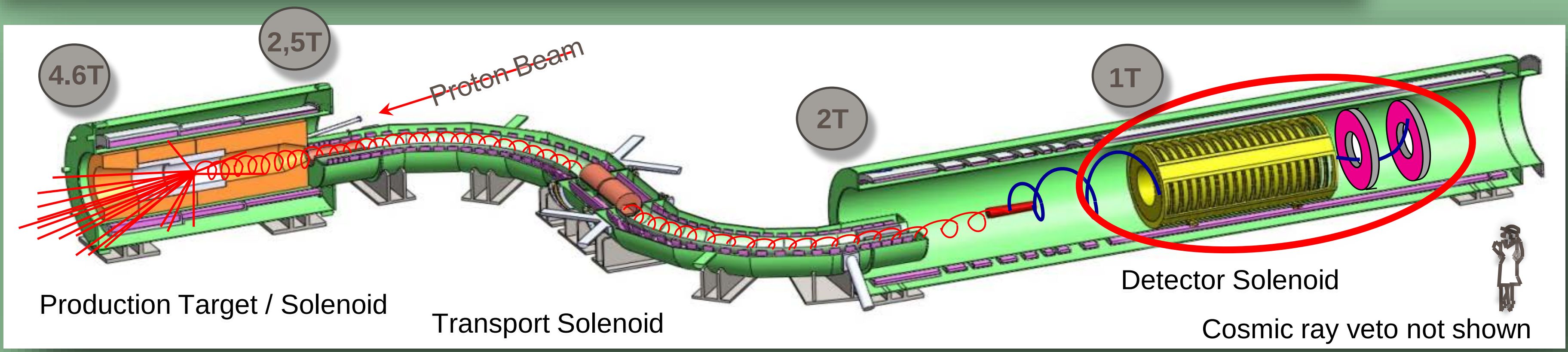

- The sensitivity goal demands a total of ~ 6×10^{17} stopped muons in a 3 year run of ~ 6×10^{7} sec This requires a muon stopping rate of 10^{10}/sec, placing demands on the detector technologies

Tracker requirements:

Momentum resolution σ_p/p < 180 keV/c at 105 MeV
Adequate rate capability:
20 kHz/cm^2 in live window
Tolerate beam flash rate of 3 MHz/cm^2
Have dE/dx capability to distinguish electrons from protons
Operate in a 1T magnetic field in a 10^{-4} Torr vacuum
Provide maximum acceptance for conversion electrons at 105 MeV

Calorimeter requirements:

Energy resolution $\sigma_E/E \sim \mathcal{O}(5\%)$ at 105 MeV
Time resolution $\sigma(t)$ < 500 ps
Position resolution < 1 cm
Adequate rate capability
Operate in a 1T magnetic field in a 10^{-4} Torr vacuum
Redundant photosensors and DAQ
Survive in the neutron (10^{12} n/cm^2) and gamma (100 krad) radiation environment of Mu2e
Provide close to full acceptance for conversion electrons at 105 MeV

What happens during a microbunch ?

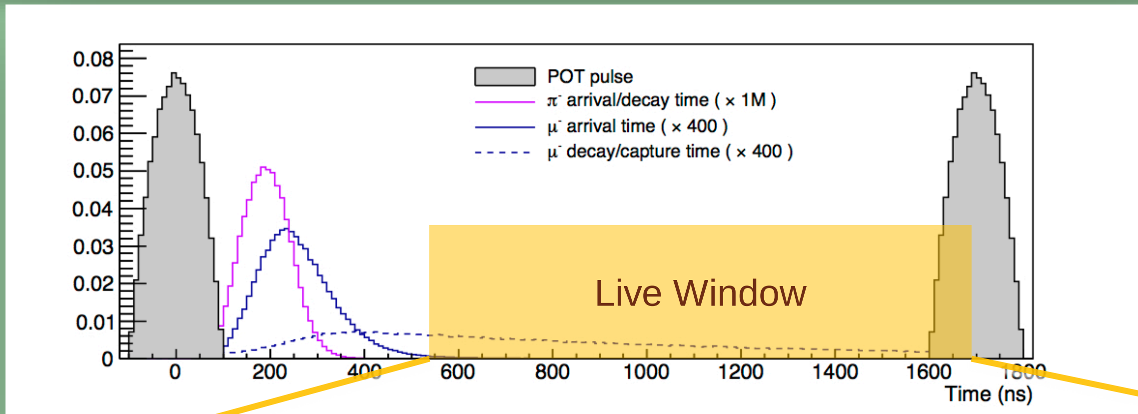

Use of pulsed proton beam and a delayed live gate allows suppression of prompt backgrounds by many orders of magnitude

Proton pulses must be narrow

Out-of-time protons must be suppressed by $\mathcal{O}(10^{10})$

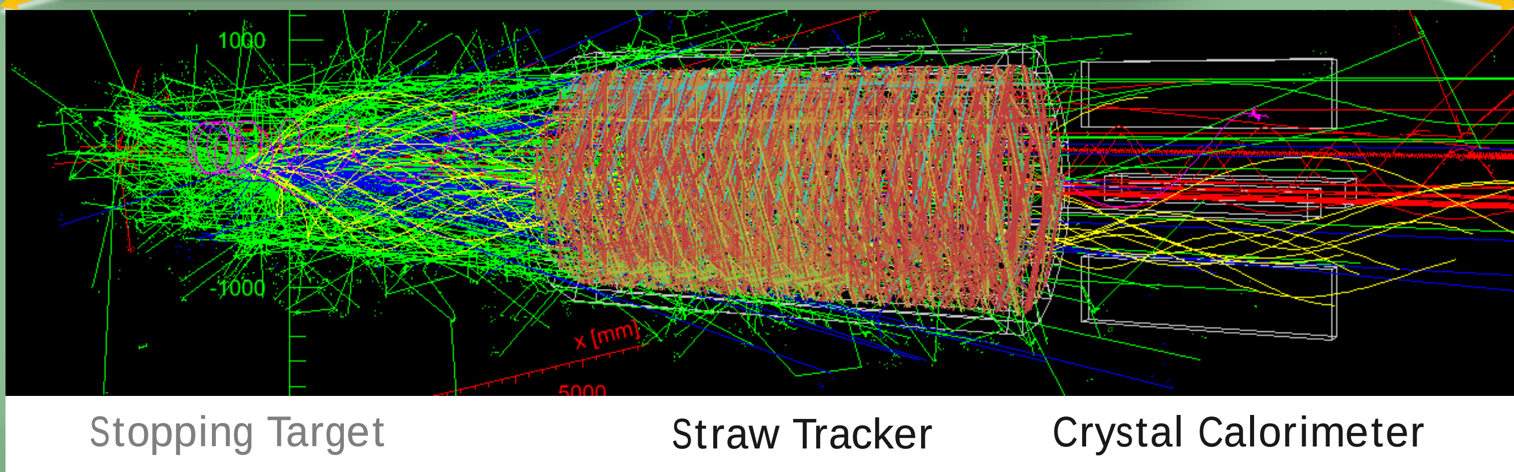

- Simulations encompass a full ~1μs, including all the background overlays from the beam flash, μ capture products, neutrons, *etc*. and properly account for contributions from previous bunches.

What happens during a microbunch ?

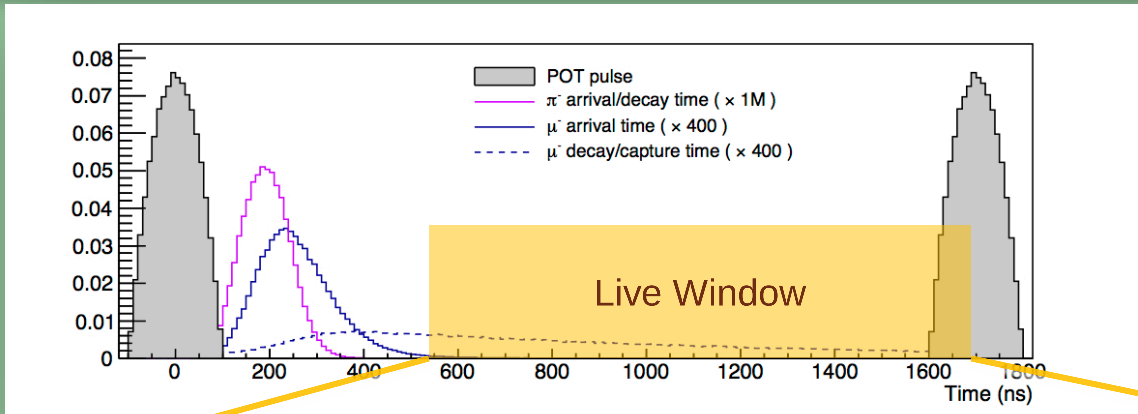

Use of pulsed proton beam and a delayed live gate allows suppression of prompt backgrounds by many orders of magnitude

Proton pulses must be narrow

Out-of-time protons must be suppressed by $\mathcal{O}(10^{10})$

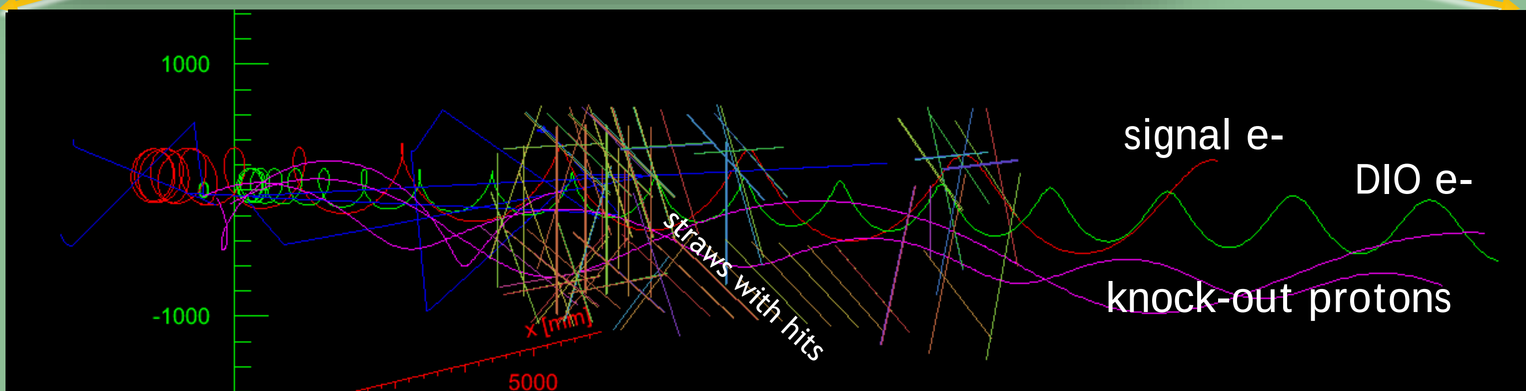

(particles with hits within +/-40 ns of signal electron t_{mean})

- Simulations encompass a full ~1μs, including all the background overlays from the beam flash, μ capture products, neutrons, *etc*. and properly account for contributions from previous bunches.

Tracker and calorimeter design

Both have a central hole to allow DIOs and beam flash events to pass through

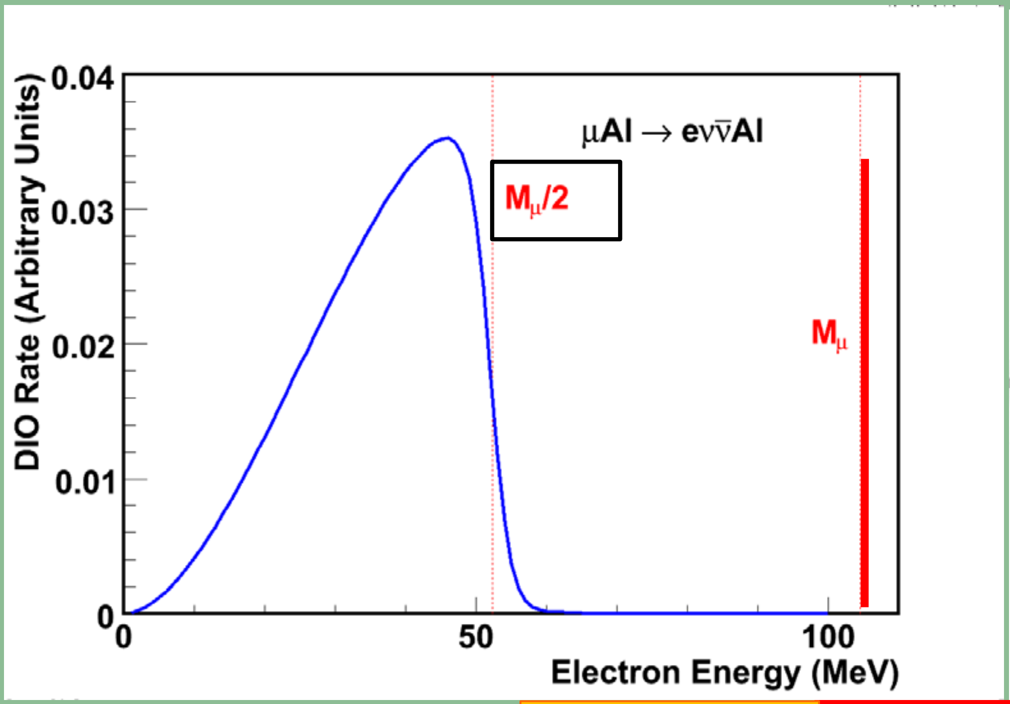

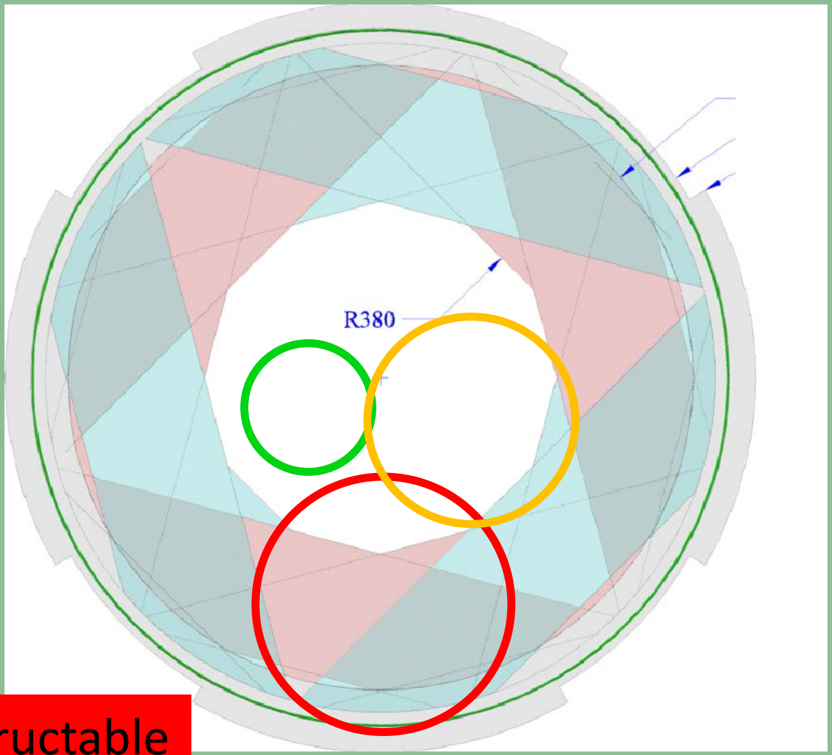

no hits in tracker	some hits in tracker, tracks not reconstructable	reconstructable Tracks

Tracker and calorimeter design

Both have a central hole to allow DIOs and beam flash events to pass through

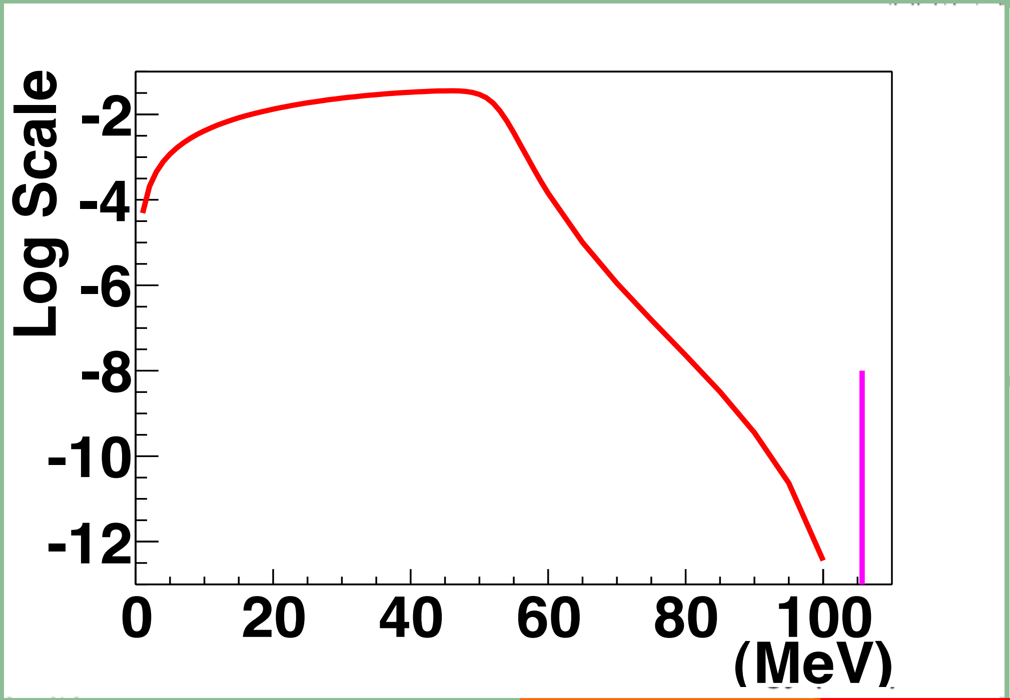

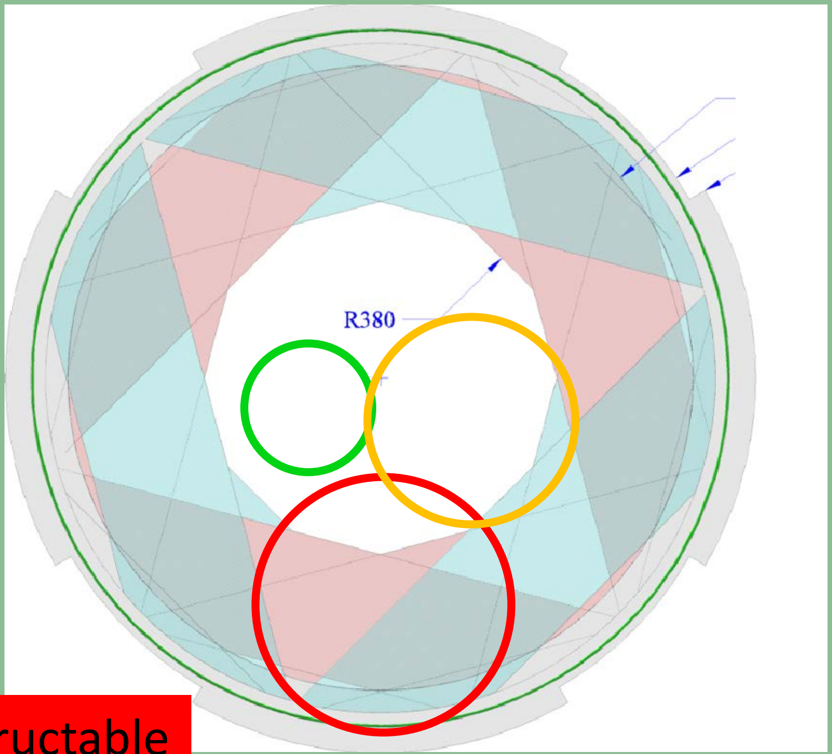

no hits in tracker	some hits in tracker, tracks not reconstructable	reconstructable Tracks

Tracker : straws ⇨ panels ⇨ planes

Straws: 5 mm OD; 15 μm metalized mylar wall

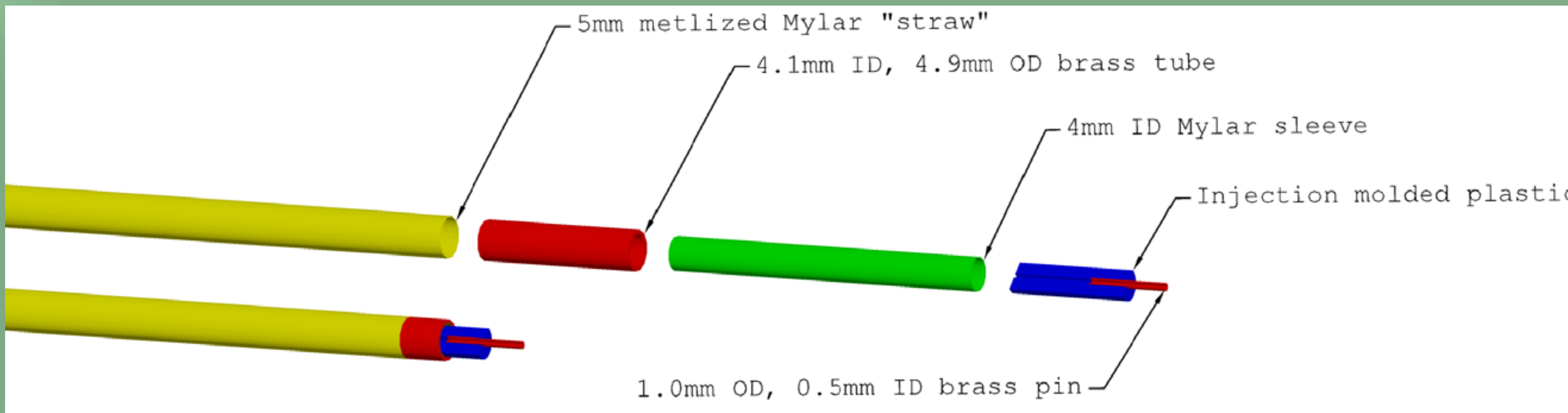

Panel: 2 layers, 48 straws each

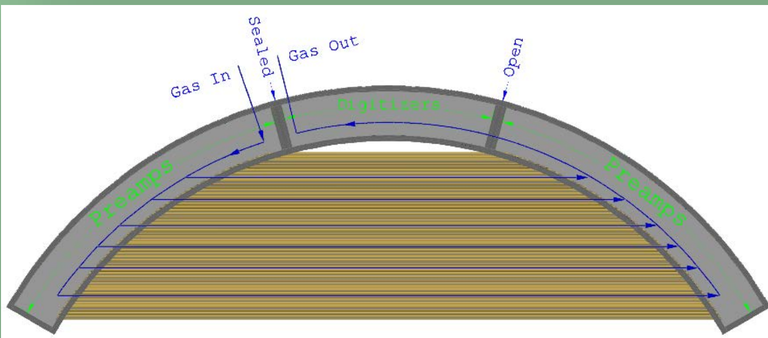

Custom ASIC for time division:
$\int \approx$ 5 mm at straw center

Plane: 6 self supporting panels

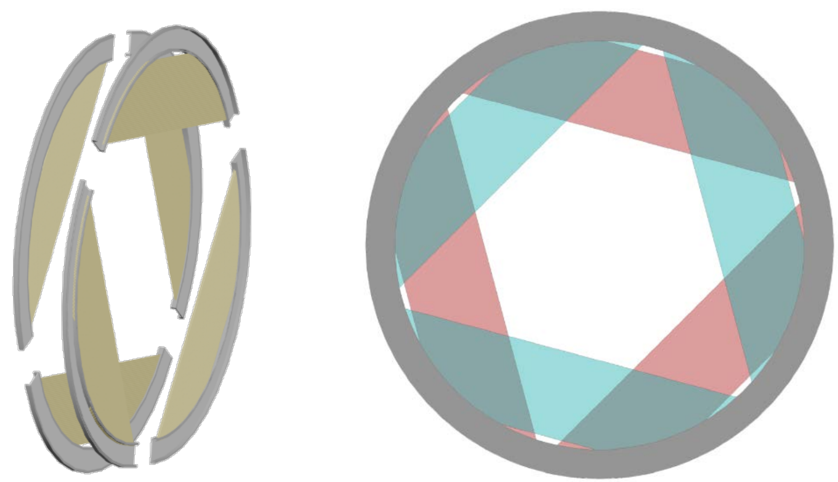

⇨ Stations ⇨ Tracker

Station: 2 planes

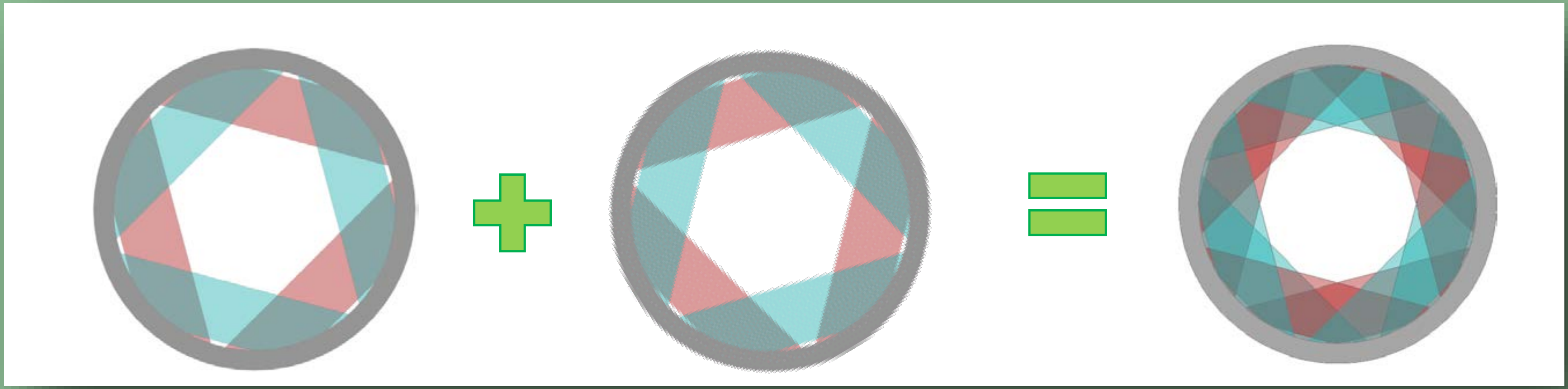

Tracker: 18 stations

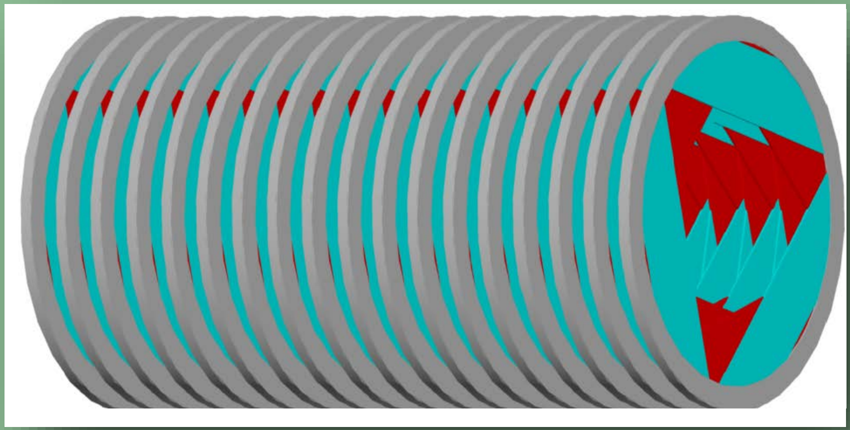

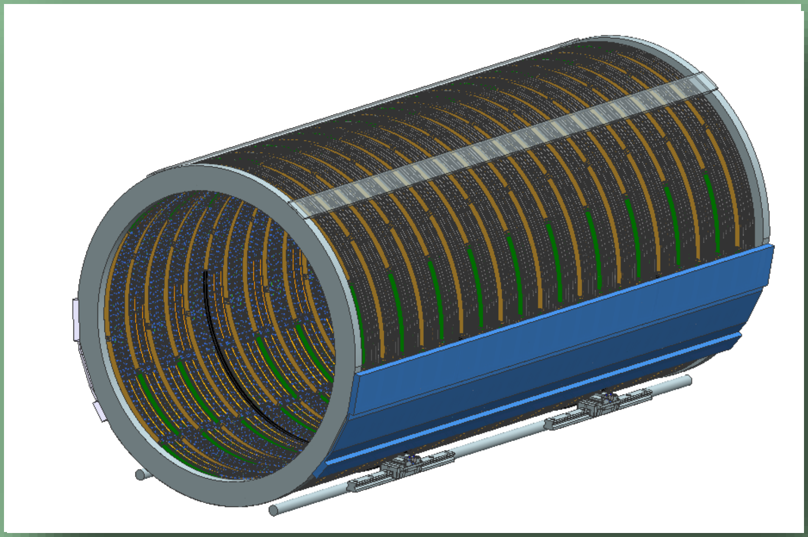

Panel assembly and straw tensioning

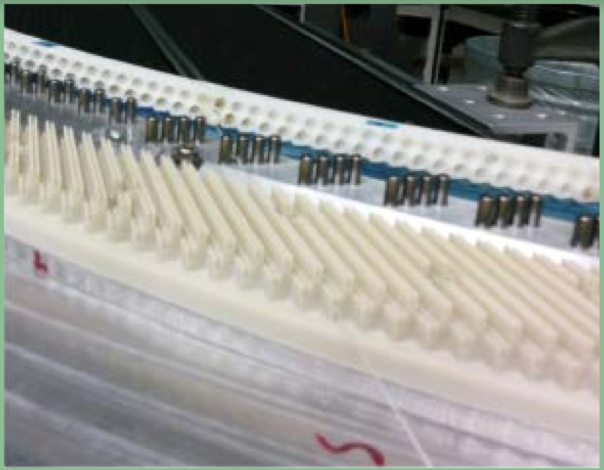

Calorimeter: two annular disks of CsI crystals

- Disks are spaced apart by ½ wavelength of the pitch of a 105 MeV/*c* helical track

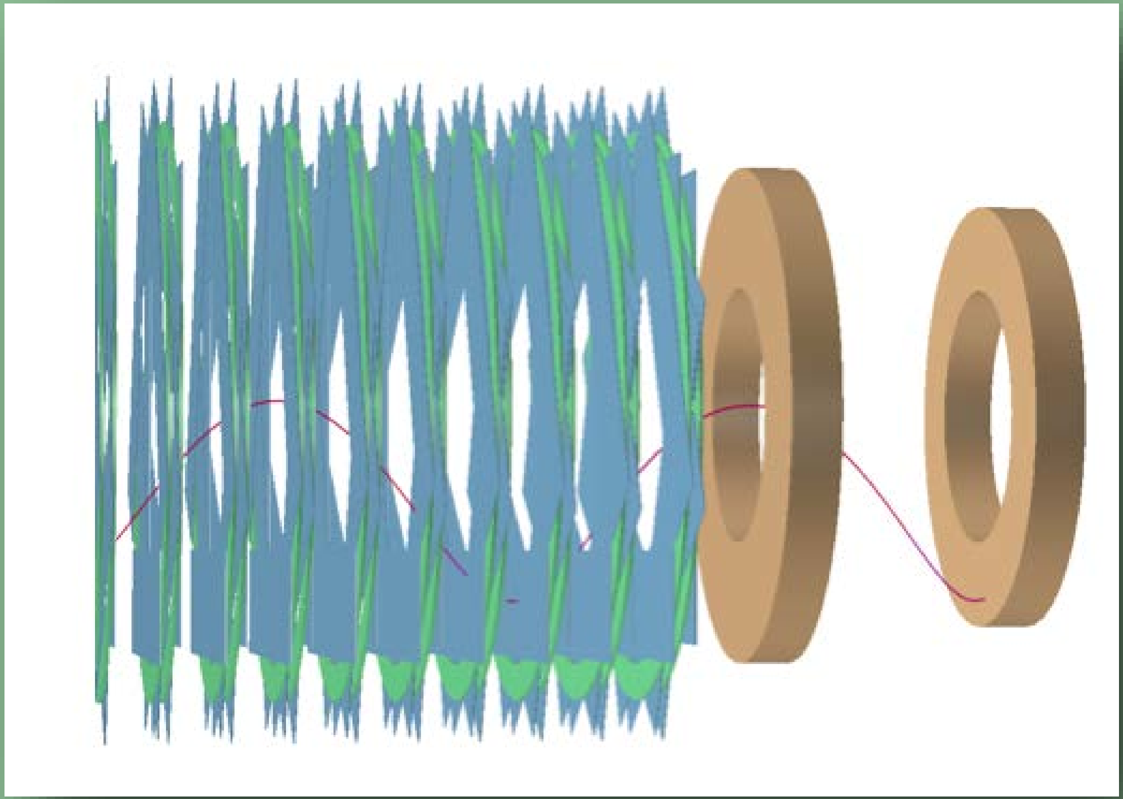

Calorimeter design

- The central hole region in the tracker and calorimeter allows us to be largely insensitive to DIO and beam flash backgrounds
- The calorimeter has two identical annuli, spaced apart by 700 mm (½ λ of the helical trajectory of the conversion electron)
- $r_{inner} = 374$ mm
  $r_{outer} = 660$ mm
  depth = 10 X_0 (200 mm)
- Each annulus contains 674 square CsI crystals with dimensions 34 x 34 x 200 mm^3
- Each crystal is read out by two large area (14x20 mm^2) six element UV-extended SiPMs

  The analog front end electronics is directly mounted on the SiPM

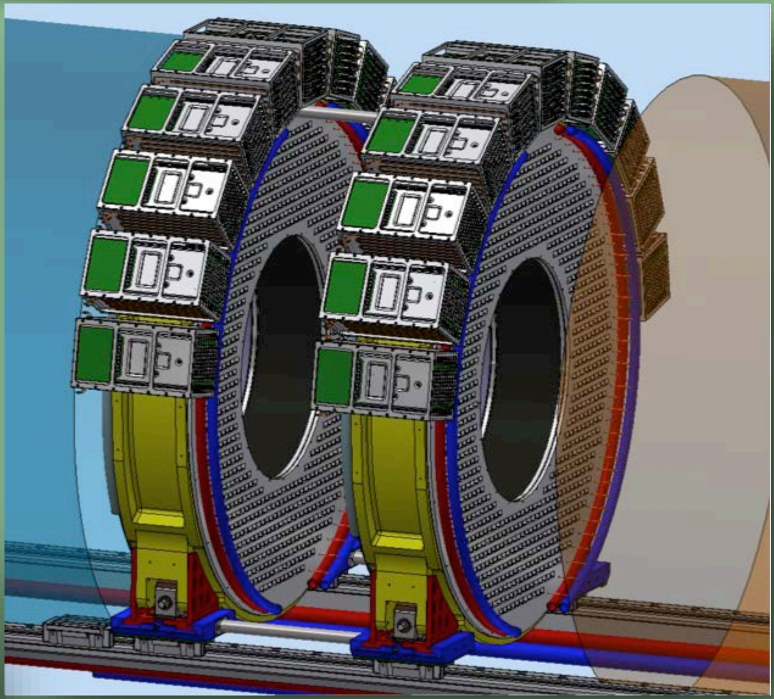

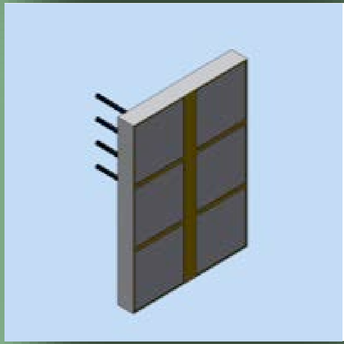

- The digital electronics and voltage regulators are located in electronics crates mounted on the periphery
- Calibration and monitoring are provided by a 6 MeV radioactive source and a laser system

Calorimeter structure exploded view

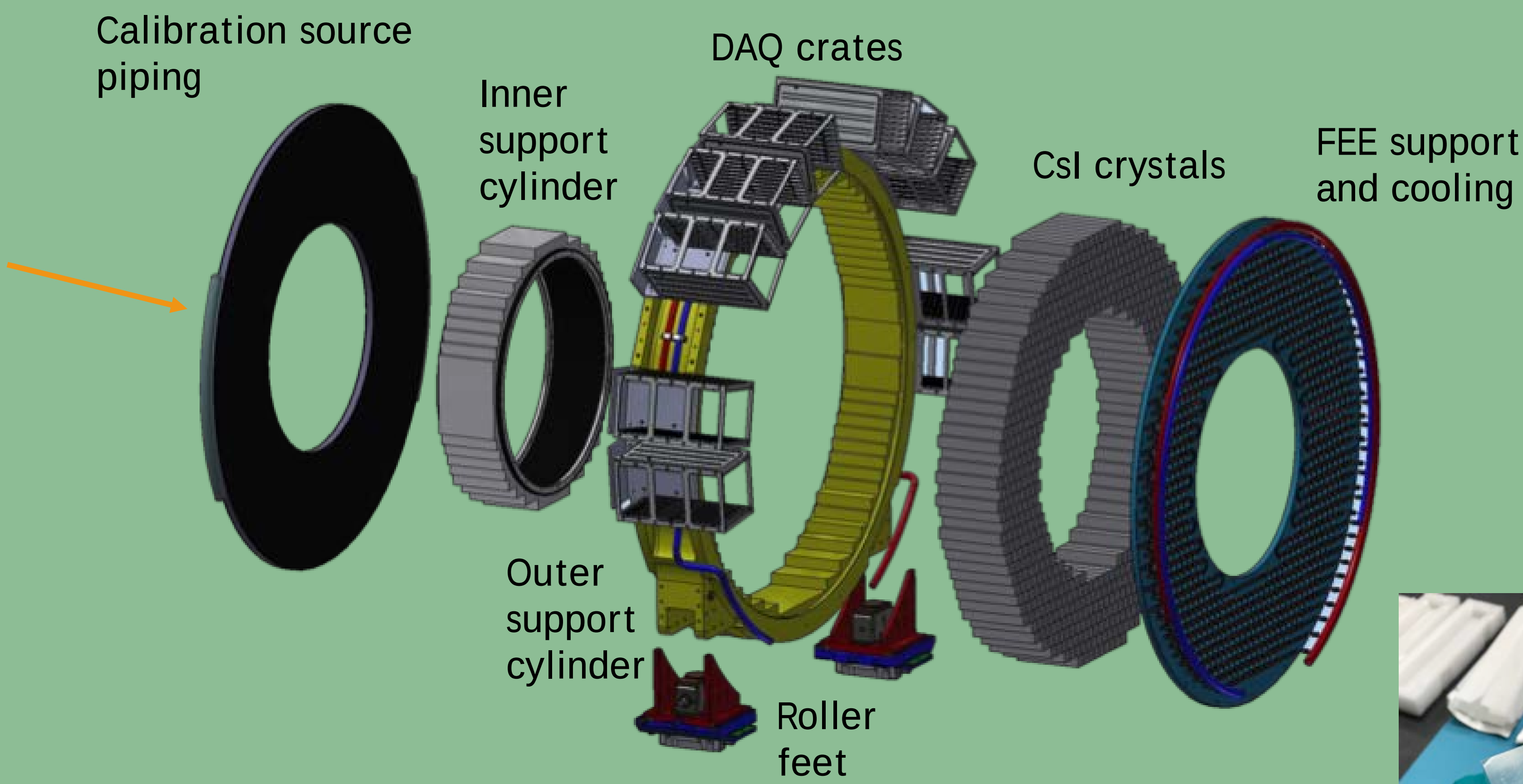

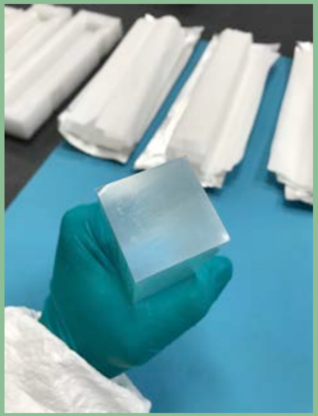

Three views of a disk

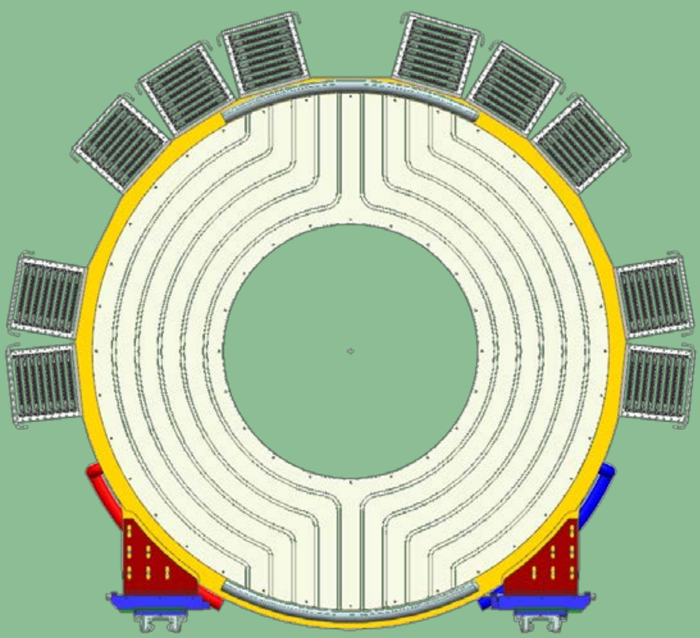

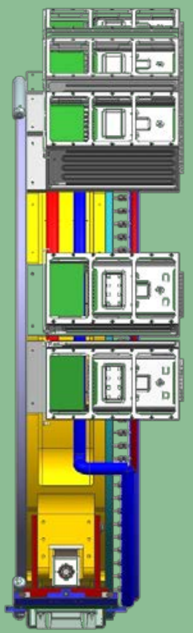

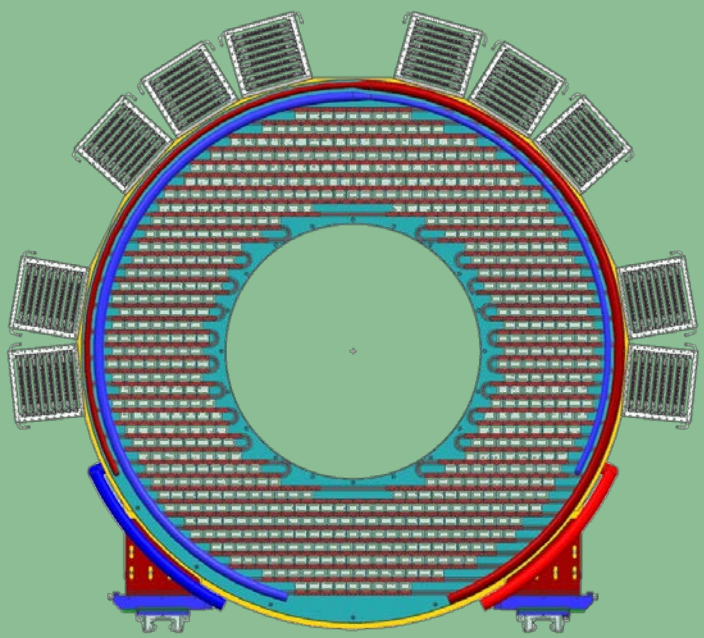

The front faces of the disk include thin Al tubing (à la *BABAR*) through which flows irradiated fluorinert to provide a 6.13 MeV calibration γ

There is no internal crystal support structure: Tyvek-wrapped crystals are selected by dimension, leveled and shimmed to minimize placement error

Three views of a disk

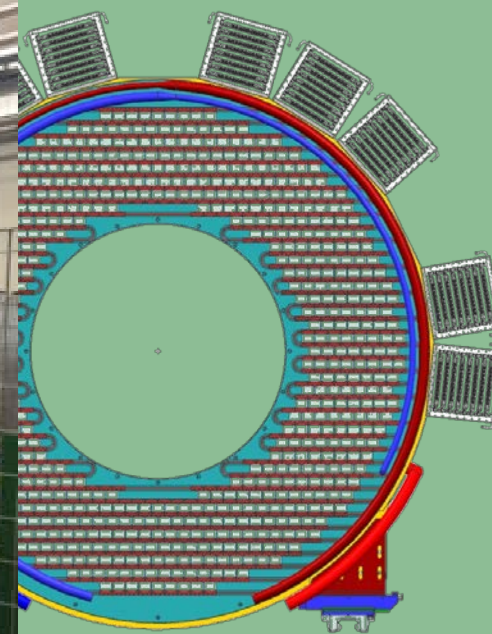

The front faces of the
thin Al tubing (à la *BA*
which flows irradiated
provide a 6.13 MeV ca

nternal crystal support
vek-wrapped crystals are
dimension, leveled and
minimize placement error

Calorimeter cluster-seeded track finding

The speed and efficiency of track reconstruction is improved by selecting tracker hits compatible with the time (|Δt| < 50 ns) and azimuthal angle of calorimeter clusters

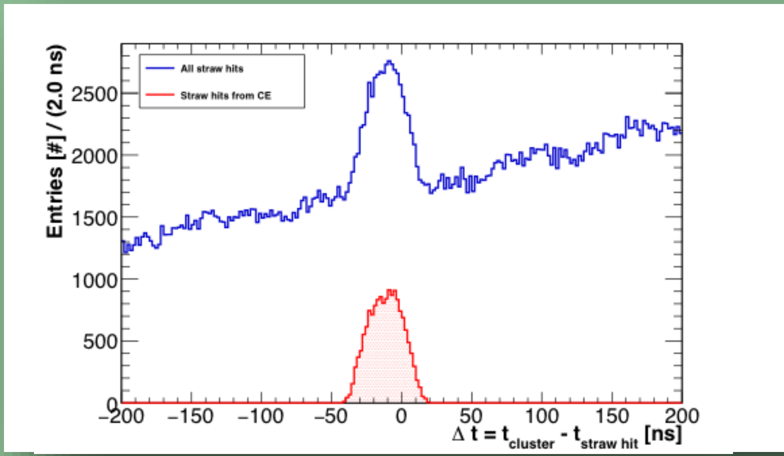

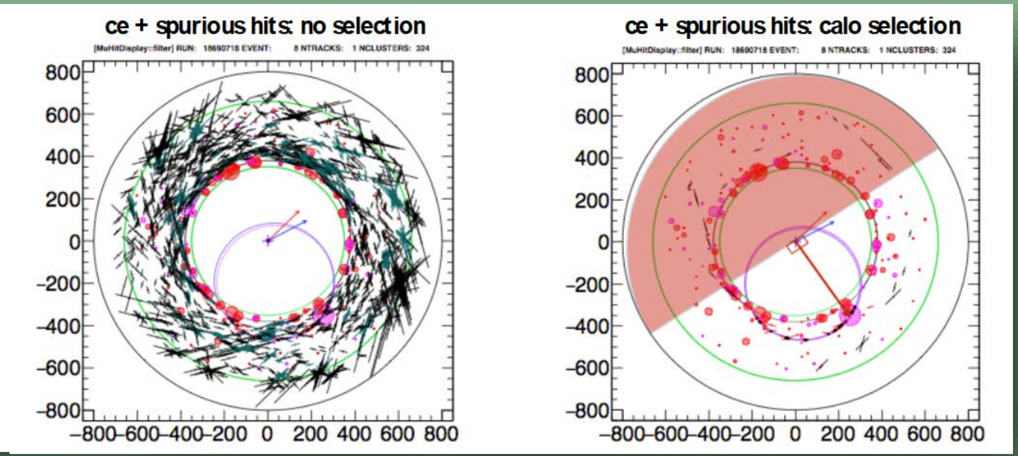

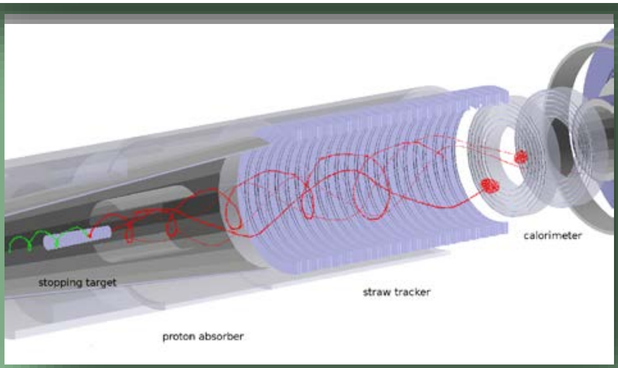

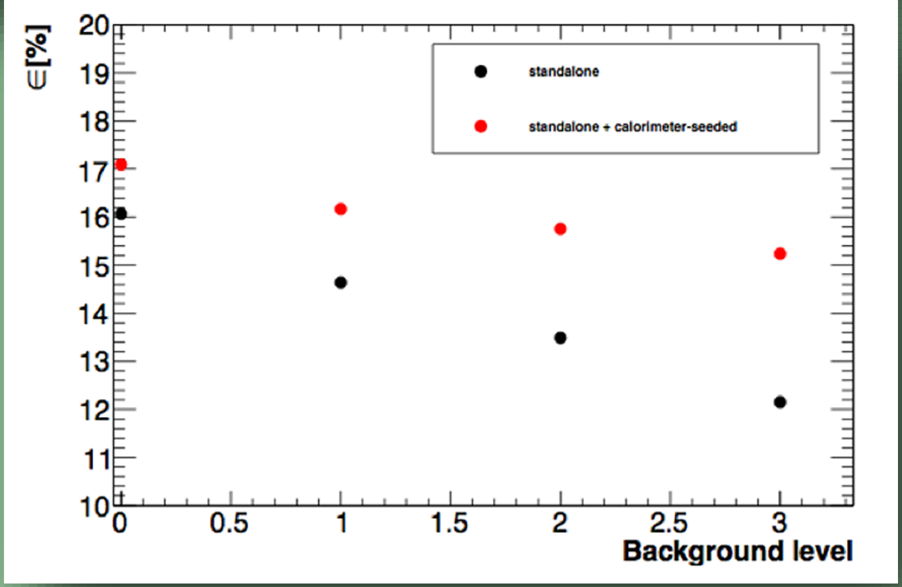

Calorimeter-seeded track finding improves the relative efficiency for tracks in the signal region (103.5 < p <105 MeV/c) by ~11% and is more robust against background

PID: e/μ separation by TOF, E/p

CRV studies show that with a CRV inefficiency of 10^{-4}, an additional rejection factor of ~200 is needed in order to have < 0.1 fake events from cosmics in the signal window

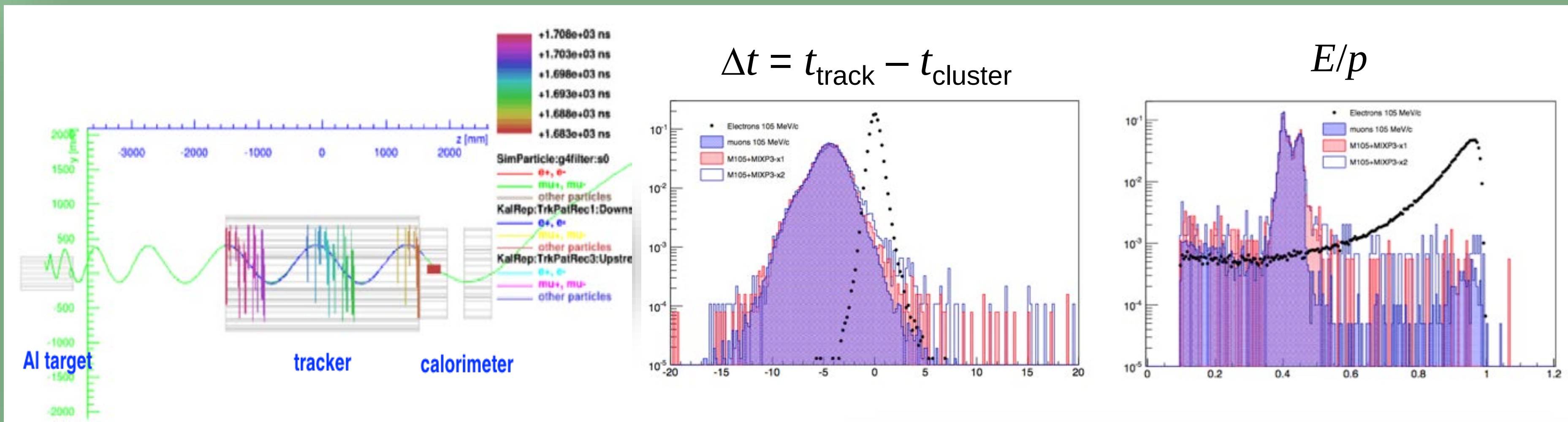

Rare cosmic ray muon events can mimic a conversion electron signal event

Events of this type can be vetoed using the timing information from the calorimeter

A rejection factor of 200 can be achieved with ~95% conversion electron efficiency

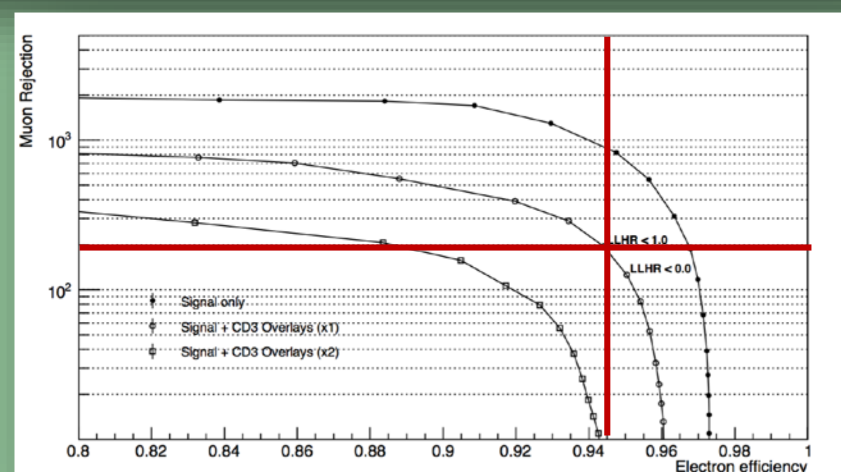

Calorimeter energy resolution

- Achieving best possible energy resolution requires efficient shower clustering algorithm with detached cluster recovery and pile-up rejection
  - Cluster algorithm with detached cluster recovery

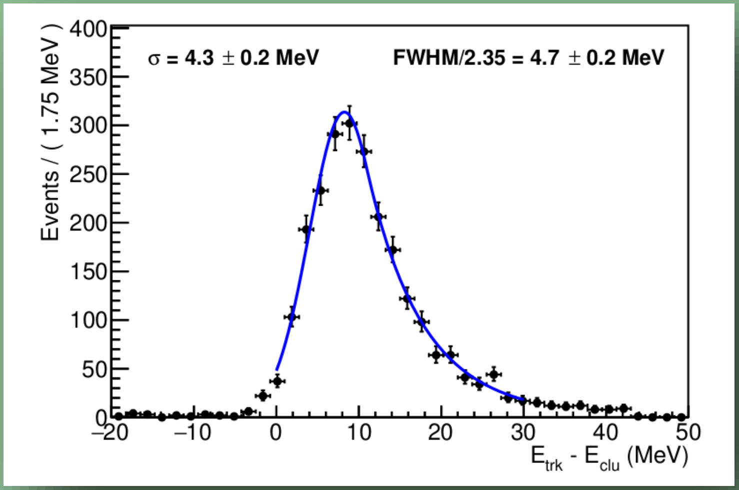

GEANT4 simulation

  - Pile-up rejection using waveform digitization

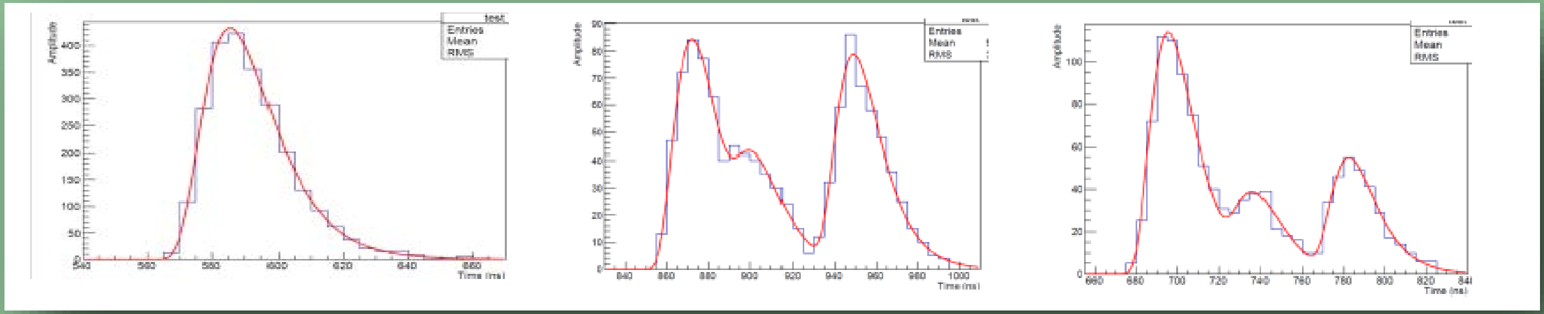

Calorimeter spatial, time resolution

Spatial resolution

Compare predicted and Monte Carlo positions with signal events

$\sigma_x = 6.3 \pm 0.2$ mm

$\sigma_y = 5.8 \pm 0.2$ mm

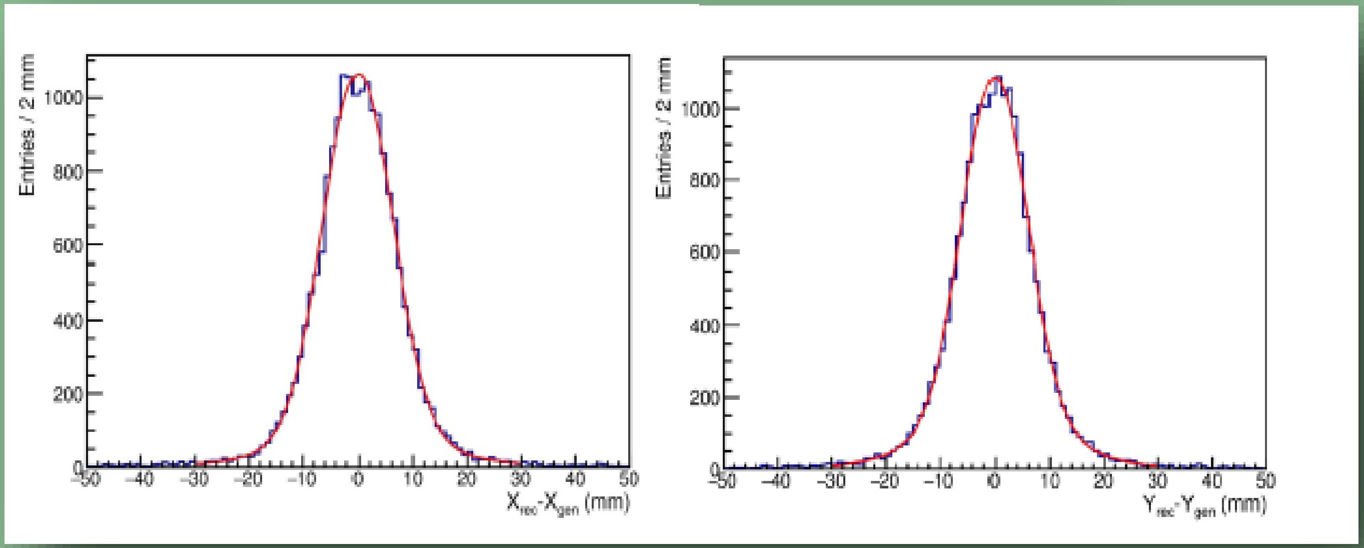

Time resolution

Cluster time defined using the energy-weighted crystal times

$\sigma_t = 109 \pm 1$ ps

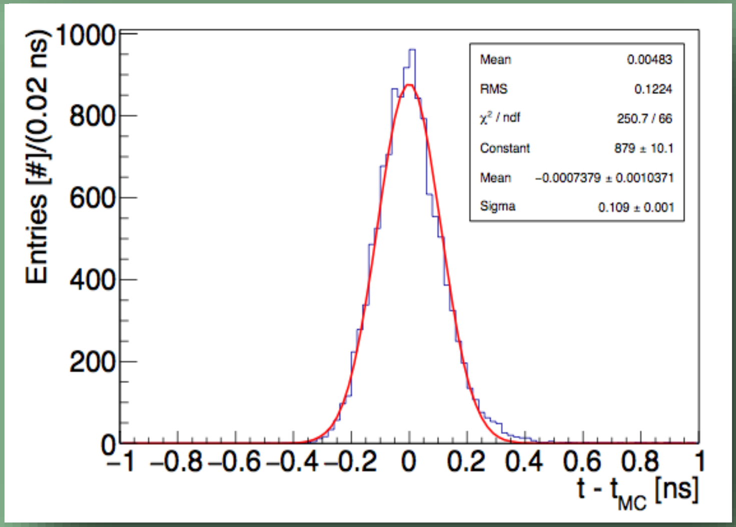

GEANT4 simulation

Extended response SiPMs match CsI spectrum

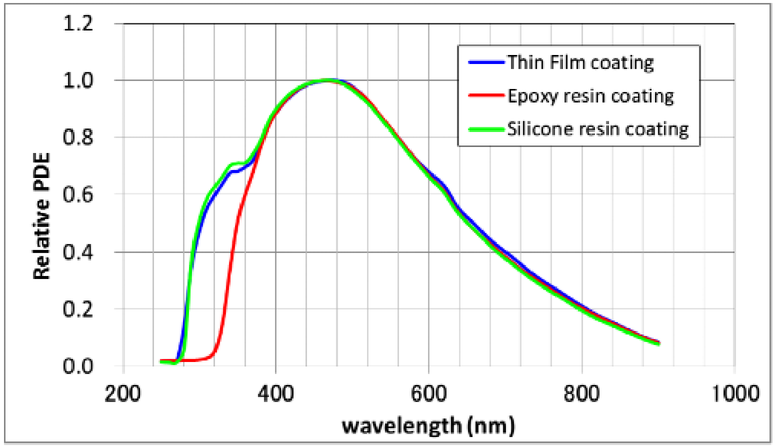

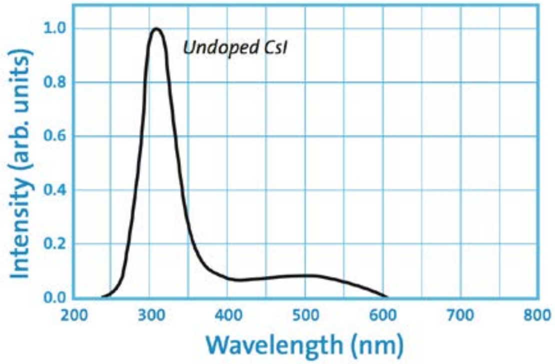

- Six 6x6mm cells in a 2x3 array
    - 50 mm pixels
    - Biased in series/parallel

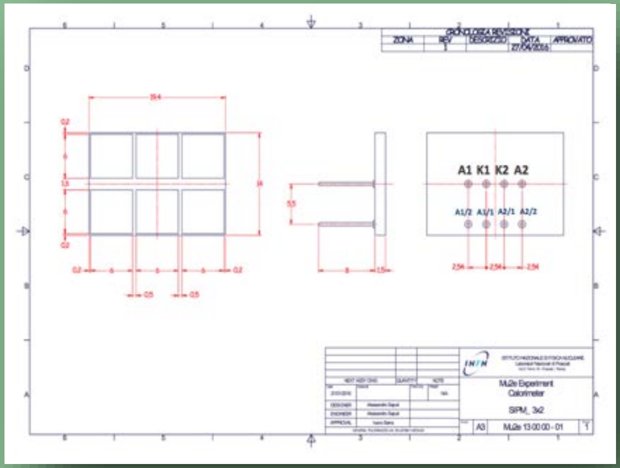

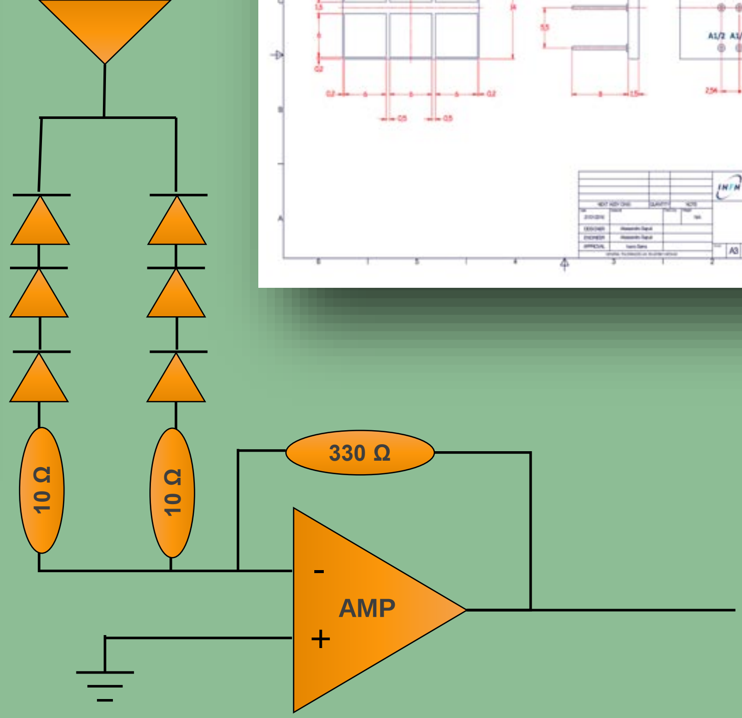

Frascati test beam results: CsI/SiPM array

- Test beam with 70-115 MeV electrons @ LNF
- 51 30x30x200 mm^3 CsI crystals
- Readout: Hamamatsu, SENSL, Advansid MPPCs
- Results
  - Energy resolution $\sigma_E/E \leq 7\%$ dominated byshower leakage and beam energy spread
  - Time resolution $\sigma(t)$=1<200 ps.

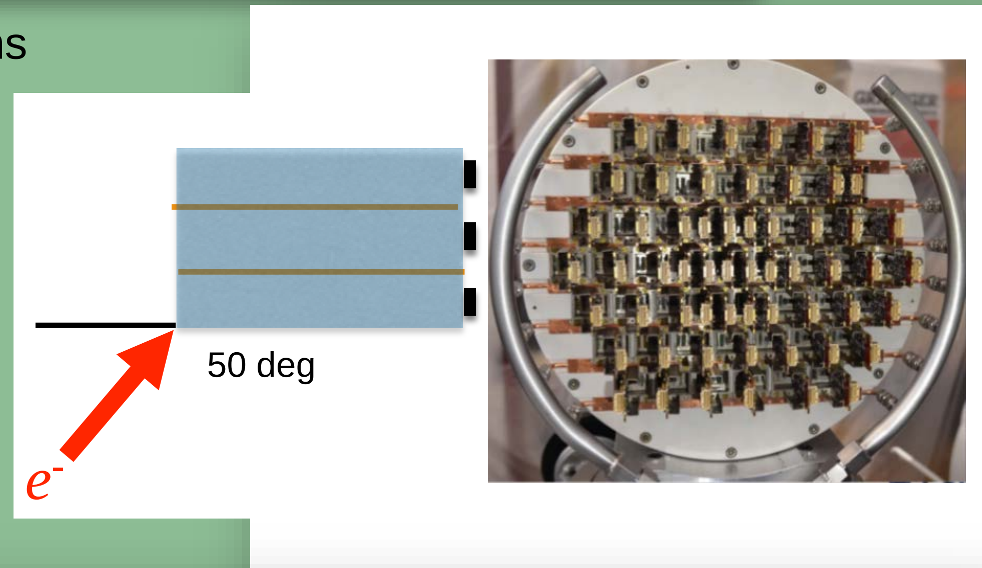

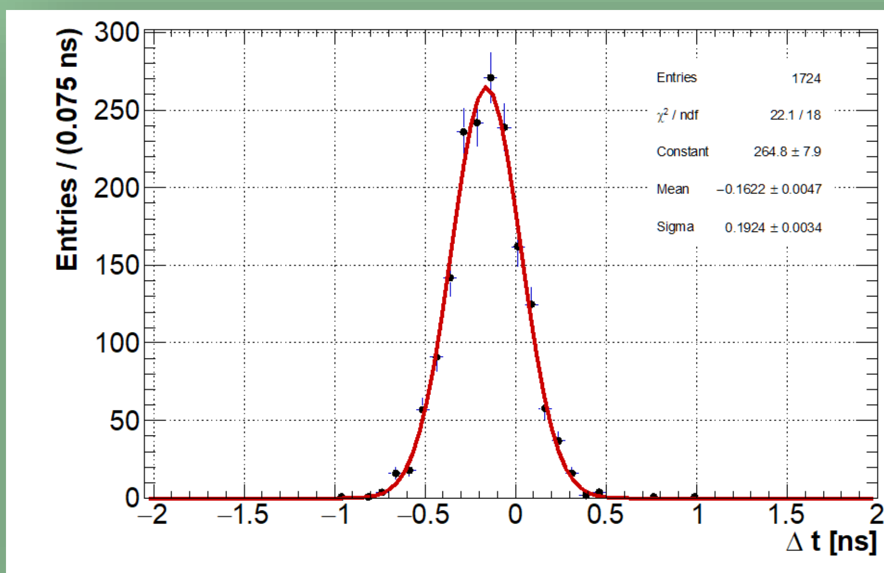

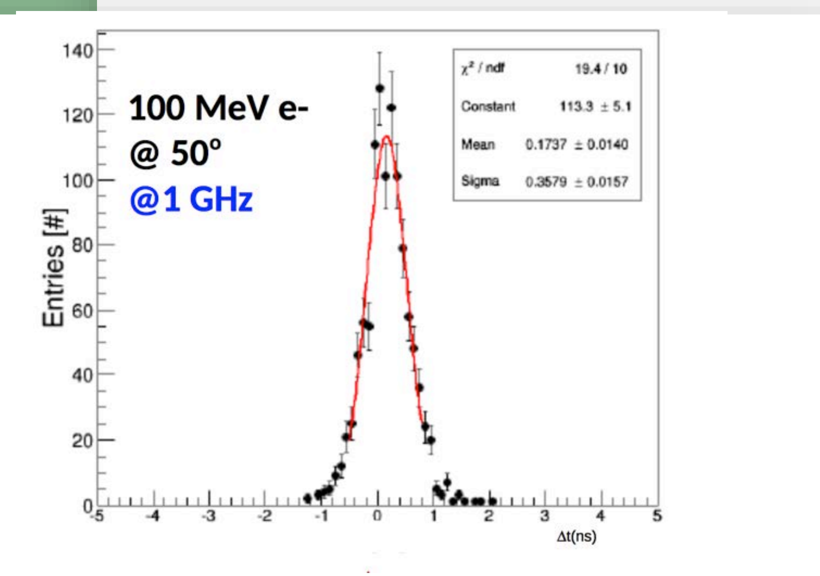

Calibration and monitoring

1) The *BaBar* calibration source has been rebuilt to provide 6.13 MeV γ s on demand

$$
\begin{aligned}
{}^{19}F + n \rightarrow\ & {}^{16}N + \alpha \\
{}^{16}N\ \rightarrow\ & {}^{16}O^{*} + \beta \qquad t_{1/2} = 7\ \mathrm{s} \\
& {}^{16}O^{*} \rightarrow {}^{16}O + \gamma(6.13\ \mathrm{MeV})
\end{aligned}
$$

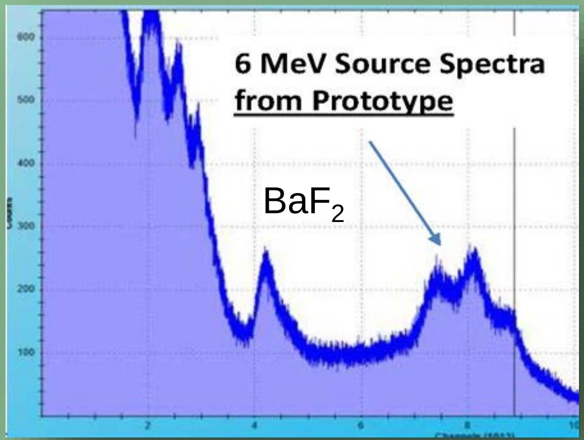

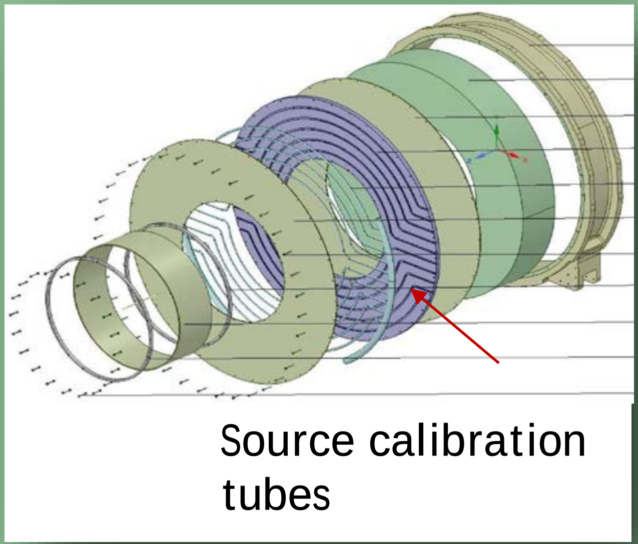

2) Laser system to monitor SiPM performance

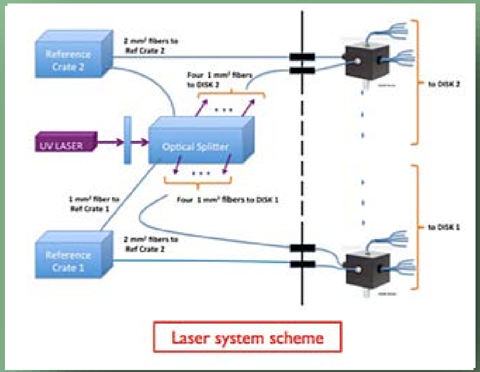

3) Cosmics + E/p for DIOs at reduced B field

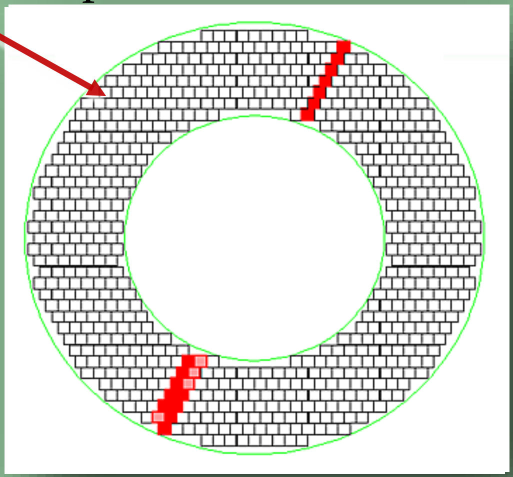

Cosmic ray veto (four layers)

Covers as much of the transport and detector solenoids as possible
Nonetheless, timing properties of the calorimeter are required to achieve required cosmic ray rejection

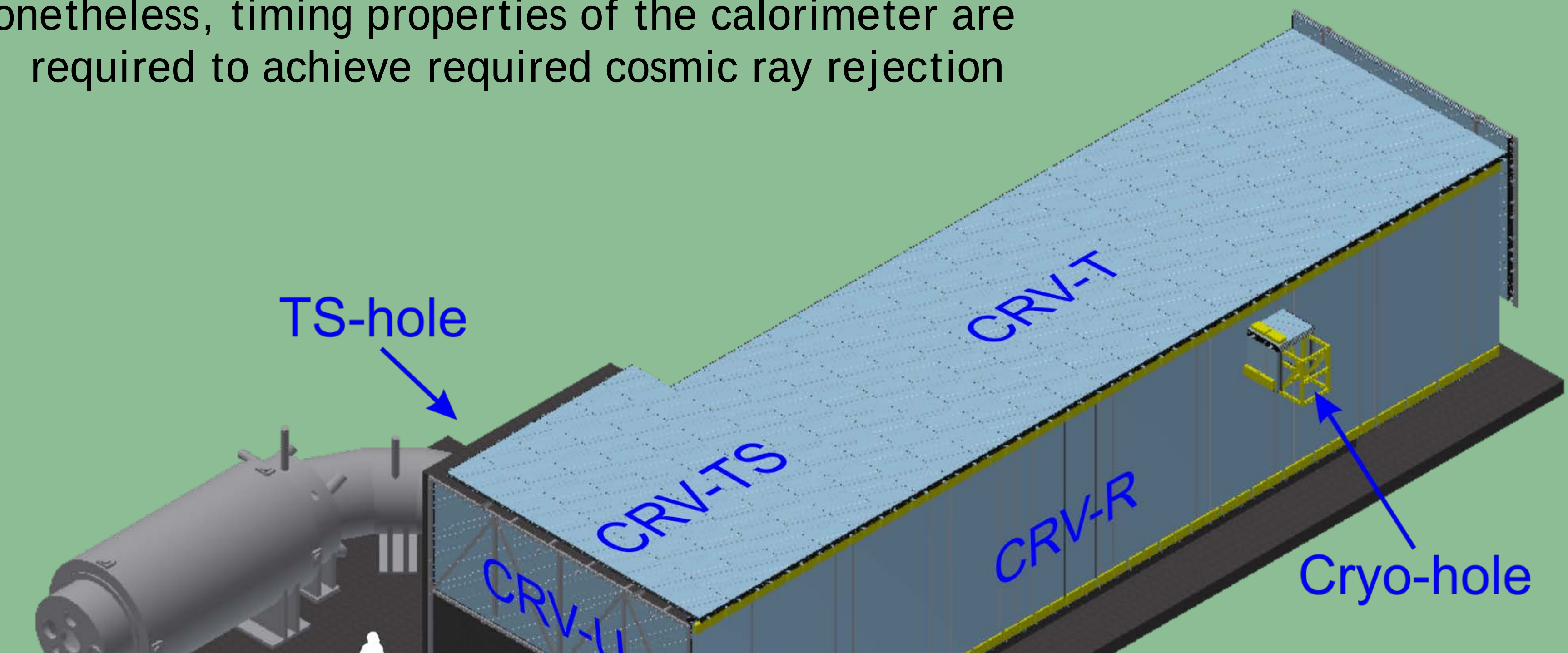

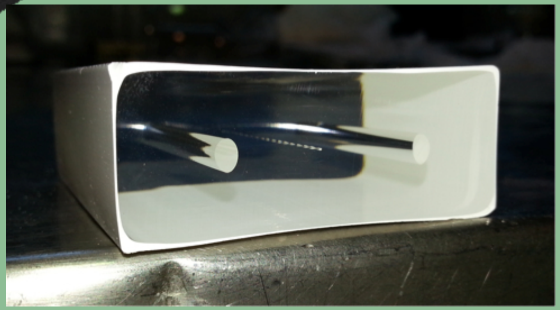

Signal sensitivity for a three year run

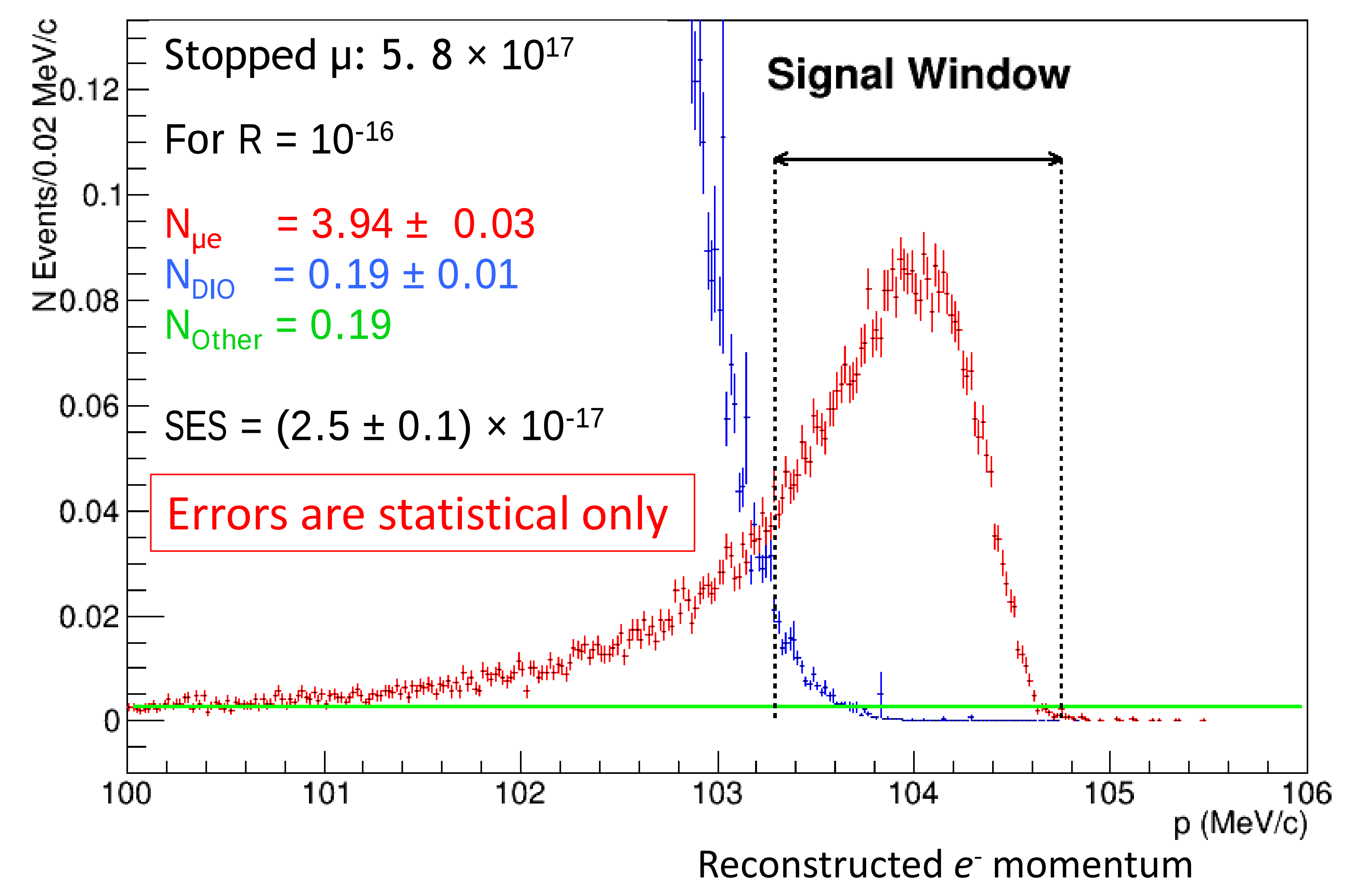

Mu2e Schedule

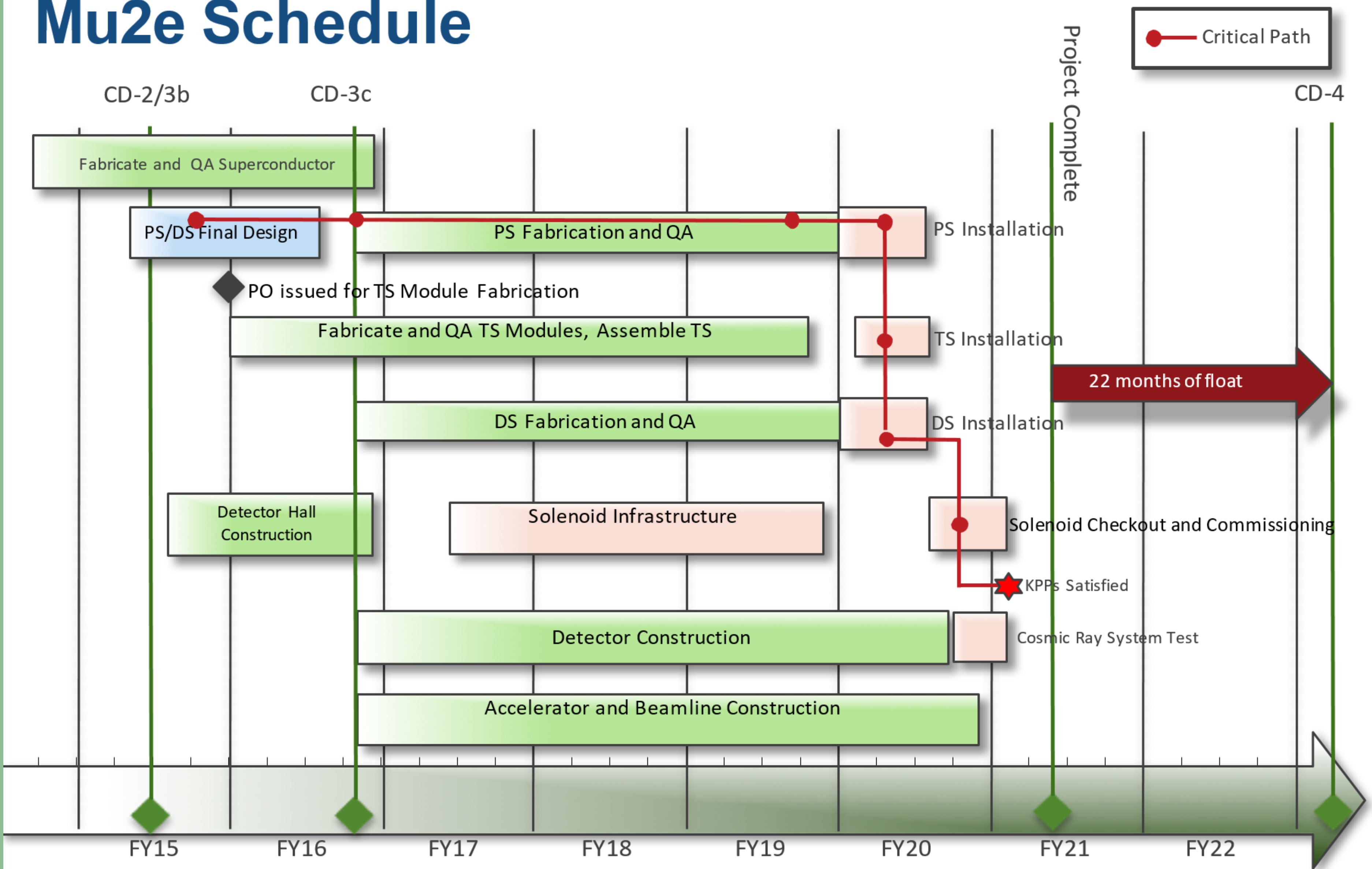

COMET Phase I

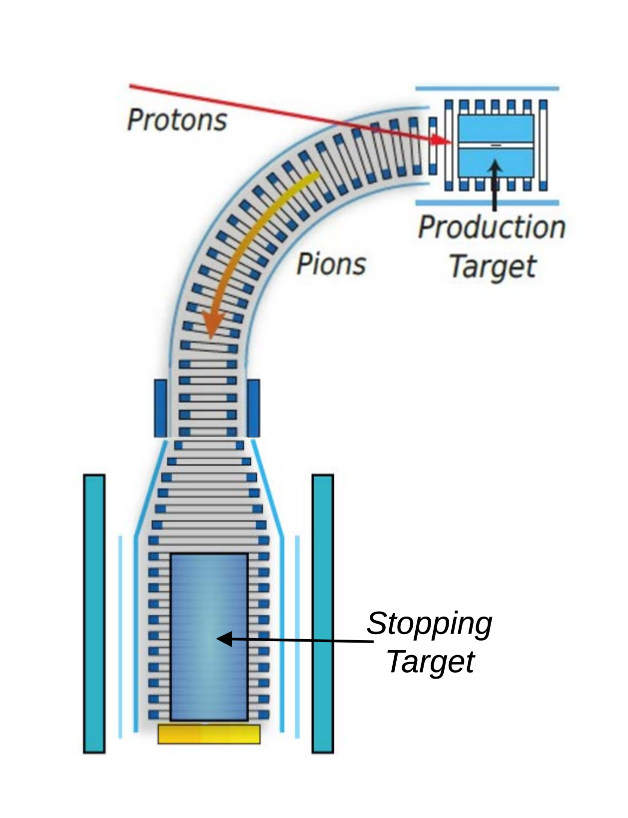

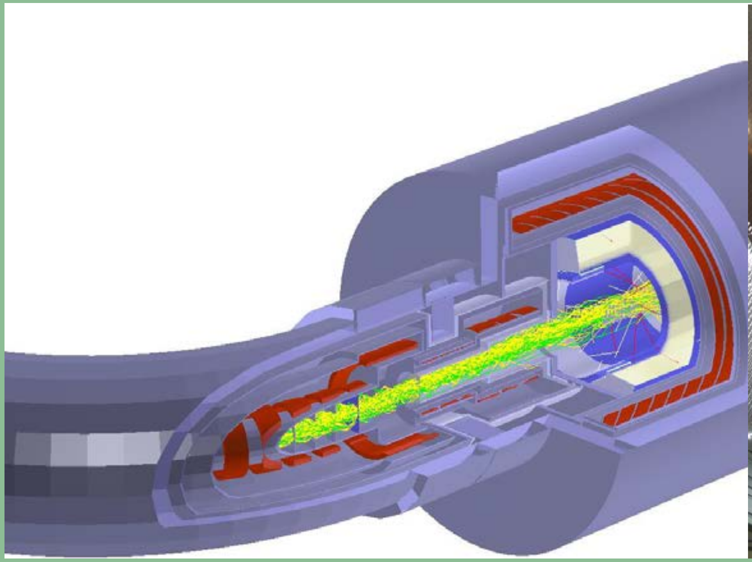

SES   3 x 10^{-15}
 or < 6 x 10^{-15} @ 90% CL
for 150 days at 3.2 kW

COMET Phase II

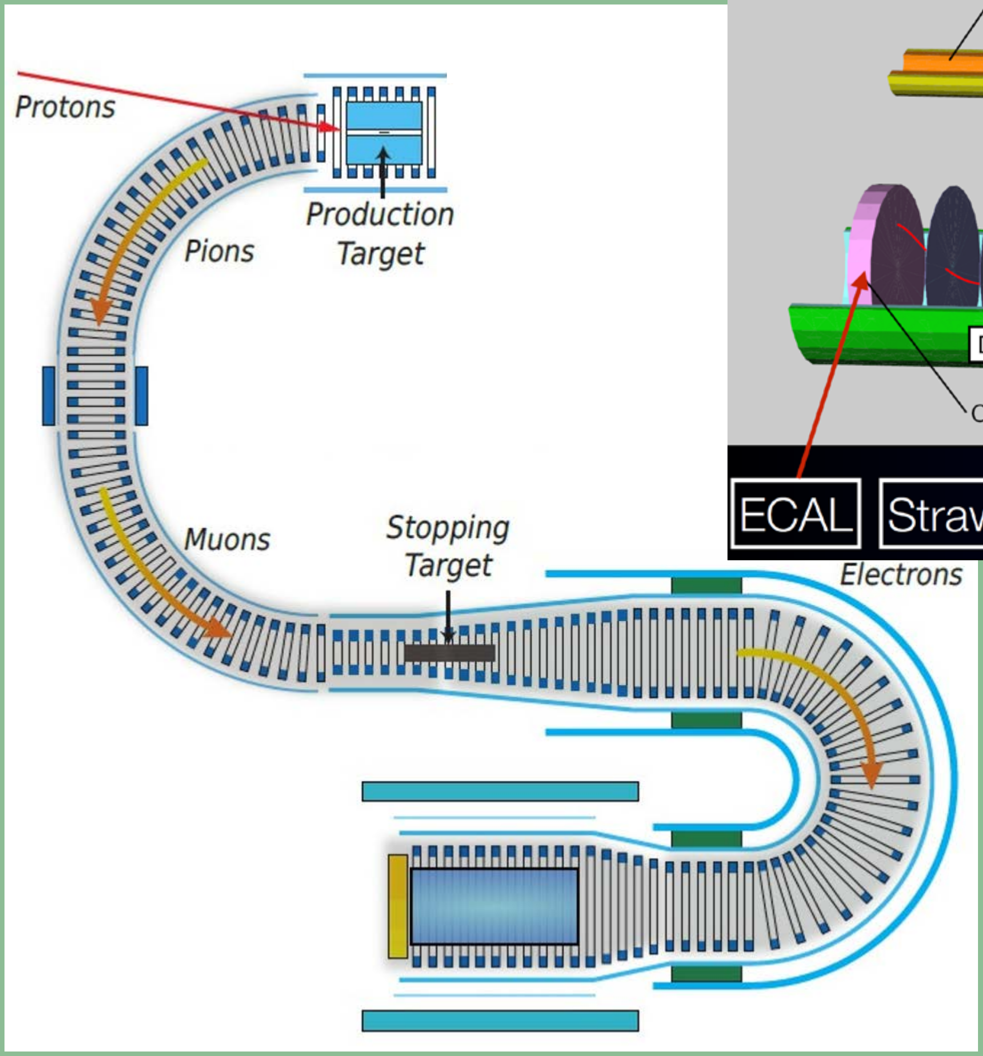

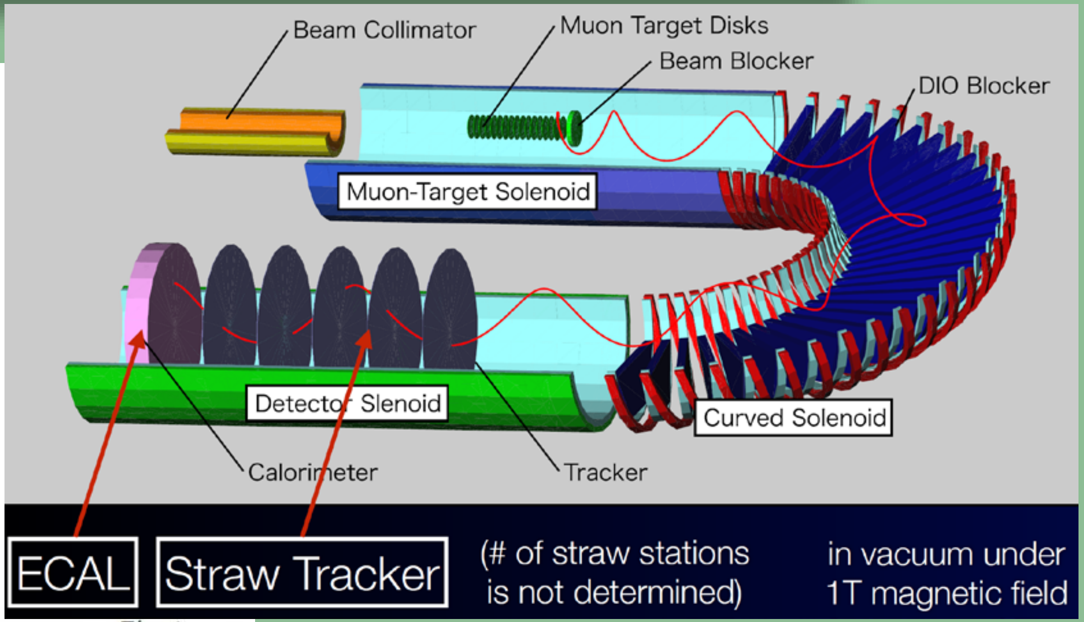

SES (1.0 – 2.6) x 10^{-17}
for 2 x 10^{7} s at 56kW

COMET schedule

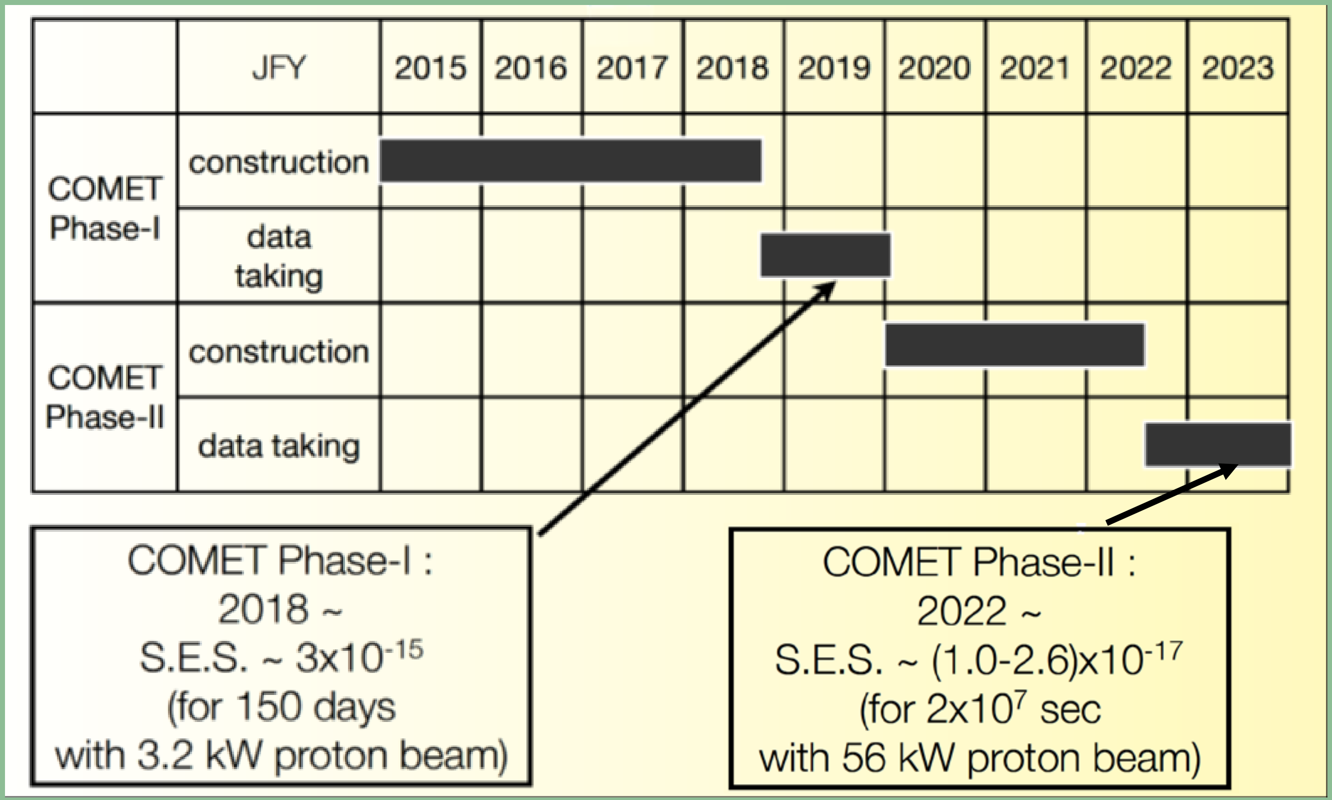

Z dependence of μ to e conversion

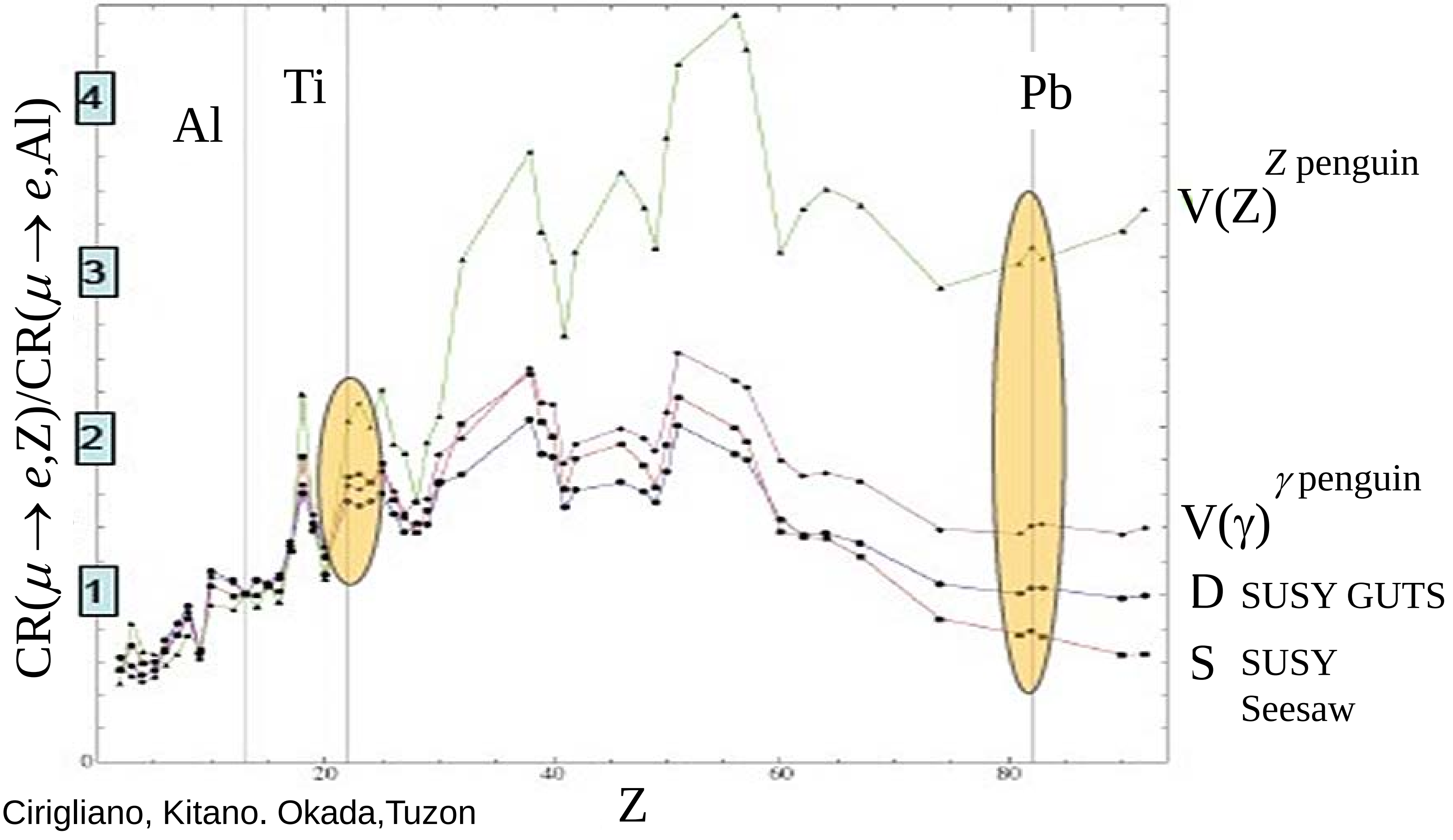

Cirigliano, Kitano. Okada,Tuzon

PIP2/Mu2e II

- PIP2 is an 800 MeV, 120 kW superconducting linac for LBNF and the muon campus
  - Currently under design
- There is also an active study of an upgrade of Mu2e
  - An order of magnitude increase in muon stops, but only a x3-5 increase in instantaneous rate
  - Detector systems must be upgraded
- Goals:
  - If $\mu \rightarrow e$ conversion has been found, use heavier targets to ascertain the (A, Z)-dependence of conversion rate
  - If conversion is not seen, improve sensitivity by an order of magnitude

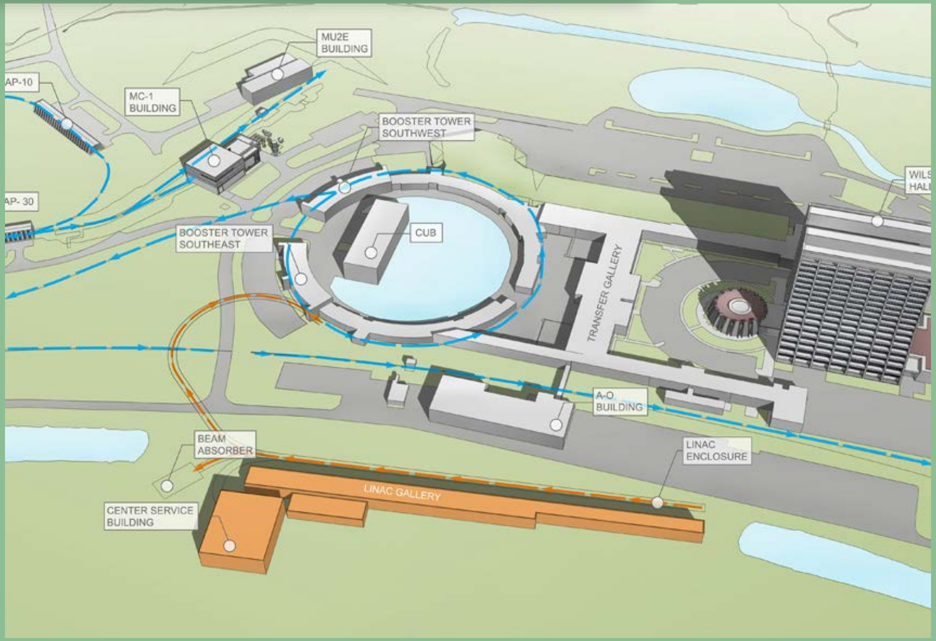

Prism/PRIME

Phase Rotated Intense Slow Muon source

PRISM Muon Electron conversion

- A muon storage ring, feeding a COMET-like channel and detector
- High muon intensity:
- (10^{11}-10^{12} μ^-/s):

  large 6D acceptance (FFAG),
- Pulsed beam >100 Hz,
- Low momentum, quasi-mono-energetic muons
- Pion contamination <10^{-18}
- Requires a multi-GeV 1-4 MeV proton driver
- Aims for SES- 3×10^{-19}
- Time scale beyond 2030

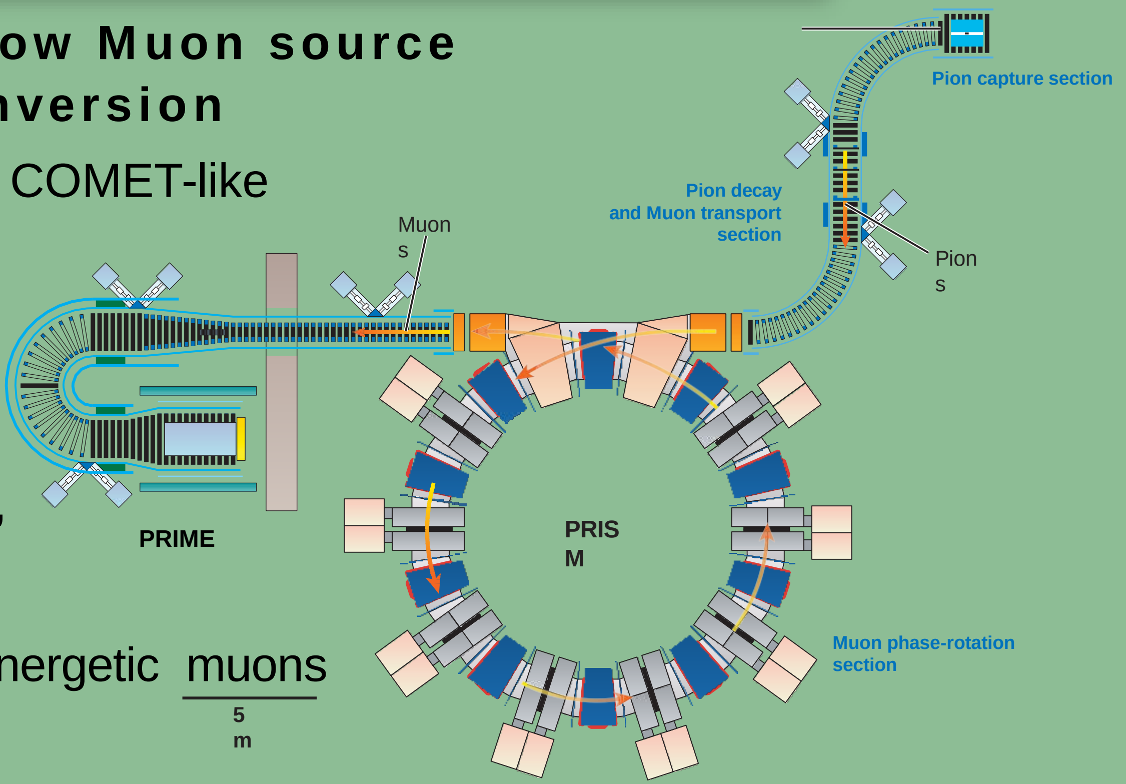

Outlook

- Current limits on charged lepton flavor violation provide useful constraints on New Physics models
- Over the next decade, improved τ decay, μ decay, leptonic and semileptonic meson decay and $\mu \rightarrow e$ conversion experiments will have the sensitivity to probe the regime predicted by many New Physics models
  - Sensitivities reach beyond what is possible in direct production of new particles at the LHC
  - Should evidence for CLFV be found, comparison of branching ratios and conversion rates would be diagnostic of specific models

R_K and R_{K*}

$$R_K = \frac{\int_{q^2_{\rm min}}^{q^2_{\rm max}} \frac{{\rm d}\Gamma[B^+ \to K^+\mu^+\mu^-]}{{\rm d}q^2}{\rm d}q^2}{\int_{q^2_{\rm min}}^{q^2_{\rm max}} \frac{{\rm d}\Gamma[B^+ \to K^+e^+e^-]}{{\rm d}q^2}{\rm d}q^2}$$

also R_{K*}, with $B^0 \to K^{*0}\ell^+\ell^-$

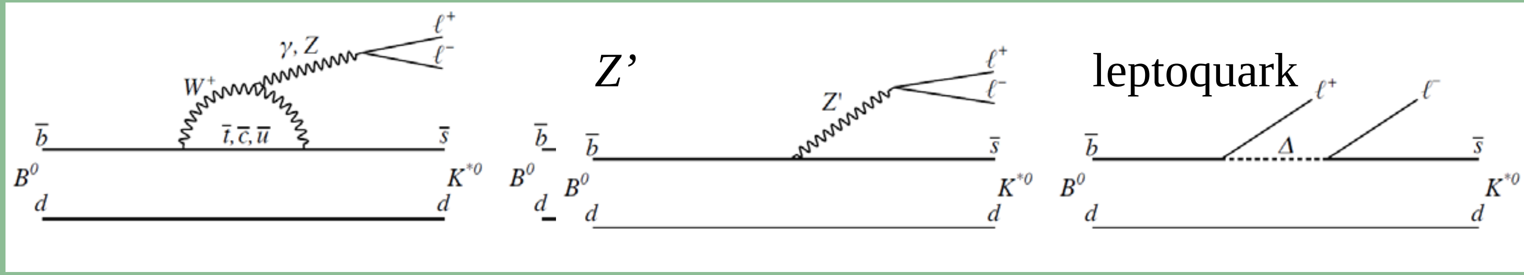

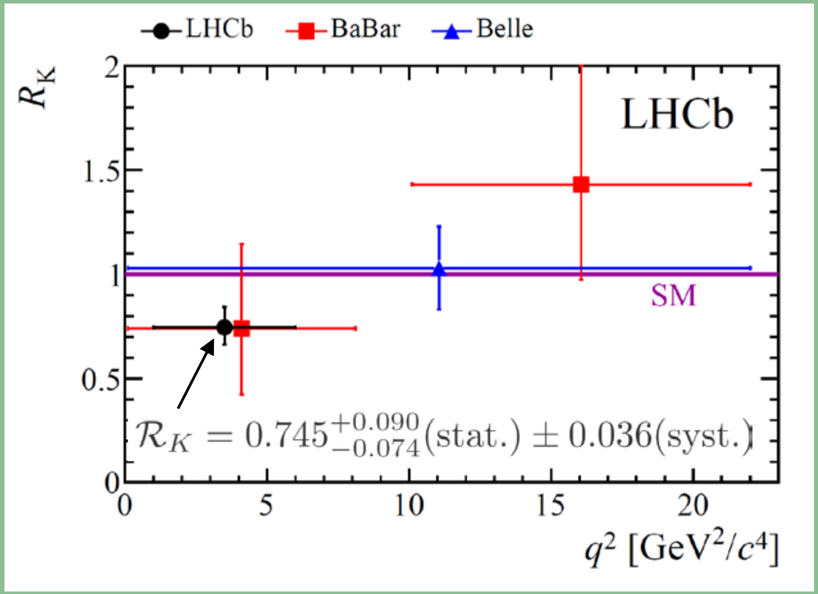

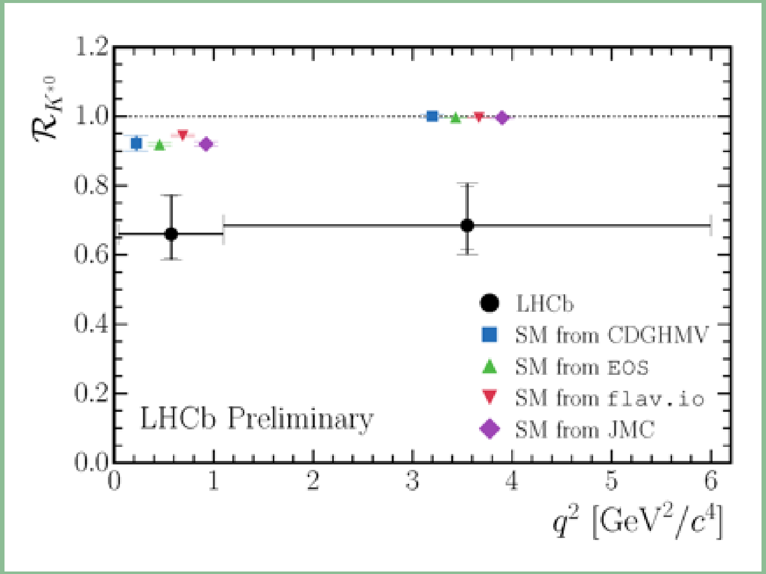

Series coupling improves decay time

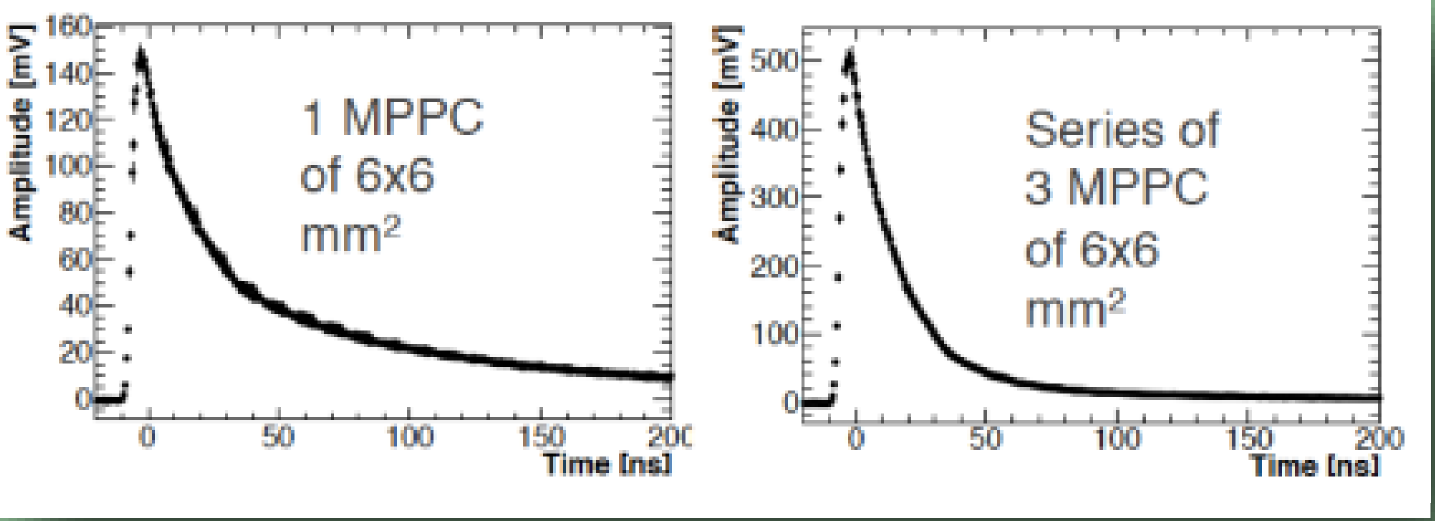

The radiation environment

- The calorimeter radiation dose is driven by the beam flash (the interaction of the proton beam on target).
- The dose from muon capture is 10x smaller
- Dose is mainly to the inner radius (up to 400 mm)
- Highest dose/year ~ 10 krad
- Highest n flux/year on crystal. ~ 2x10 ^{11} n /cm^2
- Highest dose/year on SIPM ~ 6x10^{10} n_1Mev eq/cm^2

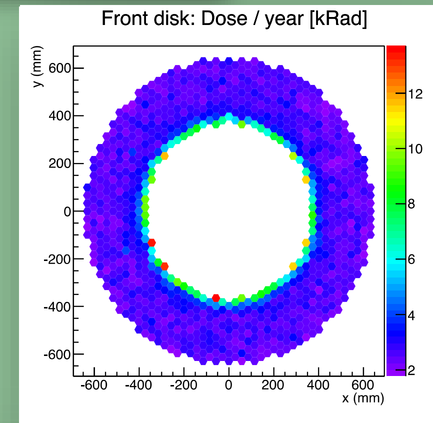

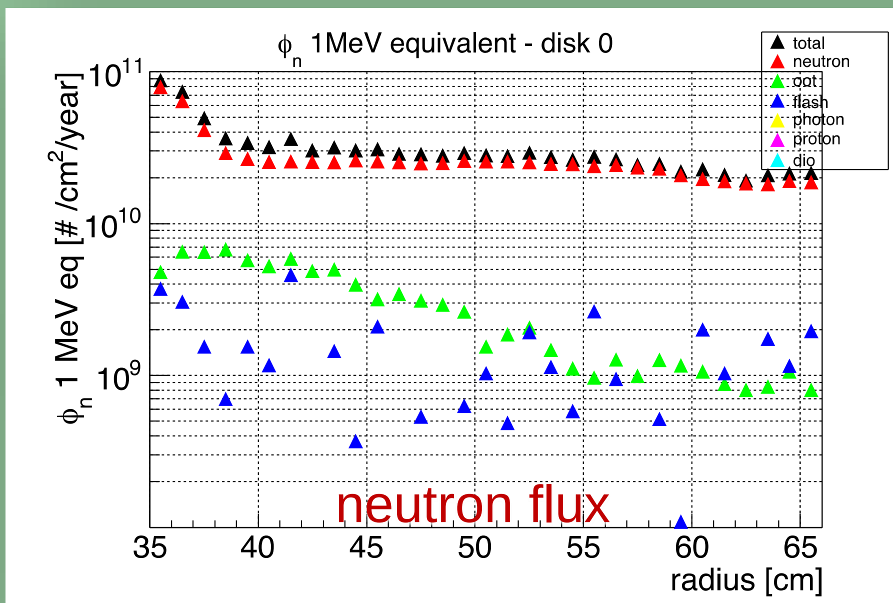

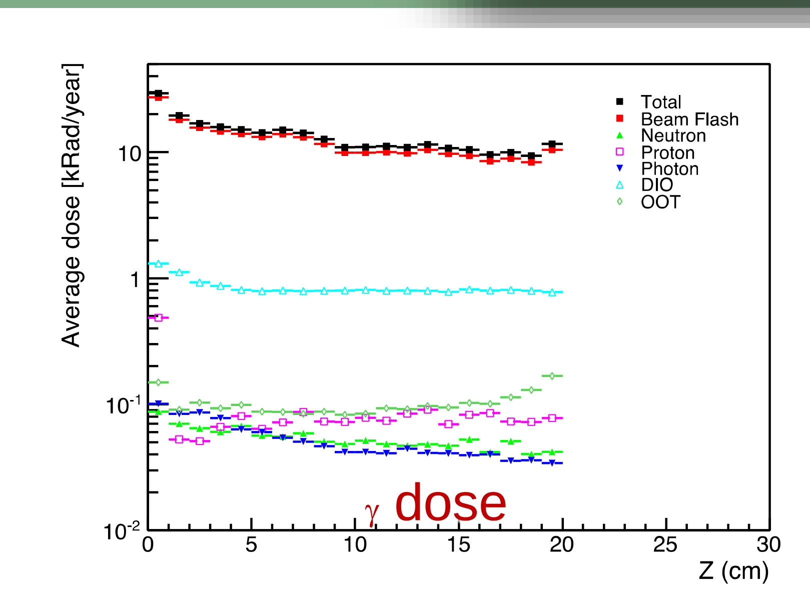

- Qualify crystals up to 100 krad, 10 ^{12} n/cm^2
- Qualify photo-sensors up to 3x10^{11} n_1MeV/cm^2

Includes a safety factor of 3 for a 3 year run

Measured CsI crystal properties

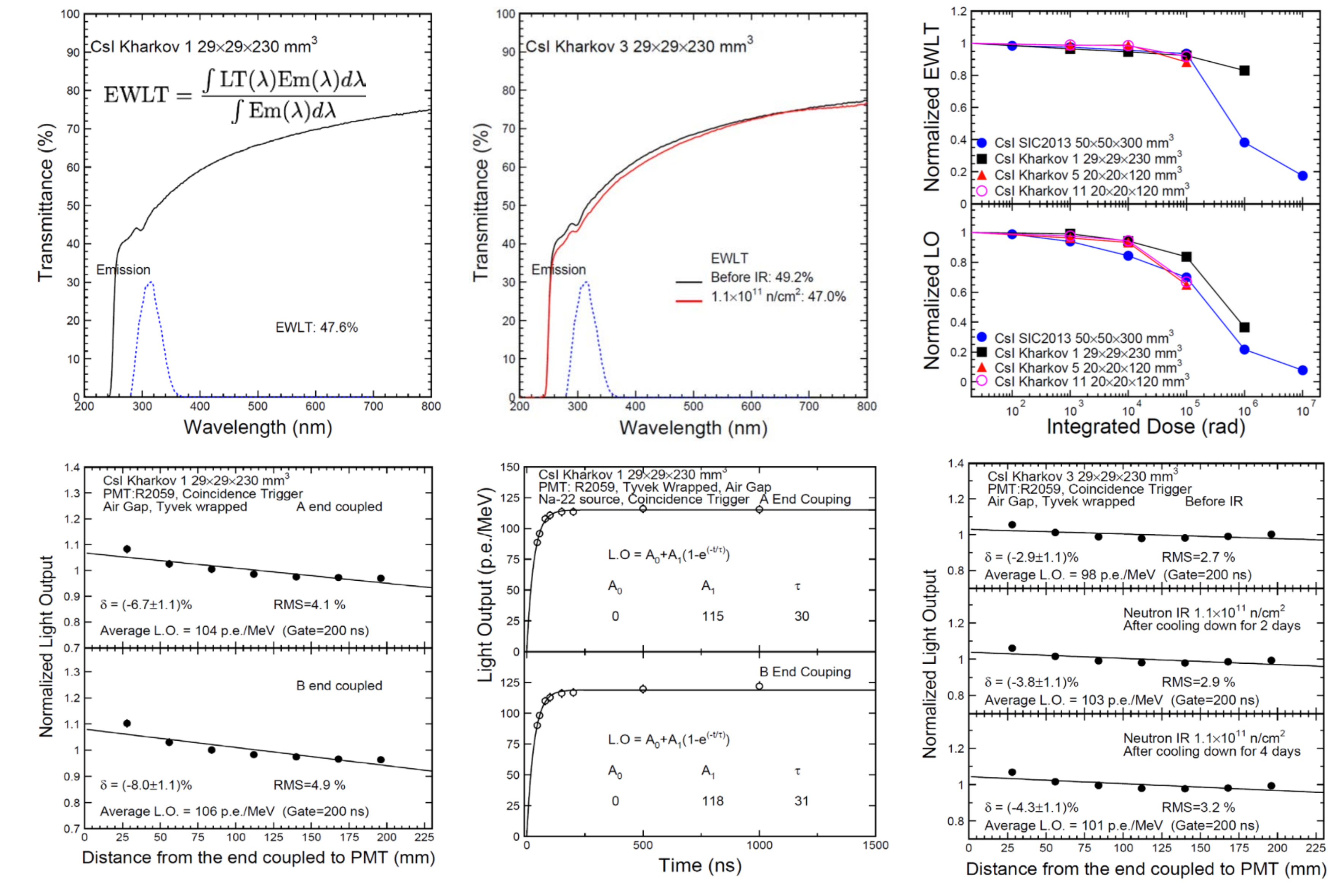

Radiation-induced noise (PMT+SiPM)

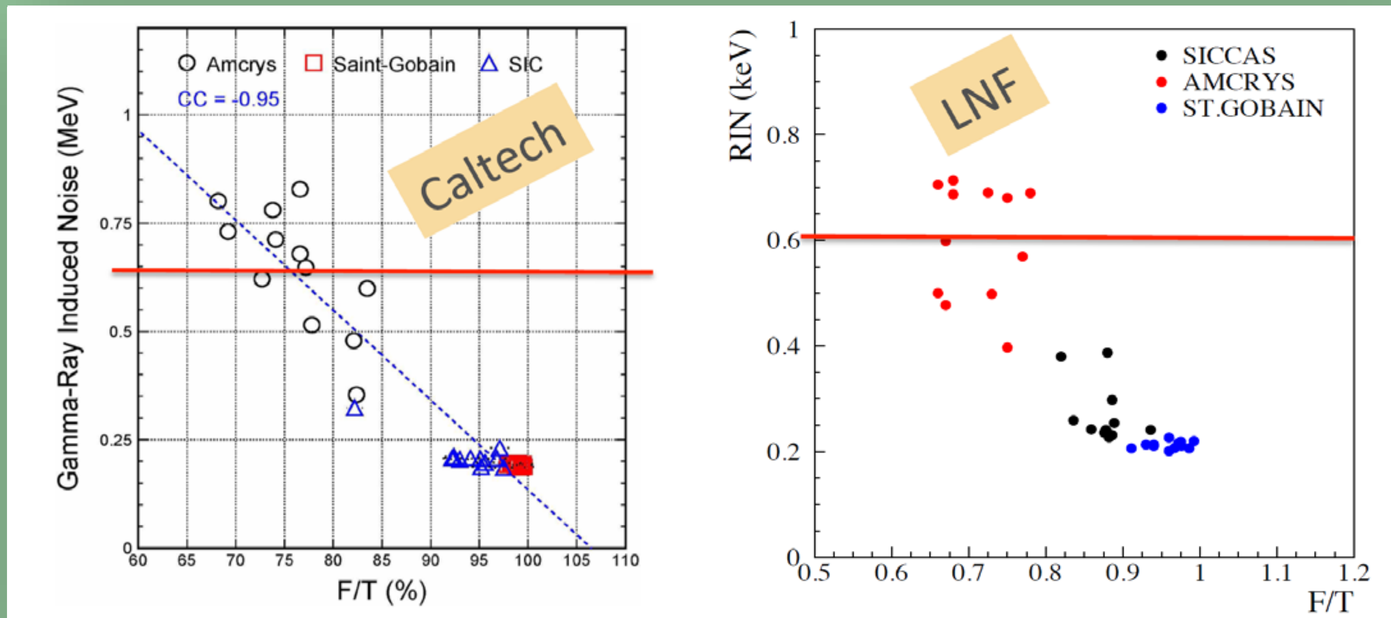

- RIN measurements of preproduction crystals from three manufacturers at Caltech and LNF are in agreement
- RIN and fast/slow component ratio are correlated
  This will be useful in developing final acceptance criteria

Side A	RIN PMT (KeV)	RIN SIPM (KeV)
C0011 - S	629	718
C0020 - A	713	1299
C0053 - SG	226	385